INFORMATION TO USERS

This manuscript has been reproduced from the microfilm master. UMI films the text directly from the original or copy submitted. Thus, some thesis and dissertation copies are in typewriter face, while others may be from any type of computer printer.

The quality of this reproduction is dependent upon the quality of the copy submitted. Broken or indistinct print, colored or poor quality illustrations and photographs, print bleedthrough, substandard margins, and improper alignment can adversely affect reproduction.

In the unlikely event that the author did not send UMI a complete manuscript and there are missing pages, these will be noted. Also, if unauthorized copyright material had to be removed, a note will indicate the deletion.

Oversize materials (e.g., maps, drawings, charts) are reproduced by sectioning the original, beginning at the upper left-hand corner and continuing from left to right in equal sections with small overlaps.

Photographs included in the original manuscript have been reproduced xerographically in this copy. Higher quality 6" x 9" black and white photographic prints are available for any photographs or illustrations appearing in this copy for an additional charge. Contact UMI directly to order.

ProQuest Information and Learning
300 North Zeeb Road, Ann Arbor, MI 48106-1346 USA
800-521-0600

DISSERTATION

MOLECULAR BASIS OF HYPOXIA-INDUCED PULMONARY VASOCONSTRICTION: ROLE OF VOLTAGE-GATED POTASSIUM CHANNELS

Submitted by

Elizabeth Ann Coppock

Department of Physiology

In partial fulfillment of the requirements

For the Degree of Doctor of Philosophy

Colorado State University

Fort Collins, Colorado

Spring 2001

COLORADO STATE UNIVERSITY

January 12, 2001

WE HEREBY ROCOMMEND THAT THE DISSERTATION PREPARED UNDER OUR SUPERVISION BY ELIZABETH COPPOCK ENTITLED MOLECULAR-BASIS FOR HYPOXIA-INDUCED PULMONARY VASOCONSTRICTION: ROLE OF VOLTAGE-GATED POTASSIUM CHANNELS, BE ACCEPTED AS FULFILLING IN PART REQUIREMENTS FOR THE DEGREE OF DOCTOR OF PHILOSOPHY.

Committee on Graduate Work

Advisor

Co-Advisor

Department Head

ABSTRACT OF DISSERTATION

MOLECULAR BASIS OF HYPOXIA-INDUCED PULMONARY VASOCONSTRICTION: ROLE OF VOLTAGE-GATED POTASSIUM CHANNELS

Pulmonary artery smooth muscle cells (PASMCs) isolated from small resistance pulmonary arteries depolarize and contract in response to hypoxia while PASMCs isolated from large conduit arteries usually do not respond. The hypoxia-induced membrane depolarization, smooth muscle cell contraction, and subsequent constriction of resistance pulmonary arteries, is thought to occur via inhibition of PASMC K^+ channels that are open at the resting membrane potential. As inhibition of these channels has been clearly implicated as an important step in hypoxic pulmonary vasoconstriction (HPV), recent attention has focused on identifying the K^+ channel(s) involved in this response. Previous studies implicated a delayed-rectifier voltage-gated K^+ (Kv) channel in both the maintenance of the resting membrane potential, and the hypoxia-induced depolarization of PASMCs from resistance arteries. Although progress has been made in identifying which Kv channel proteins are expressed in PASMCs, there are conflicting reports regarding which channels contribute to the native O_2-sensitive K^+ current. In this study, the O_2-sensitivity of cloned Kv channels, expressed in a heterologous expression system, and the expression of Kv channel α and β subunits along the pulmonary arterial tree were

were examined in order to identify, from a molecular perspective, which Kv channels are likely to contribute to the O_2-sensitive current expressed in resistance PASMCs. Additionally, since the targeting of Kv channels to lipid raft microdomains rich in signaling molecules, such as protein kinases, could represent a mechanism by which hypoxia alters Kv channel function, the targeting of the O_2-sensitive Kv channel, Kv2.1, to lipid rafts was examined in PASMCs from conduit and resistance vessels.

The effects of hypoxia on Kv1.2, Kv1.5, Kv2.1 and Kv9.3 α subunits expressed in mouse L-cells were examined using the whole-cell configuration of the patch-clamp technique. Hypoxia (PO_2 ~ 30 mmHg) reversibly inhibited Kv1.2 and Kv2.1 currents at potentials more positive than 30 mV. In contrast, hypoxia had no effect on Kv1.5 current. Currents generated by the coexpression of Kv2.1 with Kv9.3 α subunits were reversibly inhibited by hypoxia in the voltage range of the resting membrane potential as were currents generated by the coexpression of Kv1.2 and Kv1.5 α subunits. These results indicate that 1) Kv1.2 and Kv2.1, but not Kv1.5, homomeric channels are reversibly inhibited by hypoxia, 2) Kv1.2 and Kv1.5 α subunits can assemble to form a functional heteromeric channel that is sensitive to hypoxia, and 3) only the heteromeric channels, Kv1.2/Kv1.5 and Kv2.1/Kv9.3, are inhibited by hypoxia in the voltage range of the PASMC resting membrane potential, suggesting that these heteromeric channels are likely components of the native pulmonary arterial O_2-sensitive K^+ current.

In the second part of this study, expression of Kv1.2, Kv1.5, Kv2.1 and Kv3.1b was confirmed and expression of Kvβ1.1, Kvβ1.2, Kvβ1.3, but not Kvβ2.1, channel proteins was demonstrated in PASMCs from conduit and resistance vessels. Additionally, immunoblotting with densitometry was used to demonstrate that expression

levels of Kv3.1b and Kvβ1.1, Kvβ1.2 and Kvβ1.3, dramatically increases from the main conduit pulmonary artery to the small resistance pulmonary arteries where HPV is thought to occur. The expression level of Kv1.5 protein was modestly greater in resistance than in conduit PASMCs, while expression levels of both Kv1.2 and Kv2.1 channel proteins were similar between conduit and resistance PASMCs. Furthermore, mRNA levels of Kv9.3 appeared to be greater in resistance than in conduit PASMCs. The differential expression of Kv3.1b and Kv9.3 α subunits and members of the Kvβ1 subfamily suggests that they may be involved in the differential responses of conduit and resistance pulmonary arteries to hypoxia.

In the third part of the study the targeting of Kv2.1 to lipid rafts in the pulmonary artery was examined. It was demonstrated that Kv2.1 targets to lipid rafts in both conduit and resistance PASMCs. It is not likely that Kv2.1 raft association alone accounts for the differential responses of conduit and resistance pulmonary arteries to hypoxia; however, the targeting of Kv channels to these important signaling centers may prove to be a key component of PASMC O_2-sensing.

Elizabeth Ann Coppock
Department of Physiology
Colorado State University
Fort Collins, CO 80523
Spring 2001

ACKNOWLEDGEMENTS

I would like to thank my co-advisor, Dr. Alan Tucker, for sharing his knowledge and excitement about pulmonary physiology, helping to spur on my own interests in hypoxic pulmonary vasoconstriction. Thank you for giving of yourself and your time, and for your warm personality that always helped me to keep a positive outlook and attitude. I would like to thank my committee members, Drs. Ivan McMurtry, Kurt Beam and Richard Bowen, for sharing their expertise, advice and time. I would like to thank my advisor, Dr. Mike Tamkun, for being an outstanding role model, mentor and friend. Thank you for making me feel like an important part of your laboratory group and for sharing your wealth of knowledge regarding everything from molecular biology techniques and K^+ channels to the politics of science and academia to family car camping. Thank you for taking countless hours to train me, read my papers, and give heartfelt advice in both career and family decisions.

DEDICATION

It is with great pleasure that I dedicate this dissertation to my best friend and husband, Eric. Without your constant love, prayer and support this never would have been possible.

TABLE OF CONTENTS

Chapter 1

Introduction 1

Statement of the Problem 2

Specific Aims and Hypotheses 2

Specific Aim 1 4

Specific Aim 2 4

Specific Aim 3 5

References 6

Chapter 2

Review of the Literature 8

Introduction and Background 8

Hypoxic Pulmonary Vasoconstriction 9

HPV is Unique to Small Pulmonary Arteries 11

Potassium Channels in the Pulmonary Vasculature 12

Potassium Channels in HPV 14

Identification of Kv Channel Genes Involved in Pulmonary Arterial O_2-Sensing 16

Complexity and Diversity of Kv Channels 16

Recent Progress Towards the Identification of Kv Channel α Subunits Likely to Contribute to the Pulmonary Arterial O_2-Sensitive K^+ Current 18

Kv channel expression in the pulmonary vasculature 18

Antibody dissection of the O_2-sensitive K^+ current 19

O_2-sensitivity of cloned channels 20

Kv2.1 21

Kv2.1/Kv9.3 21

Kv1.5 22

Kv1.2 22

Kv1.2/Kv1.5 23

Kv3.1b 23

Summary 24

Role of the Kv β Subunit in O_2-Sensing 26

Potential Mechanisms of Kv Channel Inhibition by Hypoxia 27

Membrane Bound Heme-Linked Protein and/or NADPH Oxidase Mechanism of O_2-Sensing 28

Mitochondria as O_2-Sensors 30

Intracellular Ca^{2+} Release as a Mechanism of Kv Channel Inhibition by Hypoxia 32

Kv Channel Targeting to Lipid Rafts as a Mechanism of O_2-Sensing 33

Kv Channel Regulation by Chronic Hypoxia 33

Summary 35

Tables 36

References 37

Chapter 3

Oxygen-Sensitivity of Voltage-Gated K^+ Channels Expressed in the Pulmonary Vasculature 50

Introduction 50

Materials and Methods 52

Isolation of Bovine Pulmonary Arteries 52

Isolation of Total RNA 53

RT-PCR Analysis 54

Southern Blot Analysis 54

Northern Blot Analysis 55

Cloning of Kv9.3 and Production of the Channel cDNA Constructs 56

Transfection and Tissue Culture 57

Heteromeric Formation of Kv1.2/Kv1.5 and Kv2.1/Kv9.3 Channels 58

Electrophysiology 59

Solutions 60

Pulse Protocols and Analysis 60

Statistical Analysis 61

Results 61

mRNA Expression of Kv Channel Subunits in Bovine PASMCs 61

Cloning of Rat Kv9.3 62

O_2-Sensitivity of Kv2.1 Expressed in Mouse L-Cells 62

O_2-Sensitivity of Kv2.1/Kv9.3 Expressed in Mouse L-Cells 63

O_2-Sensitivity of Kv1.5 and Kv1.2 Homomeric Channels Expressed in Mouse L-Cells 63

O_2-Sensitivity of Kv1.2/Kv1.5 Heteromeric Channels Expressed in Mouse L-Cells 64

Discussion 65

Tables 70

Figures 72

References 78

Chapter 4

Identification, Localization and Differential Expression of Kv α and β Subunits in the Pulmonary Artery 81

Introduction 81

Materials and Methods 84

Antibodies and Fluorophores 84

Transfection and Tissue Culture 85

Isolation of Total RNA, RT-PCT and Northern Blot Analysis 85

Cloning of Bovine Kv9.3 85

Production of Anti-Kv9.3-T Antibody 86

Production of Anti-Bovine Kv1.5-T Antibody 86

Production of GST Fusion Proteins 87

Immunofluorescence Staining of Transfected Tissue Culture Cells 88

Immunostaining of Pulmonary Artery Tissue Sections 90

Preparation of PASMC Membranes 91

Western Blotting 92

Immunoprecipitation 94

Quantification of Western Blot Signals 94

Statistical Analysis 95

Results Part 1 – Antibody Characterization 95

Anti-Kv9.3 Antibody recognizes the GST/Kv9.3 N-terminus Fusion Protein and Kv9.3-Transfected L-Cells 95

Anti-Bovine Kv1.5-T Antibody Recognizes Bovine Kv1.5 Protein 96

Anti-Kv1.2-T Antibody Recognizes GST/Kv1.2 Fusion Protein And Kv1.2-Transfected L-Cells 96

Results Part 2 – Expression and Localization of Kv α and β Subunits Within the Pulmonary Artery 97

Expression of Kv2.1 in Bovine PASMCs 97

Expression of Kv9.3 in Bovine PASMCs 98

Heteromeric Formation of Kv2.1/Kv9.3 Channels in Bovine PASMCs 99

Expression of Kv1.2 in Bovine PASMCs 99

Expression of Kv1.5 in Bovine PASMCs 100

Heteromeric Formation of Kv1.2/Kv1.5 Channels in Bovine PASMCs 101

Expression of Kv3.1b in Bovine PASMCs 102

Expression of Kv β Subunits in Bovine PASMCs 103

Results Part 3 – Differential Expression of Kv α and β Subunits In Conduit and Resistance Pulmonary Arteries 105

Differential Expression of Kv α Subunits in the Pulmonary Artery.....105

Differential Expression of Kv β Subunits in the Pulmonary Artery.....107

Discussion 108

Expression of Kv Channel α Subunits in the Pulmonary Artery 108

Expression of Kv Channel β Subunits in the Pulmonary Artery 114

Study Limitations 117

Summary 119

Tables 121

Figures 123

References 153

Chapter 5

Localization of Kv2.1 to Lipid Rafts in the Pulmonary Artery 156

Introduction 156

Materials and Methods 158

Materials 158

Immunohistochemistry 158

L-Cell Raft Isolation 158

Rat and Bovine Brain Raft Isolation 159

Rat Lung Raft Isolation 160

Bovine Pulmonary Artery Smooth Muscle Cell Raft Isolation 160

Detergent-Free Raft Isolation 160

Western Blot Analysis 161

Results 161

Kv1.5 and Caveolin Expression in Bovine PASMCs 161

Localization of Kv2.1, but not Kv4.2, to Lipid Rafts in Transfected L-Cells 162

Localization of Kv2.1 to Lipid Rafts in Rat Lung 163

Determination of Kv2.1 Localization to Lipid Rafts in Bovine Conduit and Resistance PASMCs 163

Localization of Kv2.1 to Lipid Rafts in Rat and Bovine Brain 164

Localization of Kv2.1 to Lipid Rafts in Bovine Conduit and Resistance PASMCs Using a Detergent-Free Method of Raft Extraction 165

Discussion 165

Figures 171

References 180

Chapter 6

Summary and Future Directions 184

LIST OF TABLES

Chapter 2

2.1. Summary of Candidate O_2-Sensitive Kv Channels Expressed In the Pulmonary Vasculature 36

Chapter 3

3.1. PCR Primers and Conditions 70

3.2. Summary Table of the O_2-Sensitivity of Cloned Kv Channels In Mouse L-Cells 71

Chapter 4

4.1. Summary of Antibodies Tested 121

4.2. Summary of Kv Channel Expression in Conduit vs. Resistance Pulmonary Arteries 122

LIST OF FIGURES

Chapter 3

3.1. Detection of Kv α Subunit mRNA in Conduit and Resistance Bovine Pulmonary Artery 72

3.2. Comparison of Our Rat Kv9.3 Amino Acid Sequence with the Published rat Kv9.3 Amino Acid Sequence 73

3.3. Effect of Hypoxia on Kv2.1 Current Expressed in Mouse L-Cells 74

3.4. Effect of Hypoxia on Kv2.1/Kv9.3 Heteromeric Channels Expressed in Mouse L-Cells 75

3.5. Effect of Hypoxia on Kv1.5 and Kv1.2 Current Expressed in Mouse L-Cells 76

3.6. Effect of Hypoxia on Kv1.2/Kv1.5 Heteromeric Channels Expressed in Mouse L-Cells 77

Chapter 4

4.1. Amino Acid Sequence Alignment of Bovine Kv9.3 with Rat Kv9.3 123

4.2. Amino Acid Sequence Alignment of Bovine, Human, Rat and Rabbit Kv1.5 α Subunits 124

4.3. Western Blot Analysis of GST/Kv9.3 N-Terminus Fusion Protein 125

4.4. Kv9.3 Immunostaining of Transfected L-Cells 126

4.5. Kv1.5 Western Blot Analysis and Corresponding Peptide Block 127

4.6. Western Blot Analysis of Kv1.2 and Corresponding GST Block 128

4.7. Kv1.2 Immunostaining of Transfected L-Cells 129

4.8. Western Blot Analysis of Kv2.1 Expression in Bovine Conduit and Resistance PASMCs 130

4.9. Kv2.1 Immunostaining of Transfected L-Cells 131

4.10. Immunolocalization of Kv2.1 in Tissue 132

4.11. Northern Blot Analysis of Kv9.3 mRNA Expression in Bovine Conduit and Resistance PASMCs, Rat Lung and Rat Brain 133

4.12. Immunolocalization of Kv1.2 α Subunit in Bovine Resistance Pulmonary Arteries 134

4.13. Immunolocalization of Kv1.2 α Subunit and α Smooth Muscle Actin In Bovine Conduit and Resistance Pulmonary Arteries 135

4.14. Western Blot Analysis of Kv1.2 Protein Expression in Rat Brain And Bovine Conduit and Resistance PASMCs 136

4.15. Western Blot Analysis of Kv1.5 Protein Expression in Bovine Conduit and Resistance PASMCs 137

4.16. Kv1.5 Immunostaining of Transfected L-Cells 138

4.17. Immunolocalization of Kv1.5 α Subunit in Bovine Resistance Pulmonary Arteries 139

4.18. Immunolocalization of Kv1.5 α Subunit and α Smooth Muscle Actin In Bovine Conduit and Resistance Pulmonary Arteries 140

4.19. Western Blot Analysis of Kv3.1b Protein Expression in Bovine Conduit and Resistance PASMCs 141

4.20. Western Blot Analysis of Kv β Subunit Expression in Bovine Conduit and Resistance PASMCs 142

4.21. Immunolocalization of Kvβ1.2 in Bovine Resistance Pulmonary Arteries 143

4.22. Immunolocalization of Kvβ1.2 and α Smooth Muscle Actin In Bovine Conduit and Resistance Pulmonary Arteries 144

4.23. Western Blot Analysis of Kv α Subunit Expression in the Pulmonary Artery 145

4.24. Bar Graph Highlighting the Differences in Kv α Subunit Expression Between Conduit and Resistance PASMCs 146

4.25. Immunolocalization of Kv1.2 α Subunit in the Bovine Pulmonary Artery 147

4.26. Immunolocalization of Kv1.5 α Subunit in the Bovine Pulmonary Artery 148

4.27. Northern Blot Analysis of Kv9.3 mRNA Expression in the Bovine Pulmonary Artery 149

4.28. Western Blot Analysis of Kv β Subunit Expression in the Pulmonary Artery 150

4.29. Bar Graph Highlighting the Differences in Kv β Subunit Expression Between Conduit and Resistance PASMCs 151

4.30. Immunolocalization of Kvβ1.2 Subunit in the Bovine Pulmonary Artery 152

Chapter 5

5.1. Immunolocalization of Caveolin and Kv1.5 to Bovine Conduit and Resistance Pulmonary Arteries 171

5.2. Sucrose Density Gradient Centrifugation of 1% Triton X-100-Solubilized Extracts from Mouse L-Cells Stably Expressing Kv2.1 or Kv4.2 172

5.3. Sucrose Density Gradient Centrifugation of detergent-free Solubilized Extracts from Mouse L-Cells Stably Expressing Kv2.1 173

5.4. Sucrose Density Gradient Centrifugation of 1% & 0.5% Triton X-100-Solubilized Extracts from Rat Lung Lysates..... 174

5.5. Sucrose Density Gradient Centrifugation of 1% & 0.5% Triton X-100-Solubilized Extracts from Bovine Conduit PASMC Lysates..... 175

5.6. Sucrose Density Gradient Centrifugation of 1% & 0.2% Triton X-100-Solubilized Extracts from Bovine Resistance PASMC Lysates..... 176

5.7. Sucrose Density Gradient Centrifugation of 1% Triton X-100-Solubilized Extracts from Rat Brain Lysates.....177

5.8. Sucrose Density Gradient Centrifugation of 1% & 0.5% Triton X-100-Solubilized Extracts from Bovine Brain Lysates 178

5.9. Sucrose Density Gradient Centrifugation of Detergent-Free Solubilized Extracts from Bovine Conduit and Resistance PASMC Lysates 179

CHAPTER 1

INTRODUCTION

Pulmonary hypertension (PHT) is a potentially devastating complication of a variety of respiratory diseases and of chronic high altitude exposure. The most common cause of PHT is chronic alveolar hypoxia and the associated hypoxic pulmonary vasoconstriction (HPV) (13). Chronic hypoxic exposure, induced experimentally, caused by residence at high altitude, or associated with lung disease, leads to pathological changes within the pulmonary vascular tree, termed vascular remodeling, which ultimately maintain PHT in the absence of hypoxia (13). Oxygen therapy, return to low altitude, and/or treatment with vasodilators do not necessarily reverse or even substantially limit disease progression remodeling has occurred (5). Consequently, established PHT often results in death due to heart failure.

The initiating event in chronic hypoxic PHT appears to be sustained HPV. Since the closing of pulmonary arterial smooth muscle cell (PASMC) O_2-sensitive potassium channels is implicated as an important first-step in this cascade of events, a clearer understanding of the molecular nature of these O_2-sensitive channels will aid in the development of more specifically targeted therapies.

STATEMENT OF THE PROBLEM

Many studies implicate delayed-rectifier voltage-gated potassium channels in both the maintenance of the resting membrane potential, and the hypoxia-induced depolarization of PASMCs. These channels have been described based on their biophysical and pharmacological properties; however, both the precise identity of these channels, and the mechanism by which they "sense" hypoxia in the pulmonary circulation is unknown. Therefore, the purpose of this study was to examine, from a molecular perspective, which specific Kv channels are responsive to hypoxia and their cellular and subcellular localization within the pulmonary vasculature.

SPECIFIC AIMS AND HYPOTHESES

Based on the work of several independent investigators, Kv1.2, Kv1.5, Kv2.1, Kv3.1 and Kv9.3 α subunits are likely to be molecular components of the O_2-sensitive potassium current within the pulmonary vasculature. However, because of the contradictions within the literature and some of the limitations of previous studies, their role in O_2-sensing needs to be examined more fully. For instance, while Kv1.5 is considered by some to be an important player in HPV (3,16), this channel has been discounted by others unable to detect its expression within the pulmonary vasculature (7). Furthermore, a significant amount of work in this field has utilized cultured PASMCs (14,16). A potential problem with studies of vascular smooth muscle in short-tem cultures is that, with time, myocytes show alterations in the expression of outward currents (7).

In PASMCs isolated from resistance vessels, hypoxia leads to membrane depolarization (6), an increase in intracellular Ca^{2+} concentration (10), contraction (6,10), and subsequent constriction of resistance pulmonary arteries (2,6,9,15), but has little or no effect on conduit PASMCs (6,10). Proposed mechanisms for the contrasting vasoactive response to hypoxia between conduit and resistance pulmonary arteries includes differential expression of Kv channel α subunits (2); however, this has not been examined on a molecular level. Furthermore, although recent studies suggest a role for Kv β subunits in O_2-sensing (4,8), protein expression of Kv β subunits within the pulmonary vasculature has not been studied. A general theme in modern biology is that signaling molecules, e.g. protein kinases, are localized near their specific substrates in order to maximize signaling and minimize cross-talk between systems. The localization of numerous signaling proteins, tyrosine kinases, nitric oxide synthase, protein kinase C, and G-proteins, to caveolae and caveolae-like domains (1) is one example of this compartmentalization. Furthermore, like hypoxia, tyrosine kinase inhibitors have been shown to markedly inhibit whole cell K^+ current with no other effects on channel kinetics (11). Recently the tyrosine kinase pathway has been implicated as playing a role in HPV (12). It is possible that targeting of K^+ channels to lipids rafts and their associated signaling molecules represents a mechanism by which hypoxia alters Kv channel function. Therefore, targeting of pulmonary arterial Kv channels to lipid rafts within the pulmonary vasculature must be examined.

Specific Aim 1: To determine the oxygen sensitivities of cloned channels, Kv1.2, Kv1.5, Kv2.1, Kv1.2/Kv1.5 and Kv2.1/Kv9.3, expressed in a heterologous expression system.

Hypothesis: One or more Kv channel currents will be significantly inhibited by hypoxia when expressed in a heterologous expression system.

Cloned channels will be expressed in mouse L-cells and assayed for sensitivity to hypoxia using the whole-cell method of the patch-clamp technique.

Specific Aim 2: To determine the expression of Kv1.2, Kv1.5, Kv2.1, Kv3.1b, Kv9.3, Kvβ1.1, Kvβ1.2, Kvβ1.3 and Kvβ2.1 subunits in PASMCs and, if they are expressed, to compare their cellular localization and expression levels between conduit and resistance pulmonary arteries. Furthermore, to examine heteromeric assembly between Kv1.2 and Kv1.5 α subunits, and between Kv2.1 and Kv9.3 α subunits, in the pulmonary vasculature.

Hypotheses: Kv1.2, Kv1.5, Kv2.1, Kv3.1b and Kv9.3 are expressed in PASMCs and one or more of these subunits is differentially expressed between conduit and resistance PASMCs (resistance greater than conduit). One or more Kv β subunit(s) is expressed in PASMCs and this expression differs between conduit and resistance PASMCs. Kv1.2/Kv1.5 and/or Kv2.1/Kv9.3 heteromeric channels are expressed in PASMCs.

Immunohistochemistry, immunoblotting, RT-PCR and Northern blotting will be used to assay protein and mRNA expression of Kv α and β subunits in bovine PASMCs. Differences in protein expression between conduit and resistance PASMCs will be determined via Western blot analysis and densitometry. Heteromeric channel assembly will be examined using immunoprecipitation techniques.

Specific Aim 3: To examine the possibility of Kv2.1 channel localization to lipid rafts within the pulmonary vasculature.

Hypothesis: Kv2.1 is localized to a lipid raft in resistance PASMCs but not in conduit PASMCs.

Kv2.1 will be examined for raft association in bovine conduit and resistance PASMCs using both a detergent and non-detergent based extraction method.

REFERENCES

1. Anderson RG. The caveolae membrane system. *Annu Rev Biochem* 67: 199-225, 1998.

2. Archer SL, Huang JM, Reeve HL, Hampl V, Tolarova S, Michelakis E, and Weir EK. Differential distribution of electrophysiologically distinct myocytes in conduit and resistance arteries determines their response to nitric oxide and hypoxia. *Circ Res* 78: 431-442, 1996.

3. Archer SL, Souil E, Dinh-Xuan AT, Schremmer B, Mercier JC, El Yaagoubi A, Nguyen-Huu L, Reeve HL, and Hampl V. Molecular identification of the role of voltage-gated K^+ channels, Kv1.5 and Kv2.1, in hypoxic pulmonary vasoconstriction and control of resting membrane potential in rat pulmonary artery myocytes. *J Clin Invest* 101: 2319-2330, 1998.

4. Gulbis JM, Mann S, and MacKinnon R. Structure of a voltage-dependent K^+ channel beta subunit. *Cell* 97: 943-952, 1999.

5. Kennedy TP, Michael JR, and Summer W. Calcium channel blockers in hypoxic pulmonary hypertension. *Am J Med* 78: 18-26, 1985.

6. Madden JA, Dawson CA, and Harder DR. Hypoxia-induced activation in small isolated pulmonary arteries from the cat. *J Appl Physiol* 59: 113-118, 1985.

7. Patel AJ, Lazdunski M, and Honore E. Kv2.1/Kv9.3, a novel ATP-dependent delayed-rectifier K^+ channel in oxygen-sensitive pulmonary artery myocytes. *EMBO J* 16: 6615-6625, 1997.

8. Perez-Garcia MT, Lopez-Lopez JR, and Gonzalez C. Kvbeta1.2 subunit coexpression in HEK293 cells confers O_2 sensitivity to Kv4.2 but not to Shaker channels. *J Gen Physiol* 113: 897-907, 1999.

9. Post JM, Gelband CH, and Hume JR. $[Ca^{2+}]_i$ inhibition of K^+ channels in canine pulmonary artery. Novel mechanism for hypoxia-induced membrane depolarization. *Circ Res* 77: 131-139, 1995.

10. Sham JS, Crenshaw BR, Jr., Deng LH, Shimoda LA, and Sylvester JT. Effects of hypoxia in porcine pulmonary arterial myocytes: roles of K(V) channel and endothelin-1. *Am J Physiol Lung Cell Mol Physiol* 279: L262-L272, 2000.

11. Sobko A, Peretz A, and Attali B. Constitutive activation of delayed-rectifier potassium channels by a src family tyrosine kinase in Schwann cells. *EMBO J* 17: 4723-4734, 1998.

12. Uzun O, Demiryurek AT, and Kanzik I. The role of tyrosine kinase in hypoxic constriction of sheep pulmonary artery rings. *Eur J Pharmacol* 358: 41-47, 1998.

13. Vender RL. Chronic hypoxic pulmonary hypertension. Cell biology to pathophysiology. *Chest* 106: 236-243, 1994.

14. Wang J, Juhaszova M, Rubin LJ, and Yuan XJ. Hypoxia inhibits gene expression of voltage-gated K^+ channel alpha subunits in pulmonary artery smooth muscle cells. *J Clin Invest* 100: 2347-2353, 1997.

15. Yuan XJ, Tod ML, Rubin LJ, and Blaustein MP. Contrasting effects of hypoxia on tension in rat pulmonary and mesenteric arteries. *Am J Physiol* 259: H281-H289, 1990.

16. Yuan XJ, Wang J, Juhaszova M, Golovina VA, and Rubin LJ. Molecular basis and function of voltage-gated K^+ channels in pulmonary arterial smooth muscle cells. *Am J Physiol* 274: L621-L635, 1998.

CHAPTER 2

REVIEW OF THE LITERATURE

INTRODUCTION AND BACKGROUND

Membrane potassium channels play an essential role in cellular homeostasis and nerve and muscle excitability. In vascular smooth muscle, voltage-gated potassium channels are integral in the regulation of membrane potential and, therefore, vascular tone (43,62). Closure of vascular smooth muscle cell (VSMC) K^+ channels, open at the resting membrane potential, causes membrane depolarization. This change in membrane potential activates voltage-gated Ca^{2+} channels, leading to an increase in intracellular calcium concentration, and vasoconstriction (62). Activation of VSMC K^+ channels leads to hyperpolarization, inhibition of voltage-gated Ca^{2+} channels and vasodilation (62). Vascular smooth muscle cells have a high input resistance; therefore, even a small change in K^+ channel activity can have a significant effect on membrane potential and consequently vascular tone (62,95). Indeed, many factors which modulate vessel tone do so through activating or inhibiting VSMC K^+ channels (43,62,95). This review will focus on the pulmonary arterial VSMC K^+ channels thought to be inhibited by hypoxia leading to pulmonary vasoconstriction.

In the systemic circulation, small arteries dilate in response to low levels of oxygen (hypoxia) in order to increase oxygen delivery to the tissues. In contrast,

small resistance arteries in the pulmonary circulation constrict in response to alveolar hypoxia, a process known as hypoxic pulmonary vasoconstriction (HPV) (98). In the fetal circulation, HPV contributes to the high pulmonary arterial resistance, diverting placental blood through the ductus arteriosus (57). In the adult, HPV reduces the flow of blood through atelectatic or underventilated areas of the lung where ventilation is not adequate for oxygenation (57). In this manner, acute HPV is a mechanism that helps to match perfusion to ventilation, diverting blood flow away from poorly ventilated portions of the lung in order to maximize arterial saturation (111). When only a small region of the lung is hypoxic, HPV can occur without a significant effect on pulmonary arterial pressure (61). However, if hypoxia is generalized, as seen with many lung diseases and with high altitude exposure, the subsequent pulmonary vasoconstriction causes an increase in pulmonary arterial pressure, which can potentially lead to pulmonary hypertension, heart failure, and death (35).

Hypoxic Pulmonary Vasoconstriction

Since first described by Von Euler and Liljestrand in 1946 (107), HPV has been extensively studied. However, the exact mechanisms underlying HPV remain unknown. Although endothelial-derived vasoactive factors are clearly important and appear to be necessary for the full expression of HPV *in vivo* (for review see Ward and Aaronson (109)), it seems likely that HPV is initiated, at least partially, through a mechanism intrinsic to pulmonary arterial smooth muscle cells (PASMCs). Responsiveness to acute hypoxia has been demonstrated not only in isolated lungs

(39,56,75,106), but in pulmonary arterial rings denuded of endothelium (4,38,50,117), and in single PASMCs (4,17,28,51,65,71,74,75,116).

It is currently hypothesized that alveolar hypoxia acts to directly depolarize the PASMC membrane, thus causing an influx of Ca^{2+} through L-type voltage-gated Ca^{2+} channels and subsequent contraction. Indeed, in isolated PASMCs, acute hypoxia has been shown to significantly depolarize the membrane potential by about 15-20 mV (4,32,50,116) leading to contraction of individual PASMCs (51). In 1976, McMurtry and coworkers were the first to demonstrate that HPV is inhibited by the voltage-gated Ca^{2+} channel antagonists, verapamil and SKF 525, in the isolated perfused lung (56). They (55) and others (100) also demonstrated that HPV is potentiated by BAY K 8644, a calcium channel agonist. In 1985, Harder et al were the first to demonstrate that the hypoxia-induced constriction of small pulmonary arteries (<300 μm) was associated with membrane depolarization which could be inhibited by verapamil (38). More recently, Salvaterra and Goldman, using isolated adult PASMCs (85), and Cornfield et al using isolated fetal PASMCs (17), demonstrated that the hypoxia-induced increase in intracellular Ca^{2+} was inhibited by L-type Ca^{2+} channel blockers. These studies clearly illustrate the importance of Ca^{2+} influx through membrane voltage-gated Ca^{2+} channels in HPV. Indeed, Franco-Obregon and Lopez-Barneo have shown that hypoxia causes a potentiation of the Ca^{2+} current in the majority of cells isolated from rabbit resistance pulmonary arteries (28). However, since these channels are relatively inactive at the resting membrane potential of PASMCs (28), it is likely that hypoxia acts first to depolarize the membrane by inhibiting the K^+ channels involved in setting the resting membrane

potential (111). Hypoxic inhibition of K^+ channels was first demonstrated in 1988 by Lopez-Barneo and coworkers in carotid body type I cells (48). Later, Hume and coworkers showed that hypoxia causes both an inhibition of whole cell K^+ current and membrane depolarization in isolated PASMCs (75). An alternative, or perhaps additional hypothesis, is that hypoxia causes the release of Ca^{2+} from intracellular stores independent of Ca^{2+} influx and that this rise in intracellular Ca^{2+} leads to inhibition of membrane Kv channels (32,42,74). Additionally, Ca^{2+} sensitivity may be increased in HPV (109). The relative importance of these mechanisms is not clear, however, the aforementioned studies suggest that hypoxia acts through multiple pathways to induce pulmonary vasoconstriction.

Hypoxic Vasoconstriction is Unique to Small Pulmonary Arteries

Vascular smooth muscle cells (VSMCs) show different responses to hypoxia according to the size and type of vessel from which they were isolated. Small resistance pulmonary arteries (3^{rd} intrapulmonary artery branches or greater) constrict in response to hypoxia (4,50,74,117), while large, conduit pulmonary arteries (main pulmonary artery and right and left branches) usually do not respond, or dilate slightly (4,50,74), although hypoxic responses have been described in some preparations (40,117). In addition, the response of small pulmonary arteries is in marked contrast to that of small arteries isolated from the systemic circulation, which dilate in response to hypoxia (117). At the single cell level, hypoxia causes small contractions (50,90) and increased intracellular Ca^{2+} (90) in resistance PASMCs, but has little or no effect in conduit PASMCs or VSMCs isolated from small systemic arteries (50,90). Furthermore, hypoxia causes a significant depolarization of the

membrane potential from approximately –51 mV to –37 mV in resistance PASMCs, while in conduit PASMCs the membrane potential is not significantly affected (50). Proposed mechanisms for the contrasting vasoactive response to hypoxia between conduit and resistance pulmonary arteries and vessels from other vascular beds include differential expression of an O_2-sensitive K^+ channel, (1,4), differential expression of an O_2-sensitive L-type Ca^{2+} channel (26,29), and/or the presence of distinct O_2-sensing mechanisms.

Potassium Channels in the Pulmonary Vasculature

Four main classes of potassium channels have been described in vascular smooth muscle based on their biophysical and pharmacological properties: ATP-sensitive (K_{ATP}), inward rectifier (K_{IR}), large-conductance Ca^{2+}-activated K^+ (BK_{Ca}) and voltage-gated (Kv) (95){(43). Of these, the Kv channels are most likely to control the PASMC membrane potential and thus regulate vessel tone (24,115).

ATP-sensitive K^+ channels are sensitive to changes in levels of intracellular adenosine triphosphate (ATP) and are, therefore, regulated by cellular metabolic status (44,62). K_{ATP} currents are enhanced by ADP and inhibited by ATP. The antidiabetic sulfonylurea drugs, such as glibenclamide, inhibit this channel, while antihypertensive drugs such as minoxidil activate this channel (62). These channels probably do not contribute to HPV, as glibenclamide has no effect on pulmonary perfusion pressure in normoxia or moderate hypoxia (39). However, these channels may serve as an important negative feedback mechanism, preventing excessive HPV under conditions of severe hypoxia, when ATP levels are reduced (113).

Furthermore, blockade of the endothelin subtype A receptor leads to activation of K_{ATP} channels and subsequent inhibition of HPV (86).

Inward rectifier channels conduct maximum current at membrane potentials negative to the K^+ equilibrium potential (E_K) and smaller outward currents at membrane potentials positive to the E_K (62). This channel is very sensitive to inhibition by extracellular Ba^{2+}. The presence of these channels in the pulmonary vasculature has not as yet been confirmed.

BK_{Ca} channels are sensitive to both membrane depolarization and increases in intracellular Ca^{2+}, with increasing Ca^{2+} levels essentially shifting the activation curve in the hyperpolarizing direction. BK_{Ca} channels have a single-channel conductance of 250 pS in symmetrical K^+ and are sensitive to block by tetraethylammonium (TEA), charybdotoxin (CTX) and iberiotoxin (62). BK_{Ca} channels play a role in the control of arterial smooth muscle membrane potential by serving as a negative feedback mechanism, regulating the degree of membrane depolarization and the constriction induced by increased cytoplasmic Ca^{2+} (15,62). PASMC BK_{Ca} channels are activated at membrane potentials positive to the resting membrane potential (which explains why CTX does not depolarize PASMCs (4,65,115)); thus, under conditions of hypoxia, it is likely that the membrane depolarization and increased $[Ca^{2+}]_i$ activate BK_{Ca} channels leading to membrane hyperpolarization (77). Therefore, it is more likely that BK_{Ca} channels prevent excessive HPV rather than initiate it.

All vascular smooth muscle cells examined to date have at least one component of voltage-sensitive K^+ current, and many studies report more than one

type of current (62). These currents include "delayed rectifier" (IK_{DR}) and "transient outward" (IK_{TO}) types (15). Recently, a third non-inactivating Kv current (IK_N), which is activated at the resting membrane potential, has also been described in rabbit, rat and pig PASMCs (25,64,65). These channels provide an important K^+ channel conductance in the physiological membrane potential range of pulmonary arteries (62). Indeed, several groups of investigators have shown that the membrane potential in PASMCs is controlled by one or more subtypes of K_{DR} (4,63,65,93,119). Pharmacologically, most Kv currents can be isolated by selective inhibition to 4-aminopyridine (4-AP). Outward K^+ current in PASMCs is inhibited by low-doses of 4-AP (4,63), but not by TEA (4) or CTX (4). In addition, 4-AP (4,65,115,119), but not TEA (4,65), CTX (4,65,115), iberiotoxin (65), or glibenclamide (115), depolarizes PASMCs. Furthermore, exposure to 4-AP, but not glibenclamide or CTX, leads to an increase in $[Ca^{2+}]_i$ (20). Taken together, these studies clearly emphasize the importance of Kv channels in the regulation of PASMCs membrane potential and pulmonary arterial tone.

Potassium Channels in HPV

Agents which block K^+ channels, such as 4-AP and TEA, depolarize the membrane (4,74,115), increase tension in pulmonary arterial rings (4,75), and increase pulmonary arterial pressure in isolated perfused lungs (39). Hypoxia acts in a similar manner to inhibit whole-cell outward K^+ current (4,74,75), cause membrane depolarization (4,75,116), constriction of small pulmonary arteries (4), and an increase in pulmonary artery pressure (39). The fact that PASMC membrane depolarization and pulmonary artery constriction can be mimicked by K^+ channel

blockers suggests that the depolarization induced by hypoxia is due to inhibition of K^+ channels open at the resting membrane potential.

Two types of PASMC K^+ channels have been suggested to be modulated by hypoxia leading to HPV, BK_{Ca} (70,75) and Kv (which includes IK_{DR} and IK_N); however, the majority of electrophysiological and pharmacological evidence points to members of the Kv family as the main PASMC O_2-sensors (see McCulloch et al for further review (54)). The O_2-sensitive K^+ current described in most rat PASMC preparations is a delayed-rectifier, which is sensitive to 4-AP and insensitive to CTX (7). Indeed, hypoxic-inhibition of PASMC K_{DR} current has been shown in whole-cell and single-channel studies in the presence of BK_{Ca} channel inhibitors (4,66). Furthermore, hypoxia and 4-AP constrict resistance arteries, while CTX has no effect (4). In addition, pretreatment of isolated dog PASMCs with 4-AP (1 mM), but not TEA (1 mM), prevents the hypoxic effect on outward K^+ current (74). Taken together, these data suggest that Kv channels that exhibit delayed-rectifier currents, and are sensitive to 4-AP but insensitive to CTX, are responsible for the O_2-sensitive K^+ current in PASMCs. However, pretreatment with 4-AP does not always prevent, and may even potentiate, hypoxic constriction, as has been demonstrated in rat and dog lungs (8,39), rat resistance pulmonary arteries (4), and in isolated pig PASMCs (90). While these studies seem to argue against a role for Kv channels in HPV, several points need to be considered. For instance, increased sensitivity to hypoxia has been demonstrated after an initial priming depolarization (101), and in the presence of agonist-induced pretone (110). Therefore, in some cases, pretreatment with 4-AP may act as a priming agent, causing decreased background K^+

permeability and a potentiation of the hypoxic response. Additionally, as 4-AP sensitivity varies between Kv channel subtypes and between species (18), the use of 4-AP as a pharmacological tool for determining the O_2-sensitive K^+ current is limited. For instance, the heteromeric Kv2.1/Kv9.3 channel, which is a good candidate for at least one O_2-sensitive K^+ current, is insensitive to 4-AP at 1-10 mmol/l (71), the concentration used in the above mentioned studies where 4-AP did not attenuate hypoxic constriction. Therefore, it is likely that the pulmonary arterial O_2-sensitive K^+ current represents an ensemble of current from distinct Kv channel isoforms, some of which may be 4-AP insensitive. Additionally, the variability in the 4-AP sensitivity of the hypoxia response may be due to species specific α subunit combinations responsible for the hypoxia sensitive current. Thus, the variable response to hypoxia in the presence of 4-AP does not exclude a role for Kv channels in HPV. Given that the majority of published studies suggest the involvement of a voltage-sensitive K^+ current in PASMC O_2-sensing, the remainder of this review will focus on the role of Kv channels in HPV.

IDENTIFICATION OF Kv CHANNEL GENES INVOLVED IN PULMONARY ARTERIAL O_2-SENSING

Complexity and Diversity of Kv Channels

The first complete nucleotide sequence encoding a voltage-gated K^+ channel was reported in 1987 with the cloning of the *Drosophila Shaker* channel (67). Low stringency screening of *Drosophila* cDNA libraries with the *Shaker* cDNA, led to the isolation of K^+ channel cDNAs, *Shab, Shal* and *Shaw*, derived from three distinct *Drosophila* genes (11). The sequences are homologous to *Shaker* having

approximately 40% identity. Each *Drosophila* gene has been shown to have one or more mammalian homologues (84), currently grouped into the Kv1, Kv2, Kv3 and Kv4 subfamilies. The Kv1 family, which has greater than 60% homology to *Shaker* in the core region, is the largest with at least 7 members (13). In addition to the 4 mammalian subfamilies relating to *Shaker, Shab, Shal* and *Shaw*, 5 additional subfamilies (Kv5-9) have also been described {Salinas, Duprat, et al. 1997 386 /id}. Currently, over 30 Kv channels have been cloned and expressed in heterologous expression systems (13). These channels often display differences in voltage sensitivity, current kinetics and steady state activation and inactivation (84).

Kv channels exist as tetramers formed by four, six transmembrane spanning α subunits combining to form a functional channel (49). Not only can identical α subunits combine to form a functional channel, but distinct α subunits can also combine to form functional heteromeric channels both *in vitro* and *in vivo* (14,83,91). These heteromeric channels have unique properties that often represent a blend of the observed properties of the corresponding homomeric channels. Furthermore, several Kv α subunits are nonfunctional when expressed alone. For example, the Kv9.3 subunit, the most recently identified member of the mammalian Kv family, does not form a functional homomeric channel itself, but rather functions only in heteromeric complexes where it confers altered voltage sensitivity and activation kinetics (71).

Accessory β subunits can combine with Kv α subunits to add even more diversity to Kv channel function (37). Currently, four Kv β subunit gene families have been described (22,23,27,58,79). All are cytoplasmic proteins, approximately 40 kDa in mass, with a conserved core sequence and variable N termini. Kv β

subunits have been shown to confer functional effects onto α subunits, including both fast and slow inactivation, altered voltage-sensitivity, and slowed deactivation (59,104). Additionally, the β subunit may play a role as a cellular redox sensor for it appears to confer O_2-sensitivity upon the Kv4.2 channel in heterologous expression systems (73). Thus, the roles of Kv β subunits are many and indeed they may be important not only in the functional modulation of Kv α subunits, but also in the PASMC response to hypoxia.

Recent Progress Towards the Identification of Kv Channel α Subunits Likely to Contribute to the Pulmonary Arterial O_2-Sensitive K^+ Current

Although the electrophysiological and pharmacological profile of the O_2-sensitive currents in the pulmonary artery has been extensively characterized, the molecular nature of this current is only starting to be elucidated. Beginning in 1997, several groups of investigators examined the expression of Kv channels in the pulmonary artery, antibody dissection of PASMC whole-cell K^+ current, and the O_2-sensitivity of cloned Kv channels expressed in heterologous expression systems, in an attempt to identify the molecular components of the O_2-sensivite Kv current in PASMCs.

Kv channel expression in the pulmonary vasculature

Yuan and coworkers used reverse transcription polymerase chain reaction (RT-PCR) and immunoblotting to show that Kv1.5 and Kv1.2 mRNA and protein were expressed in primary cultures of rat PASMCs (108). Patel et al, using degenerate RT-PCR, detected mRNA expression of Kv1.2, Kv1.3, Kv2.1 and a novel Kv channel α subunit, Kv9.3, in rat PASMCs. Despite several approaches, these

investigators failed to detect Kv1.5 and thus concluded it was not expressed in the rat pulmonary artery (71). Archer and colleagues, using immunohistochemistry and immunoblotting of dissociated rat resistance PASMCs, reported expression of Kv1.1, Kv1.2, Kv1.3, Kv1.5 and Kv2.1, but not Kv1.4 (6). About the same time, Yuan and coworkers, using RT-PCR of primary cultures of rat PASMCs, confirmed expression of Kv1.1, Kv1.2, Kv1.5, Kv1.6, Kv2.1, and Kv9.3 mRNA and reported mRNA expression of Kv1.4 (120). Using immunoblotting, they detected Kv1.2, Kv1.4, Kv1.5, but not Kv1.3 (120). Hulme et al detected expression of Kv1.2 and Kv1.5 in PASMCs from rat lung tissue sections (41). Most recently, Osipenko et al reported expression of Kv3.1b protein in freshly dissociated PASMCs from rats and rabbits using immunocytochemistry (66). Additionally, our group has data showing that Kv1.2, Kv1.5, Kv2.1, Kv9.3, and Kv3.1b subunits are expressed in bovine resistance PASMCs (unpublished observations). Taken together, these results strongly suggest the expression of the following α subunits in resistance PASMCs: Kv1.2, Kv1.5, Kv2.1, Kv3.1b, Kv9.3 (see Table 1). Not as convincingly, the presence of Kv1.1, Kv1.4 and Kv1.6 is also suggested.

Antibody dissection of the O_2-sensitive K^+ current

Recently, antibodies against Kv channels have been utilized in the intracellular patch pipette solution in an attempt to dissect the O_2-sensitive K^+ current in PASMCs during whole-cell recordings in normoxic and hypoxic conditions. When Archer and coworkers added anti-Kv2.1 to the patch pipette, they found inhibition of outward K^+ current and membrane depolarization in rat resistance PASMCs, suggesting that Kv2.1 plays a role in setting the resting membrane potential (6).

When anti-Kv1.5 was added to the patch pipette, whole cell K^+ current was significantly decreased and both the hypoxia and 4-AP-induced increase in intracellular Ca^{2+} concentration of isolated PASMCs was attenuated (6). However, anti-Kv1.5 did not consistently depolarize the membrane in isolated PASMCs. Based on their findings, the Archer group hypothesized that hypoxic inhibition of Kv2.1 leads to membrane depolarization which shifts the resting membrane potential into a range where Kv1.5 is active and can thus be inhibited by hypoxia, leading to further inhibition of whole cell K^+ current (6). Somewhat contrary to these results, others found that application of anti-Kv1.5 in the patch pipette increased intracellular Ca^{2+} concentration and caused membrane depolarization in rat PASMCs (32). Additionally, subsequent hypoxic challenge resulted in a further increase in intracellular Ca^{2+} with no effect on membrane potential. In related studies, Conforti et al used an antibody against Kv1.2 in the patch pipette in order to specifically inhibit Kv1.2 current from the whole cell current in rat pheochromocytoma (PC12) cells (a model for oxygen-sensing in the carotid body) (16). When exposed to hypoxia, they found no additional K^+ current inhibition suggesting that the Kv1.2 current was responsible for the hypoxic effect in PC12 cells (16).

O_2-sensitivity of cloned channels

The O_2-sensitivity of several cloned Kv channels has recently been studied in heterologous expression systems. Investigators have primarily focused on those channels, which when expressed in heterologous expression systems, meet the profile of the PASMC O_2-sensitive current: delayed-rectifier, sensitive to 4-AP and insensitive to CTX.

Kv2.1. Patel et al examined the O_2-sensitivity of Kv2.1 expressed in COS-7 cells (71). In a subset of COS cells, Kv2.1 (21% of cells) was reversibly inhibited by hypoxia by 34% (71). Hulme et al found similar results with Kv2.1 in mouse L-cells (41). Hypoxia significantly inhibited Kv2.1 current by 23% at 60 mV in nearly all of the cells studied. In both studies, only the Kv2.1 currents that were activated at more positive potentials, were significantly inhibited by hypoxia. Furthermore, little Kv2.1 current was detected at potentials more negative than –20 mV. In contrast, Conforti et al found Kv2.1 current to be O_2-insensitive when expressed in *Xenopus* oocytes (16). These data indicate that Kv2.1 is sensitive to hypoxia, at least in some expression systems. However, this sensitivity does not occur in the voltage range of the resting membrane potential of native PASMCs.

Kv2.1/Kv9.3. Patel et al cloned a novel subunit, Kv9.3, which does not form a functional channel itself, but combines with Kv2.1, as evidenced by immunoprecipitation from metabolically-labeled *Xenopus* oocytes and altered Kv2.1 biophysical and pharmacological properties (71). Most importantly, Kv9.3 causes a shift in the voltage dependence of activation into the voltage range of the resting membrane potential of PASMCs (41,71), suggesting that the Kv2.1/Kv9.3 heteromeric channel may contribute to the regulation of PASMC resting membrane potential and thus the PASMC O_2-sensitive K^+ current. In fact, in a subset of COS cells (56% of cells), Kv2.1/Kv9.3 current was reversibly inhibited by hypoxia by 28% (71). Hulme et al found similar results when Kv2.1/Kv9.3 was expressed in mouse L-cells. Hypoxia reversibly inhibited the Kv2.1/Kv9.3 current by 21% at 60 mV in all cells studied (41). In support of the role for Kv2.1/Kv9.3 current in the

physiological response of PASMCs to hypoxia, Kv2.1/Kv9.3 current was found to be sensitive to hypoxia in the voltage range of the PASMC resting membrane potential (41,71).

Kv1.5. The results from studies utilizing anti-Kv1.5 antibodies in the patch pipette have led some investigators to hypothesize that Kv1.5 is an important component of the O_2-sensitive current in the pulmonary artery (6). Furthermore, Kv1.5 meets the profile of the O_2-sensitive current in PASMCs: delayed rectifier, sensitive to 4-AP and insensitive to CTX (34). However, Kv1.5 is not sensitive to hypoxia when expressed as a homotetramer in L-cells (41), COS-7 cells (66) or MEL cells (66). Therefore, it is unlikely that Kv1.5 homomeric channels contribute to the O_2-sensitive current in PASMCs.

Kv1.2. Although it is thought to underlie the CTX- and hypoxia-sensitive current in PC12 cells (16,121), Kv1.2, due to its sensitivity to CTX, has historically been ignored as an important player in PASMC oxygen sensing (7). However, the O_2-sensitivity of this channel was recently examined by Hulme et al who found that, when expressed in mouse L-cells, Kv1.2 current was significantly inhibited by hypoxia (19% inhibition at 80 mV), though only at depolarized potentials of >40 mV (41). In agreement with this observation, Conforti and coworkers found that Kv1.2 current was significantly inhibited by hypoxia in *Xenopus* oocytes (16). To the contrary, when expressed in B82 cells, Kv1.2 current was not affected by hypoxia (66). Although these results suggest that Kv1.2 current is O_2-sensitive, at least in some preparations, because it does not activate in the voltage range of the PASMC

resting membrane potential (41), and because of its sensitivity to CTX, it is unlikely that Kv1.2 homomeric channels underlie a O_2-sensitive current in PASMCs.

Kv1.2/Kv1.5. When coexpressed, Kv1.2 and Kv1.5 assemble to form a functional heteromeric channel with kinetic and pharmacological properties distinct from those displayed by Kv1.2 and Kv1.5 homomeric channels (41,82). This heteromeric channel produces a delayed-rectifier current which is sensitive to 4-AP but insensitive to CTX (41,82). Noting that the Kv1.2/Kv1.5 current meets the characteristics of the O_2-sensitive K^+ current in PASMCs, Hulme et al examined the O_2-sensitivity of this channel (41). When expressed in L-cells, Kv1.2/Kv1.5 whole-cell current was reversibly inhibited by hypoxia (18% reduction at 80 mV) (41). Furthermore, in support of a role for Kv1.2/Kv1.5 current in the physiological response of PASMCs to hypoxia, this current was significantly inhibited by hypoxia in the voltage range of the PASMC resting membrane potential (for example, hypoxia inhibited current at –40 mV by ~65%) (41).

Kv3.1b. Most recently, the effects of hypoxia on Kv3.1b was examined by Osipenko et al (66). Hypoxia significantly and consistently reduced the whole-cell current amplitude in L929 cells expressing Kv3.1b channels by ~24% at 40 mV (66). Furthermore, an inhibitory effect of hypoxia was demonstrated at the single channel level and in membrane patches excised from the cell (66). However, the inhibitory effect of hypoxia was only apparent at positive potentials. These results clearly demonstrate that Kv3.1b is O_2-sensitive; however, when expressed alone as a homotetramer it is not likely to be a component of the PASMC O_2-sensitive K^+ current.

Summary

The results from the aforementioned studies are summarized in Table 1. Kv1.1, Kv1.3 and Kv1.5 currents were not O_2-sensitive in all cell systems studied (41,66). The O_2-sensitivity of Kv1.4 has not been examined; however, as can be seen from Table 1, there is some controversy as to if it is even expressed in PASMCs and, because it produces an A-type current, it does not meet the biophysical profile of the O_2-sensitive K^+ current in PASMCs. Several investigators have detected Kv1.2 expression (6,41,71,120); however, its O_2-sensitivity seems to vary markedly with expression systems (16,41,66,71). Kv2.1 is expressed in PASMCs (6,71,120) and is found to be significantly inhibited by hypoxia in COS cells (71) and in L-cells (41), but not in *Xenopus* oocytes (16). In L-cells, whole cell current from the Kv1.2/Kv1.5 heteromeric channel is significantly inhibited by hypoxia in the voltage range of the PASMC resting membrane potential (41). While there is no direct evidence that this heteromeric channel is expressed *in vivo*, both individual subunits have been detected in PASMCs (6,41,120). The Kv2.1/Kv9.3 heteromeric channel is sensitive to hypoxia in the voltage range of the PASMC resting membrane potential in COS cells (71) and L-cells (41). Both individual subunits are expressed in PASMCs (71,120) and evidence for assembly *in vitro* has been demonstrated (71); however, there is no direct evidence that this heteromeric channel is expressed *in vivo*. Furthermore, when expressed in *Xenopus* oocytes, Kv2.1/Kv9.3 current is significantly less sensitive to 4-AP than Kv2.1 current alone ($I.C._{50}$ = 4.5 mM for Kv2.1 vs. $I.C._{50}$ =31.6 mM for Kv2.1/9.3) (71) making the Kv2.1/Kv9.3 heteromeric channel much less sensitive to 4-AP than the O_2-sensitive current described in PASMCs. Kv3.1b is expressed in PASMCs and is O_2-sensitive when expressed in L929 cells (66). In support of the

role of Kv3.1b in O_2-sensing in the pulmonary artery, data in our laboratory in the bovine pulmonary artery indicate that protein expression of Kv3.1b markedly increases from the main conduit pulmonary artery to the 3rd and 4th intrapulmonary resistance arteries (unpublished observations). As small resistance pulmonary arteries constrict in response to hypoxia while large conduit pulmonary arteries do not (4,50,74), these findings strongly suggest a role for Kv3.1b in HPV.

Taken together, these studies support a potential role for Kv2.1/Kv9.3 and Kv1.2/Kv1.5 heteromeric channels in the physiological response of PASMC K^+ channel to hypoxia. The Kv3.1b α subunit is also a strong candidate; however, since (as a homotetramer) it is not activated at the resting membrane potential, it would have to be expressed as a heterotetramer with another α subunit, or perhaps with a β subunit, which shifts the activation potential in a more hyperpolarized direction, *in vivo*, in order to account for the physiological response of PASMCs to hypoxia. Further studies are needed to address this question.

The results from the aforementioned studies, while giving us clues into the molecular identity of the O_2-sensitive K^+ currents in the pulmonary artery, are also somewhat confusing and contradictory. The explanation may lie in the heterologous expression systems used and the presence of an, as of yet unidentified, O_2-sensor which is endogenously expressed in some of these cells. For instance, Kv2.1 and Kv2.1/Kv9.3 currents responded to hypoxia in only a subset of COS-7 cells (71) while responding to hypoxia in virtually all L-cells studied (41). Furthermore, Kv1.2 current was found to be sensitive to hypoxia in L-cells (41) and oocytes (16), while in

B82 cells it was not (66), suggesting that the hypoxic inhibition of Kv channels is more complicated than direct redox sensing by the Kv channel α subunits alone.

Role of the Kvβ Subunit in O_2-Sensing

It has been hypothesized that the Kv β subunit may play a role in cellular O_2-sensing (36). In fact, when the conserved core of Kvβ2.1 was crystallized, bound NADPH was detected in its crystal structure (36). Furthermore, comparison of the 3-D structure of the β subunit and that of aldo-keto reductases illustrates striking similarity, suggesting that the β subunit may act to couple redox state to channel function (36).

Multiple Kv β subunits have been detected in PASMCs. Yuan and coworkers, using RT-PCR of rat primary cultured resistance PASMCs, detected mRNA expression of Kvβ1.1, Kvβ1.2, and Kvβ2.1 (120). Data from our laboratory indicate that Kvβ1.1, Kvβ1.2, and Kvβ1.3 proteins are expressed in bovine PASMCs (unpublished observations). Furthermore, our data also suggest that protein expression of Kvβ1.1 and Kvβ1.2 dramatically increase from the main conduit pulmonary artery to the 3rd and 4th intrapulmonary resistance arteries. This is interesting in light of the fact that resistance pulmonary arteries constrict in response to hypoxia while conduit pulmonary arteries do not (117), suggesting that Kv β subunit expression within the pulmonary artery may be partially responsible for the differential effects of hypoxia on conduit and resistance pulmonary arteries.

The Kv β subunit has been shown to confer O_2-sensitivity to certain Kv α subunits. Indeed, in HEK293 cells, Kv4.2 alone was unaffected by hypoxia but when

coexpressed with Kvβ1.2, the current was significantly reduced (15.5% inhibition at 40 mV) (72). Recently, we compared the effects of hypoxia on Kv2.1 current in L-cells and HEK293 cells. We found that while the Kv2.1 current was significantly suppressed by hypoxia in L-cells, it was not significantly inhibited in HEK293 cells (unpublished observations). We have previously shown that mouse L-cells contain an endogenously expressed β subunit, Kvβ2.1 (103). Therefore, we determined whether this difference (the presence of Kvβ2.1) could account for the different O_2-sensitivities of Kv2.1 current expressed in L-cells versus HEK293 cells. We found that when Kv2.1 was coexpressed with Kvβ2.1 in HEK293 cells, the whole-cell K^+ current was significantly inhibited by hypoxia (unpublished observations). The results from this experiment are rather puzzling, however, as Kvβ2.1 does not immunoprecipitate with Kv2.1 (60). While the mechanism by which Kv β subunits confer O_2-sensitivity on to some Kv α subunits in heterologous expression systems is unknown, much evidence points to a functional role for Kv β subunits in PASMC O_2-sensing.

POTENTIAL MECHANISMS OF Kv CHANNEL INHIBITION BY HYPOXIA

There have been many hypotheses put forth to explain the hypoxic inhibition of Kv channels in PASMCs, but the mechanism by which these channels sense low levels of oxygen is still unclear. Kv channels could be the O_2-sensors themselves through direct interaction of O_2 with the channel, or they may be an effector, responding through some indirect mechanism (87). The indirect hypothesis seems more likely, however, as cloned Kv channels are O_2-sensitive in some heterologous

expression systems but not in others. Perhaps they must be coexpressed with some endogenous O_2-sensor that confers O_2-sensitivity to the channel. As mentioned previously, Kv2.1 and Kv2.1/Kv9.3 channels were inhibited by hypoxia in only a subset of COS cells (71). Variable expression of, and/or channel colocalization with, such an endogenous O_2-sensor would explain some of the apparent differences in the O_2-sensitivities of cloned channels expressed in heterologous expression systems.

Membrane Bound Heme-Linked Protein and/or NADPH Oxidase Mechanisms of O_2-Sensing

One possible explanation is the existence of a membrane bound heme-linked protein closely associated with the channel. In this scenario, two hypotheses have been put forth. The binding of oxygen to the sensor could affect its conformation, which in turn affects the conformation of the Kv channel and thus the K^+ current. Alternatively, hypoxia could cause a decrease in the production of reactive oxygen species (ROS) generated by a membrane bound NADPH oxidase, modulating the channel through a redox mechanism (see references (7,12,88) for further review). In support of a membrane bound O_2-sensor, Kv channel inhibition has been clearly demonstrated in excised patches in the absence of intracellular mediators in type I cells of the carotid body (31), as well as in heterologous expression systems (66,72). Furthermore, carbon monoxide, which in biological systems is only known to react with hemeproteins, significantly reverses the hypoxic inhibition of Kv channels expressed in HEK cells (72) and in rabbit carotid body type I cells (47), suggesting that the sensor is a heme protein.

In the second hypothesis, the heme protein complex also contains an NADPH oxidase that rapidly generates superoxide and H_2O_2 under normoxic conditions, creating a relatively oxidized redox state (12). During hypoxia, however, there is decreased substrate for the oxidase leading to decreased production of ROS, a more reduced state, and inactivation of redox-dependent Kv channels (12). Indeed, it is well known that K^+ channel activity can be regulated by redox modulation *in vitro* (21,81). In support of the NADPH oxidase hypothesis, reducing agents such as dithiothreitol (DTT), reduced glutathione (GSH), and NADH mimic the effects of hypoxia on PASMCs by decreasing K^+ current (68,69,118) whereas oxidizing agents such as diamide and oxidized GSH (GSSH) have the opposite effect, increasing K^+ current (69,78). NADPH oxidase is expressed in a variety of O_2-sensitive tissues including pulmonary airway chemoreceptor cells (neuroepithelial body cells) (114), carotid body (46), and PASMCs (52). Diphenyleneiodonium (DPI), an inhibitor of NADPH oxidase, has been shown to significantly inhibit HPV in isolated rat lungs (97), rabbit lungs (33) and rat pulmonary arteries (99). However, DPI, because it has been shown to inhibit both K^+ and Ca^{2+} currents (112), has been criticized as being a useful tool in evaluating the importance of NADPH oxidase in O_2-sensing (111). Furthermore, although DPI inhibits HPV, it does not cause sustained vasoconstriction in under normoxic conditions (12).

Recently, two independent groups of investigators used a NADPH oxidase-deficient mouse model to examine the role of NADPH oxidase in O_2-sensing. These groups studied the effects of hypoxia on K^+ current in neuroepithelial body (NEB) cells (30) and PASMCs (5) from these mice and found very different results.

Hypoxia had no effect on the K^+ current in NEB cells from oxidase-deficient mice while it significantly inhibited the K^+ current in NEB cells from wild-type mice (30). Additionally, DPI significantly reduced K^+ current by 30% in wild-type NEB cells, but had no effect in oxidase-deficient NEB cells. These results clearly support the role of NADPH oxidase as an O_2 sensor in pulmonary airway chemoreceptors. In contrast to these results, are the results of Archer et al in PASMCs using the same mouse model (5). They found the production of ROS to be significantly lower in the lungs of oxidase-deficient mice than in the lungs of wild-type mice. However, there was no significant difference in the hypoxic inhibition of K^+ current between wild-type and oxidase-deficient animals, suggesting that NADPH oxidase is not necessary for O_2-sensing in PASMCs. However, the NADPH $gp91^{phox}$ knockout mouse experiments do not exclude a role for a "low-output" NADPH oxidase isoforms (33).

These seemingly contradictory results emphasize the complexity of O_2-sensing and strongly suggest a diversity of O_2-sensing mechanisms between tissues.

Mitochondria as O_2-Sensors

Multiple hypotheses relating to mitochondria as O_2-sensors have been proposed (7,12,87). These include depletion of high-energy phosphates, a shift toward the reduced forms of redox couples such as NADH/NAD and GSH/GSSG and an increase in mitochondrial ROS production. A logical potential mechanism is the depletion of intracellular ATP. In isolated rat lungs, inhibitors of oxidative ATP production caused a transient pressor response and a loss of reactivity to hypoxia, suggesting that depression of oxidative ATP elicits pulmonary vasoconstriction (80). Additionally, inhibitors of glycolysis, such as 2-deoxyglucose, and inhibitors of

oxidative phosphorylation, such as rotenone, significantly inhibit outward potassium current in PASMCs (3,118). However, these responses may not be due to simple depletion of ATP, as the patch pipettes contained 5-10 mM ATP (3,118). Additionally, HPV has been shown to occur very rapidly before any changes in ATP levels (9). Severe hypoxia has been shown to decrease ATP concentration; however, the decreased ATP levels result in the opening of K_{ATP} channels, increased K^+ efflux and vasodilation (113).

An additional hypothesis is that hypoxia inhibits the activity of cytochrome oxidase, which leads to an altered mitochondrial redox state and the generation of ROS (12,87). In support of this hypothesis, hypoxia has been shown to cause a decrease in the V_{max} of cytochrome oxidase (12) and an increase in the production of ROS (45,52). However, in one report, the hypoxic generation of superoxide was attributed to a membrane bound NADPH oxidase; as DPI, but not the mitochondrial inhibitor myxathiazole, significantly attenuated this response (52).

Alternatively, hypoxia may cause an accumulation of redox couples such as NADH/NAD and GSH/GSSG and/or a decreased production of ROS (7). Mitochondria in the lung have been shown to make ROS in proportion to PO_2 (102). Furthermore, rotenone, an inhibitor of the mitochondrial electron transport chain, mimics the effect of hypoxia by decreasing whole cell K^+ current (3,118), reducing lung ROS production (3,118), and causing pulmonary artery constriction (4,80). However, there is still much controversy regarding the different responses to metabolic inhibitors in different O_2-responsive tissues (12) and some question as to

whether hypoxia causes an increase (45,52) or a decrease (7) in the production of ROS. Further studies are needed to examine these questions.

Intracellular Ca^{2+} Release as a Mechanism of Kv Channel Inhibition by Hypoxia

As mentioned earlier, there is accumulating evidence that Ca^{2+} release from intracellular stores may initiate HPV. Hypoxia has been shown to cause a rapid, transient increase in $[Ca^{2+}]_i$ in PASMCs which is unaffected by extracellular Ca^{2+} removal, or block of voltage-gated Ca^{2+} channels, but significantly decreased by caffeine depletion of Ca^{2+} from sarcoplasmic reticulum (SR) (85). Furthermore, ryanodine plus caffeine significantly inhibits HPV in dog resistance pulmonary artery (42) and thapsigargin, cyclopiazonic acid and ryanodine (used to deplete Ca^{2+} from intracellular Ca^{2+} stores) prevents HPV in rat pulmonary arterial resistance vessels (74). In PASMCs loaded with fura 2, hypoxic challenge, thapsigargin, cyclopiazonic acid, and ryanodine all resulted in a significant increase in $[Ca^{2+}]_i$ and membrane depolarization (32). However, pretreatment with thapsigargin, cyclopizonic acid or ryanodine prevented a hypoxic challenge-induced increase in $[Ca^{2+}]_i$. Taken together, these studies suggest a predominant role of Ca^{2+} release from intracellular stores in HPV. Delayed-rectifier K^+ channels are inhibited by $[Ca^{2+}]_i$ in dog PASMCs (74). Additionally, application of anti-Kv1.5 antibody within the patch pipette solution causes an increase in $[Ca^{2+}]_i$ and membrane depolarization, while subsequent hypoxic challenge results in a further increase in $[Ca^{2+}]_i$ with no effect on membrane potential (32). These results led the researchers to hypothesize that hypoxia acts to activate Ca^{2+} release from the SR leading to a rise in $[Ca^{2+}]_i$ which in turn causes the inhibition of Kv channels and membrane depolarization (32,74).

While this hypothesis is fairly well supported, it is conceivable that hypoxia acts through multiple pathways and multiple ion channels to produce HPV.

Kv Channel Targeting to Lipid Rafts as a Mechanism of O_2-Sensing

Kv channels are differentially targeted to lipid rafts within the plasma membrane (53). Indeed, the O_2-sensitive Kv2.1 channel targets to lipid rafts in mouse L-cells while Kv4.2 does not. Caveolae represent one type of lipid raft that forms an invagination at the cell surface. Numerous signaling proteins have been localized to caveolae and caveolae-like domains including tyrosine kinases, nitric oxide synthase, protein kinase C, and G-proteins (2). Like hypoxia, tyrosine kinase inhibitors have been shown to markedly inhibit whole cell K^+ current with no other effects on channel kinetics (94). Furthermore, the tyrosine kinase pathway has been recently implicated as playing a role in HPV (105). Perhaps differential targeting of K^+ channels to lipids rafts, and their associated signaling molecules, represents still another mechanism by which hypoxia alters Kv channel function. It is possible that Kvβ subunits affect this targeting which could explain how Kvβ subunits confer O_2-sensitivity upon Kvα subunits. Further studies are needed to examine these possibilities.

KV CHANNEL REGULATION BY CHRONIC HYPOXIA

Long-term hypoxic exposure leads to decreased PASMC Kv channel current (64,92,93) and membrane depolarization (19,76,92,93). While acute hypoxia modulates Kv channel current by affecting channel function, chronic hypoxic exposure is thought to modulate Kv channel current by affecting channel expression.

Indeed, Yuan and coworkers showed that prolonged exposure (24-72 hours) of rat primary cultured PASMCs to hypoxia is associated with a downregulation of Kv1.2 and Kv1.5 α subunit mRNA and protein (108). Therefore, they concluded, that the diminished trasnscription and expression of Kv α subunits most likely results in fewer functional Kv channels, a decrease in outward Kv current, and subsequent membrane depolarization.

Chronic hypoxic exposure is associated with the regulation of a number of genes in a wide variety of cell types. Protein phosphorylation and/or redox modulation of transcription factors, are thought to be part of the signaling pathway which translates a hypoxic stimulus into the regulation of gene expression (10). The mechanism by which Kv channels are downregulated by chronic hypoxia is unknown, but is likely to involve modulation of a hypoxia-inducible transcription factor. For instance, hypoxia inducible factor-1 (HIF-1), has been implicated in the regulation of an ever growing number of genes, whose gene products include; endothelin-1, erythropoietin, nitric oxide synthase 2, and vascular endothelial growth factor (89). Additionally, accumulating evidence suggests that the c-fos and c-jun family of genes can also be induced by hypoxia (10). Preliminary data by Yuan and coworkers suggests that overexpression of c-jun significantly decreases whole-cell Kv current (96), making c-jun an attractive candidate for the transcriptional downregulation of Kv channel expression during prolonged conditions of hypoxia. Whatever the mechanism for the hypoxic downregulation of Kv channel expression, it is likely to be important in the pathogenesis of chronic hypoxic pulmonary hypertension, as the

consequent reduction in outward K^+ current contributes to a sequel of events which ultimately lead to pulmonary hypertension (96).

SUMMARY

Recently, many advances have been made in the study of PASMC O_2-sensing through the use of cloned channels, heterologous expression systems and transgenic mice. Through these studies it has become evident that Kv channels play an important role in the response of PASMCs to hypoxia. Because the O_2-sensitivity of some cloned channels varies with the cell type in which they are expressed, it is most likely that Kv α subunits do not sense O_2 directly, rather, they are most likely inhibited through some indirect mechanism which involves interaction with an unidentified O_2-sensor and/or β subunit. In this manner, it is likely that the varied results represent multiple mechanisms and multiple effectors through which hypoxia is sensed throughout the body. Further work is needed to examine this possibility and to elucidate the many mechanisms by which Kv channels "sense" and respond to acute and chronic hypoxia.

Table 2.1: Summary of candidate O_2-sensitive Kv channels expressed in the pulmonary vasculature

	Channel Subunit(s) Detected in PASMCs		Channel Characteristics in Heterologous Expression Systems			
Channel	**mRNA**	**Protein**	**Slowly Inactivates**	**Sensitive to 4-AP***	**Insensitive to CTX****	**Sensitive to Hypoxia**
Kv1.1	Yes (120)	Yes (6)	Yes	Yes	Yes†	No COS cells (66), No CHO cells (66)
Kv1.2	Yes (71), Yes (120)	Yes (6), Yes (41)	Yes	Yes	No	No COS cells (71), Yes oocytes (16), Yes *L*-cells (41), No B82 cells (66)
Kv1.3	Yes (71), No (120)	No (120), Yes (6)	Yes	Yes	No	No COS cells (71)
Kv1.4	No (71), Yes (120)	Yes (120), No (6)	No	Yes	Yes	
Kv1.5	No (71), Yes (120)	Yes (120), Yes (6), Yes (41)	Yes	Yes	Yes	No L-cells (41), No COS cells (66), No MEL cells (66)
Kv1.6	No (71), Yes (120)	Yes (6)	Yes	Yes	No	
Kv2.1	Yes (71), Yes (120)	Yes (120), Yes, (6)	Yes	Yes	Yes	Yes COS cells (71), Yes, L-cells (41), No oocytes (16)
Kv3.1	Yes (66)	Yes (66)	Yes	Yes	Yes	Yes L929 cells (66)
Kv9.3	Yes (71), Yes (120)		Silent Subunit			
Kv1.2/1.5	Yes both (120), Yes Kv1.2 (71), No Kv1.5 (71)	Yes both (6), Yes both (41), Yes Kv1.2 (6)	Yes	Yes (82)	Yes (82), (41)	Yes L-cells (41)
Kv2.1/9.3	Yes both (71) Yes both (120)	Yes Kv2.1 (120), Yes Kv2.1 (6)	Yes	No (71)	Yes (71)	Yes COS cells (71), Yes L-cells (41)

*I.C. 50 $\leq$ 1.5 mM as referenced in Chandy and Gutman (13) except where indicated, **I.C. 50 $\geq$ 50 nM, as referenced in Chandy and Gutman (13) except where indicated, †rat Kv1.1 sensitive to CTX, human and mouse insensitive

REFERENCES

1. Albarwani S, Robertson BE, Nye PC, and Kozlowski RZ. Biophysical properties of Ca^{2+}- and Mg-ATP-activated K^+ channels in pulmonary arterial smooth muscle cells isolated from the rat. *Pflugers Arch* 428: 446-454, 1994.

2. Anderson RG. The caveolae membrane system. *Annu Rev Biochem* 67: 199-225, 1998.

3. Archer SL, Huang J, Henry T, Peterson D, and Weir EK. A redox-based O_2 sensor in rat pulmonary vasculature. *Circ Res* 73: 1100-1112, 1993.

4. Archer SL, Huang JM, Reeve HL, Hampl V, Tolarova S, Michelakis E, and Weir EK. Differential distribution of electrophysiologically distinct myocytes in conduit and resistance arteries determines their response to nitric oxide and hypoxia. *Circ Res* 78: 431-442, 1996.

5. Archer SL, Reeve HL, Michelakis E, Puttagunta L, Waite R, Nelson DP, Dinauer MC, and Weir EK. O_2 sensing is preserved in mice lacking the gp91 phox subunit of NADPH oxidase. *Proc Natl Acad Sci U S A* 96: 7944-7949, 1999.

6. Archer SL, Souil E, Dinh-Xuan AT, Schremmer B, Mercier JC, El Yaagoubi A, Nguyen-Huu L, Reeve HL, and Hampl V. Molecular identification of the role of voltage-gated K^+ channels, Kv1.5 and Kv2.1, in hypoxic pulmonary vasoconstriction and control of resting membrane potential in rat pulmonary artery myocytes. *J Clin Invest* 101: 2319-2330, 1998.

7. Archer SL, Weir EK, Reeve HL, and Michelakis E. Molecular identification of O_2 sensors and O_2-sensitive potassium channels in the pulmonary circulation. *Adv Exp Med Biol* 475: 219-240, 2000.

8. Barman SA. Potassium channels modulate hypoxic pulmonary vasoconstriction. *Am J Physiol* 275: L64-L70, 1998.

9. Buescher PC, Pearse DB, Pillai RP, Litt MC, Mitchell MC, and Sylvester JT. Energy state and vasomotor tone in hypoxic pig lungs. *J Appl Physiol* 70: 1874-1881, 1991.

10. Bunn HF and Poyton RO. Oxygen sensing and molecular adaptation to hypoxia. *Physiol Rev* 76: 839-885, 1996.

11. Butler A, Wei AG, Baker K, and Salkoff L. A family of putative potassium channel genes in Drosophila. *Science* 243: 943-947, 1989.

12. Chandel NS and Schumacker PT. Cellular oxygen sensing by mitochondria: old questions, new insight. *J Appl Physiol* 88: 1880-1889, 2000.

13. Chandy KG and Gutman GA. Voltage-gated K^+ channels. In North, R. A., ed. Handbook of receptors and channels: ligand- and voltage-gated ion channels. Boca Raton, FL.: 1995, p. 1-71.

14. Christie MJ, North RA, Osborne PB, Douglass J, and Adelman JP. Heteropolymeric potassium channels expressed in Xenopus oocytes from cloned subunits. *Neuron* 4: 405-411, 1990.

15. Clapp LH and Tinker A. Potassium channels in the vasculature. *Curr Opin Nephrol Hypertens* 7: 91-98, 1998.

16. Conforti L, Bodi I, Nisbet JW, and Millhorn DE. O_2-sensitive K^+ channels: role of the Kv1.2 -subunit in mediating the hypoxic response. *J Physiol (Lond)* 524(Pt 3): 783-793, 2000.

17. Cornfield DN, Stevens T, McMurtry IF, Abman SH, and Rodman DM. Acute hypoxia causes membrane depolarization and calcium influx in fetal pulmonary artery smooth muscle cells. *Am J Physiol* 266: L469-L475, 1994.

18. Deal KK, England SK, and Tamkun MM. Molecular physiology of cardiac potassium channels. *Physiol Rev* 76: 49-67, 1996.

19. Doggrell SA, Wanstall JC, and Gambino A. Functional effects of 4-aminopyridine (4-AP) on pulmonary and systemic vessels from normoxic control and hypoxic pulmonary hypertensive rats. *Naunyn Schmiedebergs Arch Pharmacol* 360: 317-323, 1999.

20. Doi S, Damron DS, Ogawa K, Tanaka S, Horibe M, and Murray PA. K^+ channel inhibition, calcium signaling, and vasomotor tone in canine pulmonary artery smooth muscle. *Am J Physiol Lung Cell Mol Physiol* 279: L242-L251, 2000.

21. Duprat F, Guillemare E, Romey G, Fink M, Lesage F, Lazdunski M, and Honore E. Susceptibility of cloned K+ channels to reactive oxygen species. *Proc Natl Acad Sci U S A* 92: 11796-11800, 1995.

22. England SK, Uebele VN, Kodali J, Bennett PB, and Tamkun MM. A novel K^+ channel beta-subunit (hKv beta 1.3) is produced via alternative mRNA splicing. *J Biol Chem* 270: 28531-28534, 1995.

23. England SK, Uebele VN, Shear H, Kodali J, Bennett PB, and Tamkun MM. Characterization of a voltage-gated K^+ channel beta subunit expressed in human heart. *Proc Natl Acad Sci U S A* 92: 6309-6313, 1995.

24. Evans AM, Osipenko ON, and Gurney AM. Properties of a novel K^+ current that is active at resting potential in rabbit pulmonary artery smooth muscle cells. *J Physiol (Lond)* 496(Pt 2): 407-420, 1996.

25. Evans AM, Osipenko ON, Haworth SG, and Gurney AM. Resting potentials and potassium currents during development of pulmonary artery smooth muscle cells. *Am J Physiol* 275: H887-H899, 1998.

26. Fearon IM, Varadi G, Koch S, Isaacsohn I, Ball SG, and Peers C. Splice variants reveal the region involved in oxygen sensing by recombinant human L-type Ca^{2+} channels. *Circ Res* 87: 537-539, 2000.

27. Fink M, Duprat F, Lesage F, Heurteaux C, Romey G, Barhanin J, and Lazdunski M. A new K^+ channel beta subunit to specifically enhance Kv2.2 (CDRK) expression. *J Biol Chem* 271: 26341-26348, 1996.

28. Franco-Obregon A and Lopez-Barneo J. Differential oxygen sensitivity of calcium channels in rabbit smooth muscle cells of conduit and resistance pulmonary arteries. *J Physiol (Lond)* 491(Pt 2): 511-518, 1996.

29. Franco-Obregon A, Montoro R, Urena J, and Lopez-Barneo J. Modulation of voltage-gated Ca^{2+} channels by O_2 tension. Significance for arterial oxygen chemoreception. *Adv Exp Med Biol* 410: 97-103, 1996.

30. Fu XW, Wang D, Nurse CA, Dinauer MC, and Cutz E. NADPH oxidase is an O_2 sensor in airway chemoreceptors: evidence from K^+ current modulation in wild-type and oxidase-deficient mice. *Proc Natl Acad Sci U S A* 97: 4374-4379, 2000.

31. Ganfornina MD and Lopez-Barneo J. Potassium channel types in arterial chemoreceptor cells and their selective modulation by oxygen. *J Gen Physiol* 100: 401-426, 1992.

32. Gelband CH and Gelband H. Ca^{2+} release from intracellular stores is an initial step in hypoxic pulmonary vasoconstriction of rat pulmonary artery resistance vessels. *Circulation* 96: 3647-3654, 1997.

33. Grimminger F, Weissmann N, Spriestersbach R, Becker E, Rosseau S, and Seeger W. Effects of NADPH oxidase inhibitors on hypoxic vasoconstriction in buffer-perfused rabbit lungs. *Am J Physiol* 268: L747-L752, 1995.

34. Grissmer S, Nguyen AN, Aiyar J, Hanson DC, Mather RJ, Gutman GA, Karmilowicz MJ, Auperin DD, and Chandy KG. Pharmacological characterization of five cloned voltage-gated K^+ channels, types Kv1.1, 1.2, 1.3, 1.5, and 3.1, stably expressed in mammalian cell lines. *Mol Pharmacol* 45: 1227-1234, 1994.

35. Grover RF. Pulmonary circulation in animals and man at high altitude. *Ann N Y Acad Sci* 127: 632-639, 1965.

36. Gulbis JM, Mann S, and MacKinnon R. Structure of a voltage-dependent K^+ channel beta subunit. *Cell* 97: 943-952, 1999.

37. Gulbis JM, Zhou M, Mann S, and MacKinnon R. Structure of the cytoplasmic beta subunit-T1 assembly of voltage- dependent K^+ channels. *Science* 289: 123-127, 2000.

38. Harder DR, Madden JA, and Dawson C. Hypoxic induction of Ca^{2+}-dependent action potentials in small pulmonary arteries of the cat. *J Appl Physiol* 59: 1389-1393, 1985.

39. Hasunuma K, Rodman DM, and McMurtry IF. Effects of K^+ channel blockers on vascular tone in the perfused rat lung. *Am Rev Respir Dis* 144: 884-887, 1991.

40. Herold CJ, Wetzel RC, Robotham JL, Herold SM, and Zerhouni EA. Acute effects of increased intravascular volume and hypoxia on the pulmonary circulation: assessment with high-resolution CT. *Radiology* 183: 655-662, 1992.

41. Hulme JT, Coppock EA, Felipe A, Martens JR, and Tamkun MM. Oxygen sensitivity of cloned voltage-gated K^+ channels expressed in the pulmonary vasculature. *Circ Res* 85: 489-497, 1999.

42. Jabr RI, Toland H, Gelband CH, Wang XX, and Hume JR. Prominent role of intracellular Ca^{2+} release in hypoxic vasoconstriction of canine pulmonary artery. *Br J Pharmacol* 122: 21-30, 1997.

43. Jackson WF. Ion channels and vascular tone. *Hypertension* 35: 173-178, 2000.

44. Jan LY and Jan YN. Cloned potassium channels from eukaryotes and prokaryotes. *Annu Rev Neurosci* 20: 91-123, 1997.

45. Killilea DW, Hester R, Balczon R, Babal P, and Gillespie MN. Free radical production in hypoxic pulmonary artery smooth muscle cells. *Am J Physiol Lung Cell Mol Physiol* 279: L408-L412, 2000.

46. Kummer W and Acker H. Immunohistochemical demonstration of four subunits of neutrophil NAD(P)H oxidase in type I cells of carotid body. *J Appl Physiol* 78: 1904-1909, 1995.

47. Lahiri S and Acker H. Redox-dependent binding of CO to heme protein controls PO_2-sensitive chemoreceptor discharge of the rat carotid body. *Respir Physiol* 115: 169-177, 1999.

48. Lopez-Barneo J, Lopez-Lopez JR, Urena J, and Gonzalez C. Chemotransduction in the carotid body: K^+ current modulated by PO_2 in type I chemoreceptor cells. *Science* 241: 580-582, 1988.

49. MacKinnon R. Determination of the subunit stoichiometry of a voltage-activated potassium channel. *Nature* 350: 232-235, 1991.

50. Madden JA, Dawson CA, and Harder DR. Hypoxia-induced activation in small isolated pulmonary arteries from the cat. *J Appl Physiol* 59: 113-118, 1985.

51. Madden JA, Vadula MS, and Kurup VP. Effects of hypoxia and other vasoactive agents on pulmonary and cerebral artery smooth muscle cells. *Am J Physiol* 263: L384-L393, 1992.

52. Marshall C, Mamary AJ, Verhoeven AJ, and Marshall BE. Pulmonary artery NADPH-oxidase is activated in hypoxic pulmonary vasoconstriction. *Am J Respir Cell Mol Biol* 15: 633-644, 1996.

53. Martens JR, Navarro-Polanco R, Coppock EA, Nishiyama A, Parshley L, Grobaski TD, and Tamkun MM. Differential targeting of Shaker-like potassium channels to lipid rafts. *J Biol Chem* 275: 7443-7446, 2000.

54. McCulloch KM, Osipenko ON, and Gurney AM. Oxygen-sensing potassium currents in pulmonary artery. *Gen Pharmacol* 32: 403-411, 1999.

55. McMurtry IF. BAY K 8644 potentiates and A23187 inhibits hypoxic vasoconstriction in rat lungs. *Am J Physiol* 249: H741-H746, 1985.

56. McMurtry IF, Davidson AB, Reeves JT, and Grover RF. Inhibition of hypoxic pulmonary vasoconstriction by calcium antagonists in isolated rat lungs. *Circ Res* 38: 99-104, 1976.

57. Michelakis ED, Archer SL, and Weir EK. Acute hypoxic pulmonary vasoconstriction: a model of oxygen sensing. *Physiol Res* 44: 361-367, 1995.

58. Morales MJ, Castellino RC, Crews AL, Rasmusson RL, and Strauss HC. A novel beta subunit increases rate of inactivation of specific voltage-gated potassium channel alpha subunits. *J Biol Chem* 270: 6272-6277, 1995.

59. Morales MJ, Wee JO, Wang S, Strauss HC, and Rasmusson RL. The N-terminal domain of a K^+ channel beta subunit increases the rate of C-type inactivation from the cytoplasmic side of the channel. *Proc Natl Acad Sci U S A* 93: 15119-15123, 1996.

60. Nakahira K, Shi G, Rhodes KJ, and Trimmer JS. Selective interaction of voltage-gated K^+ channel beta-subunits with alpha-subunits. *J Biol Chem* 271: 7084-7089, 1996.

61. Nakanishi K, Tajima F, Osada H, Nakamura A, Yagura S, Kawai T, Suzuki M, and Torikata C. Pulmonary, vascular responses in rats exposed to chronic hypobaric hypoxia at two different altitude levels. *Pathol Res Pract* 192: 1057-1067, 1996.

62. Nelson MT and Quayle JM. Physiological roles and properties of potassium channels in arterial smooth muscle. *Am J Physiol* 268: C799-C822, 1995.

63. Okabe K, Kitamura K, and Kuriyama H. Features of 4-aminopyridine sensitive outward current observed in single smooth muscle cells from the rabbit pulmonary artery. *Pflugers Arch* 409: 561-568, 1987.

64. Osipenko ON, Alexander D, MacLean MR, and Gurney AM. Influence of chronic hypoxia on the contributions of non-inactivating and delayed rectifier K currents to the resting potential and tone of rat pulmonary artery smooth muscle. *Br J Pharmacol* 124: 1335-1337, 1998.

65. Osipenko ON, Evans AM, and Gurney AM. Regulation of the resting potential of rabbit pulmonary artery myocytes by a low threshold, O_2-sensing potassium current. *Br J Pharmacol* 120: 1461-1470, 1997.

66. Osipenko ON, Tate RJ, and Gurney AM. Potential role for kv3.1b channels as oxygen sensors. *Circ Res* 86: 534-540, 2000.

67. Papazian DM, Schwarz TL, Tempel BL, Jan YN, and Jan LY. Cloning of genomic and complementary DNA from Shaker, a putative potassium channel gene from Drosophila. *Science* 237: 749-753, 1987.

68. Park MK, Bae YM, Lee SH, Ho WK, and Earm YE. Modulation of voltage-dependent K^+ channel by redox potential in pulmonary and ear arterial smooth muscle cells of the rabbit. *Pflugers Arch* 434: 764-771, 1997.

69. Park MK, Lee SH, Ho WK, and Earm YE. Redox agents as a link between hypoxia and the responses of ionic channels in rabbit pulmonary vascular smooth muscle. *Exp Physiol* 80: 835-842, 1995.

70. Park MK, Lee SH, Lee SJ, Ho WK, and Earm YE. Different modulation of Ca^{2+}-activated K^+ channels by the intracellular redox potential in pulmonary and ear arterial smooth muscle cells of the rabbit. *Pflugers Arch* 430: 308-314, 1995.

71. Patel AJ, Lazdunski M, and Honore E. Kv2.1/Kv9.3, a novel ATP-dependent delayed-rectifier K^+ channel in oxygen-sensitive pulmonary artery myocytes. *EMBO J* 16: 6615-6625, 1997.

72. Perez-Garcia MT, Lopez-Lopez JR, and Gonzalez C. Kvbeta1.2 subunit coexpression in HEK293 cells confers O2 sensitivity to Kv4.2 but not to Shaker channels. *J Gen Physiol* 113: 897-907, 1999.

73. Perez-Garcia MT, Lopez-Lopez JR, Riesco AM, Hoppe UC, Marban E, Gonzalez C, and Johns DC. Viral gene transfer of dominant-negative Kv4 construct suppresses an O2-sensitive K+ current in chemoreceptor cells. *J Neurosci* 20: 5689-5695, 2000.

74. Post JM, Gelband CH, and Hume JR. $[Ca^{2+}]_i$ inhibition of K^+ channels in canine pulmonary artery. Novel mechanism for hypoxia-induced membrane depolarization. *Circ Res* 77: 131-139, 1995.

75. Post JM, Hume JR, Archer SL, and Weir EK. Direct role for potassium channel inhibition in hypoxic pulmonary vasoconstriction. *Am J Physiol* 262: C882-C890, 1992.

76. Priest RM, Robertson TP, Leach RM, and Ward JP. Membrane potential-dependent and -independent vasodilation in small pulmonary arteries from chronically hypoxic rats. *J Pharmacol Exp Ther* 285: 975-982, 1998.

77. Reeve HL, Archer SL, and Weir EK. Ion channels in the pulmonary vasculature. *Pulm Pharmacol Ther* 10: 243-252, 1997.

78. Reeve HL, Weir EK, Nelson DP, Peterson DA, and Archer SL. Opposing effects of oxidants and antioxidants on K^+ channel activity and tone in rat vascular tissue. *Exp Physiol* 80: 825-834, 1995.

79. Rettig J, Heinemann SH, Wunder F, Lorra C, Parcej DN, Dolly JO, and Pongs O. Inactivation properties of voltage-gated K^+ channels altered by presence of beta-subunit. *Nature* 369: 289-294, 1994.

80. Rounds S and McMurtry IF. Inhibitors of oxidative ATP production cause transient vasoconstriction and block subsequent pressor responses in rat lungs. *Circ Res* 48: 393-400, 1981.

81. Ruppersberg JP, Stocker M, Pongs O, Heinemann SH, Frank R, and Koenen M. Regulation of fast inactivation of cloned mammalian IK(A) channels by cysteine oxidation. *Nature* 352: 711-714, 1991.

82. Russell SN, Overturf KE, and Horowitz B. Heterotetramer formation and charybdotoxin sensitivity of two K^+ channels cloned from smooth muscle. *Am J Physiol* 267: C1729-C1733, 1994.

83. Salinas M, Duprat F, Heurteaux C, Hugnot JP, and Lazdunski M. New modulatory alpha subunits for mammalian Shab K^+ channels. *J Biol Chem* 272: 24371-24379, 1997.

84. Salkoff L, Baker K, Butler A, Covarrubias M, Pak MD, and Wei A. An essential 'set' of K^+ channels conserved in flies, mice and humans. *Trends Neurosci* 15: 161-166, 1992.

85. Salvaterra CG and Goldman WF. Acute hypoxia increases cytosolic calcium in cultured pulmonary arterial myocytes. *Am J Physiol* 264: L323-L328, 1993.

86. Sato K, Morio Y, Morris KG, Rodman DM, and McMurtry IF. Mechanism of hypoxic pulmonary vasoconstriction involves ET(A) receptor-mediated inhibition of K(ATP) channel. *Am J Physiol Lung Cell Mol Physiol* 278: L434-L442, 2000.

87. Semenza GL. Perspectives on oxygen sensing. *Cell* 98: 281-284, 1999.

88. Semenza GL. Chairman's summary: mechanisms of oxygen homeostasis, circa 1999. *Adv Exp Med Biol* 475: 303-310, 2000.

89. Semenza GL. HIF-1: mediator of physiological and pathophysiological responses to hypoxia. *J Appl Physiol* 88: 1474-1480, 2000.

90. Sham JS, Crenshaw BR, Jr., Deng LH, Shimoda LA, and Sylvester JT. Effects of hypoxia in porcine pulmonary arterial myocytes: roles of K(V) channel and endothelin-1. *Am J Physiol Lung Cell Mol Physiol* 279: L262-L272, 2000.

91. Sheng M, Liao YJ, Jan YN, and Jan LY. Presynaptic A-current based on heteromultimeric K+ channels detected in vivo. *Nature* 365: 72-75, 1993.

92. Shimoda LA, Sylvester JT, and Sham JS. Chronic hypoxia alters effects of endothelin and angiotensin on K+ currents in pulmonary arterial myocytes. *Am J Physiol* 277: L431-L439, 1999.

93. Smirnov SV, Robertson TP, Ward JP, and Aaronson PI. Chronic hypoxia is associated with reduced delayed rectifier K+ current in rat pulmonary artery muscle cells. *Am J Physiol* 266: H365-H370, 1994.

94. Sobko A, Peretz A, and Attali B. Constitutive activation of delayed-rectifier potassium channels by a src family tyrosine kinase in Schwann cells. *EMBO J* 17: 4723-4734, 1998.

95. Standen NB and Quayle JM. K+ channel modulation in arterial smooth muscle. *Acta Physiol Scand* 164: 549-557, 1998.

96. Sweeney M and Yuan XJ. Hypoxic pulmonary vasoconstriction: role of voltage-gated potassium channels. *Respiratory Research* 1: 40-48, 2000.

97. Thomas HM, III, Carson RC, Fried ED, and Novitch RS. Inhibition of hypoxic pulmonary vasoconstriction by diphenyleneiodonium [published erratum appears in Biochem Pharmacol 1991 Oct 24;42(10):2069]. *Biochem Pharmacol* 42: R9-12, 1991.

98. Thompson BT and Hales CA. Hypoxic pulmonary hypertension: acute and chronic. *Heart Lung* 15: 457-465, 1986.

99. Thompson JS, Jones RD, Rogers TK, Hancock J, and Morice AH. Inhibition of hypoxic pulmonary vasoconstriction in isolated rat pulmonary arteries by diphenyleneiodonium (DPI). *Pulm Pharmacol Ther* 11: 71-75, 1998.

100. Tolins M, Weir EK, Chesler E, Nelson DP, and From AH. Pulmonary vascular tone is increased by a voltage-dependent calcium channel potentiator. *J Appl Physiol* 60: 942-948, 1986.

101. Turner JL and Kozlowski RZ. Relationship between membrane potential, delayed rectifier K+ currents and hypoxia in rat pulmonary arterial myocytes. *Exp Physiol* 82: 629-645, 1997.

102. Turrens JF, Freeman BA, and Crapo JD. Hyperoxia increases H2O2 release by lung mitochondria and microsomes. *Arch Biochem Biophys* 217: 411-421, 1982.

103. Uebele VN, England SK, Chaudhary A, Tamkun MM, and Snyders DJ. Functional differences in Kv1.5 currents expressed in mammalian cell lines are due to the presence of endogenous Kv beta 2.1 subunits. *J Biol Chem* 271: 2406-2412, 1996.

104. Uebele VN, England SK, Gallagher DJ, Snyders DJ, Bennett PB, and Tamkun MM. Distinct domains of the voltage-gated K+ channel Kv beta 1.3 beta-subunit affect voltage-dependent gating. *Am J Physiol* 274: C1485-C1495, 1998.

105. Uzun O, Demiryurek AT, and Kanzik I. The role of tyrosine kinase in hypoxic constriction of sheep pulmonary artery rings. *Eur J Pharmacol* 358: 41-47, 1998.

106. Voelkel NF, Morris KG, McMurtry IF, and Reeves JT. Calcium augments hypoxic vasoconstriction in lungs from high-altitude rats. *J Appl Physiol* 49: 450-455, 1980.

107. von Euler US and Liljestrand G. Observations on the pulmonary arterial blood pressure in the cat. *Acta Physiol Scand* 12: 301-320, 1946.

108. Wang J, Juhaszova M, Rubin LJ, and Yuan XJ. Hypoxia inhibits gene expression of voltage-gated K+ channel alpha subunits in pulmonary artery smooth muscle cells. *J Clin Invest* 100: 2347-2353, 1997.

109. Ward JP and Aaronson PI. Mechanisms of hypoxic pulmonary vasoconstriction: can anyone be right? *Respir Physiol* 115: 261-271, 1999.

110. Ward JP and Robertson TP. The role of the endothelium in hypoxic pulmonary vasoconstriction. *Exp Physiol* 80: 793-801, 1995.

111. Weir EK and Archer SL. The mechanism of acute hypoxic pulmonary vasoconstriction: the tale of two channels. *FASEB J* 9: 183-189, 1995.

112. Weir EK, Wyatt CN, Reeve HL, Huang J, Archer SL, and Peers C. Diphenyleneiodonium inhibits both potassium and calcium currents in isolated pulmonary artery smooth muscle cells. *J Appl Physiol* 76: 2611-2615, 1994.

113. Wiener CM, Banta MR, Dowless MS, Flavahan NA, and Sylvester JT. Mechanisms of hypoxic vasodilation in ferret pulmonary arteries. *Am J Physiol* 269: L351-L357, 1995.

114. Youngson Ç, Nurse C, Yeger H, and Cutz E. Oxygen sensing in airway chemoreceptors. *Nature* 365: 153-155, 1993.

115. Yuan XJ. Voltage-gated K+ currents regulate resting membrane potential and [Ca2+]i in pulmonary arterial myocytes. *Circ Res* 77: 370-378, 1995.

116. Yuan XJ, Goldman WF, Tod ML, Rubin LJ, and Blaustein MP. Hypoxia reduces potassium currents in cultured rat pulmonary but not mesenteric arterial myocytes. *Am J Physiol* 264: L116-L123, 1993.

117. Yuan XJ, Tod ML, Rubin LJ, and Blaustein MP. Contrasting effects of hypoxia on tension in rat pulmonary and mesenteric arteries. *Am J Physiol* 259: H281-H289, 1990.

118. Yuan XJ, Tod ML, Rubin LJ, and Blaustein MP. Deoxyglucose and reduced glutathione mimic effects of hypoxia on K+ and Ca2+ conductances in pulmonary artery cells. *Am J Physiol* 267: L52-L63, 1994.

119. Yuan XJ, Tod ML, Rubin LJ, and Blaustein MP. Hypoxic and metabolic regulation of voltage-gated K+ channels in rat pulmonary artery smooth muscle cells. *Exp Physiol* 80: 803-813, 1995.

120. Yuan XJ, Wang J, Juhaszova M, Golovina VA, and Rubin LJ. Molecular basis and function of voltage-gated K+ channels in pulmonary arterial smooth muscle cells. *Am J Physiol* 274: L621-L635, 1998.

121. Zhu WH, Conforti L, Czyzyk-Krzeska MF, and Millhorn DE. Membrane depolarization in PC-12 cells during hypoxia is regulated by an O2-sensitive K+ current. *Am J Physiol* 271: C658-C665, 1996.

CHAPTER 3

OXYGEN-SENSITIVITY OF VOLTAGE-GATED K^+ CHANNELS EXPRESSED IN THE PULMONARY VASCULATURE

INTRODUCTION

In the systemic circulation, small arteries dilate in response to hypoxia in order to increase oxygen delivery to the tissues. In contrast, small resistance pulmonary arteries constrict in response to hypoxia, a process know as hypoxic pulmonary vasoconstriction (HPV) (20). HPV contributes to the high pulmonary resistance of the fetal circulation, diverting right ventricular blood flow through the ductus arteriosus (11). In the adult, HPV reduces blood flow through atelectatic or underventilated areas of the lung where ventilation is not adequate for oxygenation (11). In this manner, acute HPV is an essential mechanism which helps to match perfusion to ventilation, diverting blood flow away from poorly ventilated regions of the lung in order to maximize arterial O_2 saturation (22). However, when hypoxia becomes generalized, as seen with many lung diseases and with high altitude exposure, the subsequent pulmonary vasoconstriction causes an increase in pulmonary arterial pressure that can lead to the development of pulmonary hypertension.

In pulmonary arterial smooth muscle cells (PASMCs), potassium channels play an essential role in setting the resting membrane potential and, consequently, vascular tone (6,16,23). It is thought that hypoxia regulates pulmonary vasoconstriction by

inhibiting Kv channels open at the resting membrane potential (22). This hypothesis is supported by numerous studies which show that hypoxia inhibits whole-cell K^+ current and causes membrane depolarization in acutely isolated and cultured PASMCs (1,2,12,15,16,24). Membrane depolarization is followed by Ca^{2+} influx through voltage-gated Ca^{2+} channels, PASMC contraction and vasoconstriction (22).

Although the biophysical and pharmacological profile of the O_2-sensitive current in the pulmonary artery has been extensively characterized, the molecular nature of this current is only beginning to be elucidated. Yuan and coworkers used RT-PCR and immunoblotting of primary cultured rat PASMCs to determine which Kv channels are expressed in the pulmonary vasculature (25). This group reported expression of Kv1.1, Kv1.2, Kv1.4, Kv1.5, Kv1.6, Kv2.1, Kv9.3, Kvβ1.1, Kvβ1.2 and Kvβ1.3 channel mRNA and Kv1.2, Kv1.4, Kv1.5, and Kv2.1 channel protein. Archer and colleagues, using a variety of techniques including immunohistochemistry and immunoblotting of freshly dissociated PASMCs from rat resistance pulmonary arteries, reported expression of Kv1.1, Kv1.2 Kv1.3, Kv1.5 and Kv2.1, but not Kv1.4 (2). This group also reported that the addition of Kv1.5 and Kv2.1 antibodies to the patch-clamp pipette solution inhibits the whole-cell O_2-sensitive K^+ current. Gelband and coworkers utilizing the same technique, found that anti-Kv1.5 antibody inhibits the hypoxia-induced membrane depolarization in rat PASMCs (7). Taken together, these results suggest that Kv1.5 and Kv2.1 channel subunits may be important components of the O_2-sensitive K^+ current of PASMCs.

Patel and colleagues, using degenerate RT-PCR of acutely dissociated and primary cultures of rat PASMCs, reported expression of Kv1.2, Kv1.3 and Kv2.1, but not

Kv1.5 (14). Furthermore, they cloned a novel subunit, Kv9.3, which does not form a functional channel itself, but rather assembles with Kv2.1 to form a functional heteromeric channel. This group also examined the O_2-sensitivity of Kv2.1 and Kv2.1/Kv9.3 expressed in COS-7 cells (14). In a subset of COS cells, Kv2.1 (21% of cells) and K2.1/Kv9.3 (56% of cells) currents were reversibly inhibited by hypoxia by 34% and 28%, respectively. Kv1.2 and Kv1.3 channels were largely disregarded as components of the PASMC O_2-sensitive current due to their CTX-sensitivity. To the contrary, Kv1.2 is thought to be an important component of the O_2-sensitive current in PC12 cells, a model for oxygen-sensing in the carotid body (4,5).

Although the Kv2.1/Kv9.3 heteromeric channel is a good candidate for the O_2-sensitive current in PASMCs, the O_2-sensitivity of other potentially important Kv channels has not been directly studied. Therefore, the present study was carried out in attempt to identify Kv channels that are likely to contribute to the O_2-sensitive K^+ current in PASMCs. Specifically, we examined the effects of hypoxia on Kv1.2, Kv1.5, Kv2.1 and Kv9.3 α subunits expressed in mouse L-cells, using the whole-cell configuration of the patch-clamp technique.

MATERIALS AND METHODS

Isolation of Bovine Pulmonary Arteries

Lungs obtained from freshly slaughtered male cattle were immediately placed in ice-cold phosphate-buffered saline (PBS). Resistance pulmonary arteries (defined as 3rd and 4th division intrapulmonary arteries, external diameter 1.5-4 mm) were isolated, removed, and maintained in ice-cold PBS. Additionally, a section of the conduit

pulmonary artery (defined as the main conduit pulmonary artery before it branches, external diameter 20-25 mm) was removed and placed in ice-cold PBS. The pulmonary arteries were dissected free of adventitia, cut open longitudinally, and then gently scraped to remove the endothelium. The resultant pulmonary arterial smooth muscle tissue was processed immediately.

Isolation of Total RNA

Total RNA was isolated using a guanidinium thiocyanate method (3). Briefly, approximately 5 g of pulmonary arterial smooth muscle was homogenized in 50 ml of 4 M guanidinium thiocyanate (4 M GTC, 25 mM Na Citrate, 0.5% N-lauroylsarcosine, pH 7.0), 0.1 M β-mercaptoethanol and 1 drop anti-foam, using a Polytron homogenizer. The lysates were then centrifuged at 1,000 rpm for 10 min at 4°C (JA25.5 rotor) and the resultant supernatant was filtered through a layer of gauze to remove any remaining tissue debris. Next, 2 g of solid cesium chloride (CsCl) was added and the homogenate rocked on a nutator at 4°C until the CsCl was in solution. This solution was divided into 15 ml Corex tubes and centrifuged at 10,000 rpm for 20 min at 4°C (Beckman JA25.5 rotor). The supernatant was layered onto 2-2.5 ml of 5.7 M CsCl cushion and centrifuged at 30,000 rpm for 24 h at 20°C (Beckman SW41 rotor). Following centrifugation, the GTC layer was aspirated with multiple RNase free Pasteur pipettes to the level of the bottom third of the CsCl cushion. The SW41 tube was cut with a hot razor blade and the remaining CsCl cushion was decanted while being careful not to contaminate the RNA pellet. The RNA pellet was dissolved in two 100 µl volumes of TE 6.5, extracted with 200 µl of 1:1 phenol/chloroform, and ethanol precipitated 3 times. The final pellet was

dissolved in approximately 50 µl TE 6.5 (10 mM Tris, 1mM EDTA, pH 6.5) and stored at –80°C until further use.

RT-PCR Analysis

First strand cDNA was prepared using Stratagene's ProStar™ First-strand RT-PCR kit. Ten µg of total RNA were reverse transcribed using 0.3 µg of oligo(dT) primers. Two µl of the resultant cDNA reaction were amplified with channel-specific primers for Kv1.2, Kv1.5, Kv2.1 and Kv9.3 α subunits using a DNA thermal cycler (Stratagene Robocycler gradient 40) under the following conditions: denaturation at 94°C for 10 min, followed by 30 cycles of denaturation at 94°C/1.5 min, annealing at 52-56°C/1.5 min, extension at 72°C/2.5 min, followed by a final extension at 72°C for 10 min. The PCR primers were designed from K^+ channel cDNA sequences reported in GenBank to yield PCR fragments of the following sizes: Kv1.2 (635 bp), Kv1.5 (355 bp), Kv2.1 (563 bp), Kv9.3 (1364 bp) and α smooth muscle actin (322 bp) (see Table 3.1 for PCR primers and conditions). The PCR products were electrophoresed through a 1% agarose gel and the DNA bands were visualized by ethidium bromide staining. Reactions without cDNA or *Taq* polymerase were used as controls. Positive PCR products were confirmed by Southern blot and/or sequenced by the Colorado State University Macromolecular Resources Facility.

Southern Blot Analysis

A Southern blot with specific K^+ channel probes was performed to confirm PCR products. The PCR gels were soaked for 1 h in denaturing solution (0.5N NaOH, 1.5 M NaCl), followed by 1 h in neutralizing solution (0.5N Tris-HCl, 1.5M NaCl, pH 8.0).

The denatured cDNA was transferred overnight to Protran® nitrocellulose membrane (Schleicher & Schuell) by capillary action. The cDNA was cross-linked via UV light to the nitrocellulose and hybridized overnight at 42°C in hybridization solution containing: 50% formamide, 4 X SSPE (600 mM NaCl, 40 mM NaH2PO4, 4 mM EDTA, pH 7.4), 5 X BFP (1 g/liter bovine serum albumin, 1 g/liter polyvinylpyrrolidone 40, 1 g/liter Ficoll, 0.001% sodium azide), 0.2% sodium dodecyl sulfate (SDS), and 0.02 mg/ml sonicated salmon sperm DNA. The templates for the random primer synthesized probes were previously sequenced rat cDNAs of the following nucleotides (the adenine of the initiating codon ATG was at +1): Kv1.2 (505-1494), Kv1.5 (1-2004), Kv2.1 (963-2119), and Kv9.3 (-1-1522). Using a RadPrime DNA labeling system (Gibco) 25 ng of each Kv channel cDNA was labeled with 50 μCi of α-^{32}P ATP. The radioactive probes were denatured, and approximately one third of the probe was added to the hybridization solution and incubated with the blots overnight at 42°C. Following hybridization, the blots were washed at 42°C 2 times for 15 min each with the following solutions: 3 X SSC + 1% SDS, 1X SSC + 1% SDS, followed by 0.2 X SSC + 1% SDS.

Northern Blot Analysis

Northern blots with specific K^+ channel probes were also performed. Ten μg of total RNA were run on a 1% agarose, 8% formaldehyde gel at 30 volts for 5-7 h. The RNA was then transferred overnight to Nitran® nylon membrane (Schleicher & Schuell) by capillary action. The RNA was cross-linked via UV light to the nylon and hybridized overnight at 65°C in hybridization solution containing: 20% formamide, 4 X SSPE, 5 X BFP, 5% SDS, 1 N HCl, 0.5 M $NaPO_4$, 10% dextran sulfate and 0.02 mg/ml sonicated

salmon sperm DNA. The templates for the random primer synthesized probes were previously sequenced rat cDNAs of the following nucleotides (the adenine of the initiating codon ATG was at +1): Kv1.2 (505-1494), Kv1.5 (1-2004), Kv2.1 (963-2119), and Kv9.3 (54-1522). Using a RadPrime DNA labeling system (Gibco), 25 ng of each Kv channel cDNA was labeled with 50 μCi of α-^{32}P ATP. The radioactive probes were denatured, added to the hybridization solution, and incubated with the blots overnight at 65°C. Following hybridization, the blots were washed 2 times for 15 min (65 °C) each with the following solutions: 3 X SSC + 1% SDS, 1X SSC + 1% SDS, followed by 0.2 X SSC + 1% SDS.

Cloning of Kv9.3 and Production of the Channel DNA Constructs

The Kv9.3 cDNA was obtained from rat lung RNA using Stratagene's ProStar™ First-strand RT-PCR kit as described above, with the exception that different primers were used. The upper primer began at –2 (the adenine of the initiating codon ATG was at +1) and the lower primer started at nucleotide 1623. PCR yielded a 1625 bp fragment that was gel-purified and subcloned into the pCR2.1 TA cloning vector (Invitrogen). The fragment was then subcloned into the *XbaI* and *SmaI* sites of a modified pBKCMV expression vector that had the β-galactosidase ATG deleted. This vector was selected to increase expression efficiency of the channel and to remove the possibility that expressed channels contain a β-galactosidase protein sequence at the N-terminus.

Kv1.2, Kv1.5 and Kv2.1 cDNAs had previously been cloned and were available for use in the Tamkun Laboratory. Previously, the 1600 bp fragment encoding the open reading frame of the rat Kv1.2 cDNA was blunted and subcloned into the $pCMV_4$ expression vector (10). The 2100 bp fragment encoding the open reading frame of the rat

Kv2.1 cDNA was previously blunted and subcloned into the pMSVNeo expression vector (18). The Kv1.5/Kv1.2 tandem was constructed by using overlap PCR to link the C-terminus of Kv1.5 to the N-terminus of Kv1.2 (as described in (10)). The tandem was blunt-end ligated into the *SmaI* site of the modified pBKCMV expression vector.

All DNA constructs were confirmed by restriction analysis and automated sequencing.

Transfection and Tissue Culture

All transfection and tissue culture was performed as previously described (10). Basically, mouse L-cells were grown on 60 mm plastic dishes in Dulbecco's modified Eagle medium (Gibco), supplemented with 10% horse serum, in the presence of G418, penicillin, streptomycin and gentamycin at 37°C and 5% CO_2. The mouse L-cell line expressing human Kv1.5 was used as previously described (18). Rat Kv2.1/pMSVNeo was transfected into mouse L-cells and stable cell lines were produced and cultured as described previously (18). Rat Kv1.2 and rat Kv9.3 were studied under transient transfection conditions. For transient transfections, 1 μg of rKv1.2/pCMV$_4$ or 0.6 μg of rKv9.3/pBKCMV was combined with 0.4 μg GFP/pCI (to assess transfection efficiency and to identify cells for voltage-clamp analysis), 15 μl lipofectamine and 0.5 ml of serum-free Dulbecco's modified Eagle medium (Gibco) and then incubated at 37 °C for approximately 30 min. Mouse L-cells, 40% to 60% confluent, were incubated with the lipofectamine mixture for 6 to 8 h after which time the mixture was removed and replaced with standard culture medium for 36 to 48 h. Cells were removed from the dish by trypsinization, centrifuged at low-speed and the resultant pellet resuspended in standard culture medium at room temperature for use within the next 12 h.

Heteromeric Formation of Kv1.2/Kv1.5 and Kv2.1/Kv9.3 Channels

Mouse L-cells stably expressing rKv2.1 were transfected with 0.6 μg of rKv9.3 while mouse L-cells stably expressing hKv1.5 were transfected with 1 μg of rKv1.2 as described above and in reference (10). After transfection, cells were incubated for 36 h in standard culture medium and then incubated with 2 μmol/liter dexamthasone for 18 to 24 h in order to induce expression of Kv1.5 or Kv2.1 and therefore allow Kv1.5/Kv1.2 and Kv2.1/Kv9.3 heteromeric channel formation.

Kv9.3 is electrically silent when expressed as a homomeric channel and modifies the activation and deactivation kinetics and shifts the activation curve in the hyperpolarizing direction of Kv2.1 when expressed as a heteromeric channel (14). Therefore, Kv2.1/Kv9.3 heteromeric channel assembly could be readily detected. Heteromeric assembly between Kv1.2 and Kv1.5 was more difficult to assess, therefore, multiple criteria were used as a guideline for heteromeric assembly. The current kinetics and activation curves generated from Kv1.2 and Kv1.5 homomeric channels and Kv1.2/Kv1.5 heteromeric channels allowed for some differentiation. Coexpression of Kv1.2 and Kv1.5 produced currents with faster activation kinetics and partial inactivation as compared with Kv1.2 alone (10). Furthermore, analysis of the voltage dependence of activation revealed that these data were best fit with a single Boltzmann equation with an activation midpoint of -4.55 ± 1.09 mV while Kv1.2 and Kv1.5 had activation midpoints of 22 mV and −13 mV respectively. When these channels were coexpressed, activation curve data which were best fit by the sum of 2 Boltzmann equations were disregarded based on the assumption that these data reflected the summation of distinct populations of

Kv1.2 and Kv1.5 homomeric channels. As a further criterion of heteromeric channel assembly, DTX sensitivity was also assessed. Kv1.2 current is sensitive to DTX (K_d=~20 nmol/liter) while Kv1.5 current is virtually insensitive (K_d>300 nmol/liter) (8). Recent studies suggest that the presence of the Kv1.5 DTX-insensitive subunit dominates the DTX-sensitivity of the Kv1.2/Kv1.5 heteromeric channel (19). In the present study Kv1.2/Kv1.5 heteromeric channels containing 1 or more DTX-insensitive Kv1.5 α subunit(s) should be insensitive to 50 nmol/liter DTX. Therefore, only currents that were insensitive to 50 nmol/liter DTX and fit a single Boltzmann equation were considered to represent heteromeric Kv1.2/Kv1.5 channel complexes and thus used for further analysis. To confirm our results, the O_2-sensitivity of the Kv1.5/Kv1.2 tandem construct was also examined.

Electrophysiology

All electrophysiological experiments were performed by Dr. Joanne Hulme. These experiments were performed in a 180 µl bath mounted on the stage of an inverted microscope (Nikon) while continuously superfused at a flow rate of approximately 0.5 to 1.0 ml/min (10). Recordings using the whole-cell configuration of the patch-clamp technique (9) were made with an Axopatch 200A amplifier (Axon Instruments). Patch pipettes, 1 to 2 MΩ, were pulled from borosilicate glass capillaries. Junction potentials were corrected with the tip of the electrode in the bath solution before gigohm seal formation was achieved with gentle suction. Once the whole-cell configuration was established, capacitive transients elicited by symmetrical 10 mV voltage clamp steps from –80 mV were recorded in order to calculate cell capacitance and access resistance. Cells with >5 nA currents were discarded. Currents were filtered at 0.5 to 2 kHz and

sampled at 1 to 5 kHz. Data acquisition and command potentials were controlled through pClamp software (version 6.04, Axon Instruments) and stored for future analysis. All experiments were performed at 21 °C to 23 °C.

Solutions

The solutions used in these experiments have been described (10). The intracellular pipette solution contained (in mmol/liter): KCl 110, HEPES 10, K_2BAPTA 5, K_2ATP 5 and $MgCl_2$ 1 adjusted to pH 7.2 with KOH. The bath solution contained (in mmol/L): NaCl 110, KCl 4, $MgCl_2$ 1, $CaCl_2$ 1.8, HEPES 10 and glucose 1.8, adjusted to pH 7.35 with NaOH. The effect of hypoxia was examined by switching between normoxic and hypoxic perfusate reservoirs. Normoxic solutions were equilibrated with 100% O_2 while hypoxic solutions were equilibrated with 100% N_2 for at least 20 min. Additionally, for hypoxic experiments, a stream of N_2 was passed over the surface of the bath. PO_2 was continuously monitored in the bath chamber using an O_2-sensitive microelectrode (IDO_2/OXEL-1, World Precision Instruments) giving PO_2 values of approximately 140 to 160 mm Hg in normoxic conditions and 30 to 40 mm Hg in hypoxic conditions. Additionally, pH and temperature were monitored regularly and maintained at 7.35 and, 21°C - 23°C, respectively.

Pulse Protocols and Analysis

Pulse protocols and analyses were performed as previously described (10). The holding potential was set at –80 mV and the cycle time within each protocol was 10 s. Current-voltage relationships and activation curves were obtained using a standard protocol which consisted of 250-ms voltage-clamp pulses applied in 10 mV steps

between –70 and 60 mV, unless otherwise indicated. Steady-state current-voltage relationships were obtained by measuring the current at the end of the voltage-clamp pulse and plotted against test potential. Currents from each cell were normalized relative to its control (normoxic) current at 60 mV. Deactivating tail currents were recorded at -40 mV. Activation curves were obtained from the maximum value of the tail current amplitude immediately after the capacitive transients.

Statistical Analysis

Data are expressed as the mean ± SEM of n cells. Comparisons between groups were made using a Student's paired t test. Values of $p<0.05$ were considered statistically significant.

RESULTS

mRNA Expression of Kv Channels Subunits in Bovine PASMCs

As there is some contradiction in the literature regarding which Kv α subunits are expressed in the pulmonary artery, we decided to test for mRNA expression of candidate O_2-sensitive α subunits before beginning the electrophysiological experiments. Therefore, RT-PCR was performed to determine the expression of Kv1.2, Kv1.5, Kv2.1 and Kv9.3 α-subunits in bovine conduit and resistance PASMCs. Kv1.2, Kv2.1 and Kv9.3 were amplified from conduit and resistance PASMCs with 30 PCR cycles (Figure 3.1 A-C). Alpha actin, an actin isoform specific for smooth muscle, was used as a control for the integrity of the smooth muscle cell RNA. Kv1.5 PCR did not yield a single predominate band, rather it gave several bands of similar intensity (data not shown); however, Southern blot analysis of the PCR products confirmed expression of

Kv1.5. Additionally, Kv1.5 mRNA expression was further confirmed via Northern blot analysis of bovine conduit and resistance PASMCs (Figure 3.1 D).

Cloning of Rat Kv9.3

Rat Kv9.3 cDNA was obtained from rat lung RNA using RT-PCR. The translated amino acid sequence was 98.3% homologous to the rat Kv9.3 sequence previously reported in Genbank (14) with two amino acid substitutions (Figure 3.2). At position number 113 our sequence had a isoleucine in place of a phenylalanine and at position 209 our sequence had a glycine in place of a glutamate.

O_2-Sensitivity of Kv2.1 Expressed in Mouse L-Cells

Representative outward currents recorded from a holding potential of –80 mV to a test potential of 60 mV, before, during and after 10 min exposure to the hypoxic solution are shown in Figure 3.3. In this example, hypoxia significantly and reversibly inhibited the Kv2.1 current by approximately 23% at 60 mV. Inhibition occurred within approximately 1 min after hypoxic exposure and continued to decrease, paralleling the decreasing PO_2, until it reached steady state after 7 min (10). Only those currents activated at potentials more positive to 30 mV were significantly inhibited by hypoxia (data not shown). Furthermore, very little Kv2.1 current was detected at potentials more negative than –20 mV. Hypoxia had no effect on the voltage dependence of activation (control, $V_{0.5}$=11.37±1.35 mV, n=15; hypoxia, $V_{0.5}$=10.73±1.27 mV, n=10), which implies that the observed decrease in Kv2.1 current was not due to a shift in the midpoint of activation (data not shown). These data suggest that while Kv2.1 seems to be sensitive

to hypoxia, it does not occur in the voltage range of PASMCs resting membrane potential.

O_2-Sensitivity of Kv2.1/9.3 Expressed in Mouse L-Cells

Cells transfected with Kv9.3 alone did not express any Kv channel activity; however, coexpression of Kv9.3 with Kv2.1 altered the biophysical properties of the Kv2.1 channel alone (10). Kv9.3 increased activation kinetics, slowed deactivation kinetics, and caused a hyperpolarizing shift in the voltage dependence of activation of Kv2.1 alone (10). Hypoxia significantly and reversibly inhibited the Kv2.1/Kv9.3 current at 60 mV (Figure 3.4 A). This hypoxic inhibition was detected in all cells studied. Mean hypoxic inhibition of Kv2.1/Kv9.3 current was 21$\pm$0.9% at 60 mV, which was not significantly different from Kv2.1 alone. Furthermore, like Kv2.1, hypoxia had no effect on the midpoint of activation of Kv2.1/Kv9.3 (data not shown). In contrast to Kv2.1, however, current from the Kv2.1/Kv9.3 heteromeric channel was sensitive to hypoxia at more physiologically relevant membrane potentials. Figure 3.4 B summarizes the mean data at negative test potentials illustrating that hypoxia significantly inhibited Kv2.1/Kv9.3 current at physiologically relevant potentials. Therefore, these data strongly support a role for the Kv2.1/Kv9.3 heteromeric channel in the physiological response of PASMCs to hypoxia.

O_2-Sensitivity of Kv1.5 and Kv1.2 Homomeric Channels Expressed in Mouse L-Cells

The effects of hypoxia on Kv1.5 channels expressed in mouse L-cells were examined. Hypoxia had no effect on Kv1.5 current at 60 mV (Figure 3.5 A). Additionally, although Kv1.5 current activated at more physiologically relevant

potentials (current was detected at –55 mV), this current was not sensitive to hypoxia at any potential (data not shown).

The effects of hypoxia on Kv1.2 were also examined and are illustrated in Figure 3.5 B and C. Kv1.2 current was significantly and reversibly inhibited by hypoxia at 60 mV (Figure 3.5 B). At 80 mV, the mean hypoxic inhibition was 19±0.2%. However, little Kv1.2 current was activated at negative potentials and current apparent at –10 mV was not significantly inhibited by hypoxia (Figure 3.5 C). These data suggest that Kv1.5 and Kv1.2 homomeric channels are not likely to contribute to the PASMCs O_2-sensitive K^+ current.

O_2-Sensitivity of Kv1.2/Kv1.5 Heteromeric Channels Expressed in Mouse L-Cells

The biophysical and pharmacological characteristics of the K^+ current generated by coexpression of Kv1.2 and Kv1.5 α subunits in mouse L-cells were examined (10). Coexpression of Kv1.2 with Kv1.5 produced currents with faster activation kinetics and partial inactivation compared with Kv1.2 alone (10). Furthermore, analysis of the voltage dependence of activation revealed that these data were best fit with a single Boltzmann equation with an activation midpoint of –4.55±1.09 mV, compared with 21.73±0.65 mV and –12.88±0.68 mV, for Kv1.2 and Kv1.5, respectively (data not shown). Additionally, Kv1.2 current was significantly inhibited by 50 nmol/liter DTX, while Kv1.5 and Kv1.2/Kv1.5 currents were unaffected (10). The electrophysiological and pharmacological data suggested the heteromeric assembly of Kv1.2 and Kv1.5 α subunits in a subset of transfected cells (10). Therefore, we examined the O_2-sensitivity of the Kv1.2/Kv1.5 current in cells with the appropriate electrophysiological and pharmacological characteristics. Hypoxia significantly and reversibly inhibited the

Kv1.2/Kv1.5 current expressed in mouse L-cells (Figure 3.6) with no effect on the midpoint of activation (data not shown). Figure 3.6 A shows a representative current tracing in which hypoxia significantly and reversibly inhibited the current by approximately 18% at 60 mV. Figure 3.6 B summarizes the mean data at negative test potentials illustrating that hypoxia significantly inhibited the Kv1.2/Kv1.5 current at physiologically relevant potentials. Therefore, these data suggest a role for the Kv1.2/Kv1.5 heteromeric channel in the physiological response of PASMCs to hypoxia.

DISCUSSION

In agreement with previous reports (2,14,25), expression of Kv2.1 was confirmed. The observation that Kv2.1 is reversibly inhibited by hypoxia is also consistent with previous findings suggesting a possible role for this channel in the O_2-sensitive current of PASMCs (2,14). When heterologously expressed as a homotetramer, however, Kv2.1 does not activate in the voltage range of the PASMC resting membrane potential (14), suggesting that it alone may not be responsible for the physiological response of PASMCs to hypoxia. Furthermore, when expressed in oocytes, Kv2.1 current was found to be insensitive to hypoxia (4). On the other hand, when coexpressed with Kv9.3, Kv2.1 and Kv9.3 α subunits assemble to form a functional heterotetramer which activates near the voltage range of the resting membrane potential for PASMCs (14). In support of this observation, coexpression of Kv2.1 and Kv9.3 α subunits in mouse L-cells generated currents that activated near the resting membrane potential of PASMCs (10). Furthermore, hypoxia inhibited the Kv2.1/Kv9.3 heteromeric channel at physiologically relevant membrane potentials, suggesting that this channel may indeed be important in

the physiological response of PASMCs to hypoxia. Patel and coworkers also found that the Kv2.1/Kv9.3 channel was inhibited by hypoxia, but these effects were only apparent in a subset (56%) of transfected COS cells (14). In contrast, hypoxia reversibly inhibited the Kv2.1/Kv9.3 channel in all L-cells studied. These data suggest that there may be an endogenously expressed O_2-sensor, which couples to the channel, that is expressed in all mouse L-cells, but only a subset of COS cells.

Many studies have reported a role for Kv1.5 in PASMC O_2-sensing. Archer et al, using antibodies specific for Kv1.5, argue in favor of Kv1.5 being an important molecular component of HPV (2). Additionally, Wang and co workers reported that chronic hypoxia down-regulates Kv1.5 mRNA expression in cultured PASMCs (21). On the other hand, Patel et al were unable to detect Kv1.5 message by PCR using defined or degenerate primers (14). In the current study, expression of Kv1.5 message was demonstrated in PASMCs via Northern analysis (Figure 3.1 D). Initially, we were unable to amplify Kv1.5 using primers specific for the C-terminus; however, we were successful in amplifying Kv1.5 using PCR primers to the N-terminus and lower annealing temperatures (data not shown). While multiple PCR products were generated, Kv1.5 amplification was confirmed via Southern blot analysis. Although Kv1.5 appears to be expressed in PASMCs, it was not found to be O_2-sensitive when expressed in mouse L-cells, despite the fact that this current activated in the range of the PASMC resting membrane potential and furthermore, that anti-Kv1.5 antibodies inhibit the native hypoxia-sensitive current (2). As with human Kv1.5, rat Kv1.5 was also found to be insensitive to hypoxia (data not shown), therefore, ruling out a species difference. This is in agreement with a more recent study that found Kv1.5 to be insensitive to hypoxia in

MEL cells (13). The inability of Kv1.5 to respond to hypoxia therefore suggests that Kv1.5 homomeric channels do not contribute to the O_2-sensitive current of PASMCs.

Expression of Kv1.2 mRNA was confirmed in PASMCs. Although Kv1.2 expression is well documented (2,14,21,25) it has been largely ignored as a molecular component of the PASMC O_2-sensitive current on the basis of its CTX sensitivity (2,14,25). Kv1.2 is significantly inhibited by CTX in the nanomolar range (K_d<20 nmol/L) (8), whereas the PASMC O_2-sensitive current is virtually CTX-insensitive (K_d>300 nmol/liter) (2,14,25). In the present study, Kv1.2 current was significantly inhibited by hypoxia when expressed in mouse L-cells. However, this current only activated at depolarized potentials. This is in agreement with a more recent study (4), which found Kv1.2 current to be significantly inhibited by hypoxia in *Xenopus* oocytes (4). Even more recently, Kv1.2 was found to be insensitive to hypoxia in B82 cells (13); however, upon further study, this same group found significant Kv1.2 current inhibition by hypoxia (personal communication with Dr. Gurney).

Kv1.2 and Kv1.5 α subunits assemble together to form a functional channel *in vitro* (8,17,19). Furthermore, the toxin-sensitivity of this heteromeric channel is dominated by the presence of the Kv1.5 DTX- and CTX-insensitive subunit (17,19). Because both subunits are expressed in the pulmonary artery, and because the Kv1.2/Kv1.5 heteromeric channel fits the profile of the pulmonary arterial O_2-sensitive K^+ current, the O_2-sensitivity of this heteromeric channel was examined in mouse L-cells. These data confirmed that Kv1.2 and Kv1.5 α subunits can assemble to form heteromeric channels with distinct electrophysiological and pharmacological properties from those of Kv1.2 and Kv1.5 homomeric channels (10). When these subunits were coexpressed,

65% of the cells analyzed were best fit with two Boltzman equations, suggesting the summation of Kv1.2 and Kv1.5 homomeric channels. Therefore, only cells whose activation curves were best fit with a single Boltzman equation (35%) were used to test the hypoxic sensitivity of the Kv1.2/Kv1.5 heteromeric channel (10).

Consistent with the idea that the presence of the Kv1.5 toxin-insensitive channel subunit dominates the pharmacology of the heteromeric channel (17,19), Kv1.2/Kv1.5 current was found to be insensitive to 50 nmol/L DTX (10). Furthermore, this current was significantly inhibited by hypoxia in the voltage range of the PASMC resting membrane potential. This is not likely due to the summation of Kv1.2 and Kv1.5 channels since current at the more negative potentials should be carried entirely by Kv1.5, which was not found to be O_2-sensitive (10). Furthermore, these data were confirmed with the Kv1.5/Kv1.2 tandem (10). The Kv1.2/Kv1.5 heteromeric channel is a likely candidate for the pulmonary arterial O_2-sensitive K^+ channel in that it responds to hypoxia in the voltage range of the PASMC resting membrane potential and it fits the electrophysiological and pharmacological profile of the O_2-sensitive channel in PASMCs.

In summary, the present study dealt with the O_2-sensitivity of cloned channels heterologously expressed in mouse L-cells in attempt to identify, from a molecular perspective, which Kv channels are likely candidates for the O_2-sensitive current expressed in PASMCs. The results of this study (summarized in Table 3.2) suggest the following: Kv1.2 and Kv2.1, but not Kv1.5, homomeric channels are reversibly inhibited by hypoxia. Kv1.2 and Kv1.5 α subunits can assemble to form a functional heteromeric channel that is sensitive to hypoxia. Furthermore, as previously shown (14), Kv2.1 and Kv9.3 α subunits also assemble to form a functional heteromeric channel that is sensitive

to hypoxia. Additionally, of the above channels, only the heteromeric channels, Kv1.2/Kv1.5 and Kv2.1/Kv9.3, were found to be significantly inhibited by hypoxia in the voltage range of the PASMC resting membrane potential, suggesting that these channels are likely components of the O_2-sensitive K^+ current in the pulmonary artery. This study was limited by the fact that we studied cloned channels expressed in a heterologous expression system, which cannot possibly mimic the environment surrounding the channel in PASMCs; however, it was an important first step in the molecular characterization of the PASMC O_2-sensitive K^+ currents. Localization of these channel proteins to resistance PASMCs and confirmation of heteromeric channel expression *in vivo* is the topic of Chapter 4.

Table 3.1 PCR Primers and Conditions

Name	*GenBank Accession #*	*Upper Primer (nt)**	*Lower Primer (nt)**	*Fragment Size (bp)*	*Annealing Temperature (°C)*	*Number of Cycles*
Kv1.2 (bovine)	X57033	379-396	997-1014	635	55	30
Kv1.5 (rat)	M27158	753-780	1108-1133	355	52	35
Kv2.1 (rat)	X16476	836-857	1378-1399	563	53	30
Kv9.3 (rat)	AF029056	-1-17	1343-1363	1364	56	30
α-actin (rat)	X06801	103-120	425-442	322	52-56	30-35

*The adenosine of the ATG start site is +1

Table 3.2. Summary table of the O_2-sensitivity of cloned Kv channels in mouse L-cells

Kv channel	*O_2-sensitivity*	*Physiological potentials*
Kv1.2	Yes	No
Kv1.5	No	No
Kv1.2/Kv1.5	Yes	Yes
Kv2.1	Yes	No
Kv2.1/Kv9.3	Yes	Yes

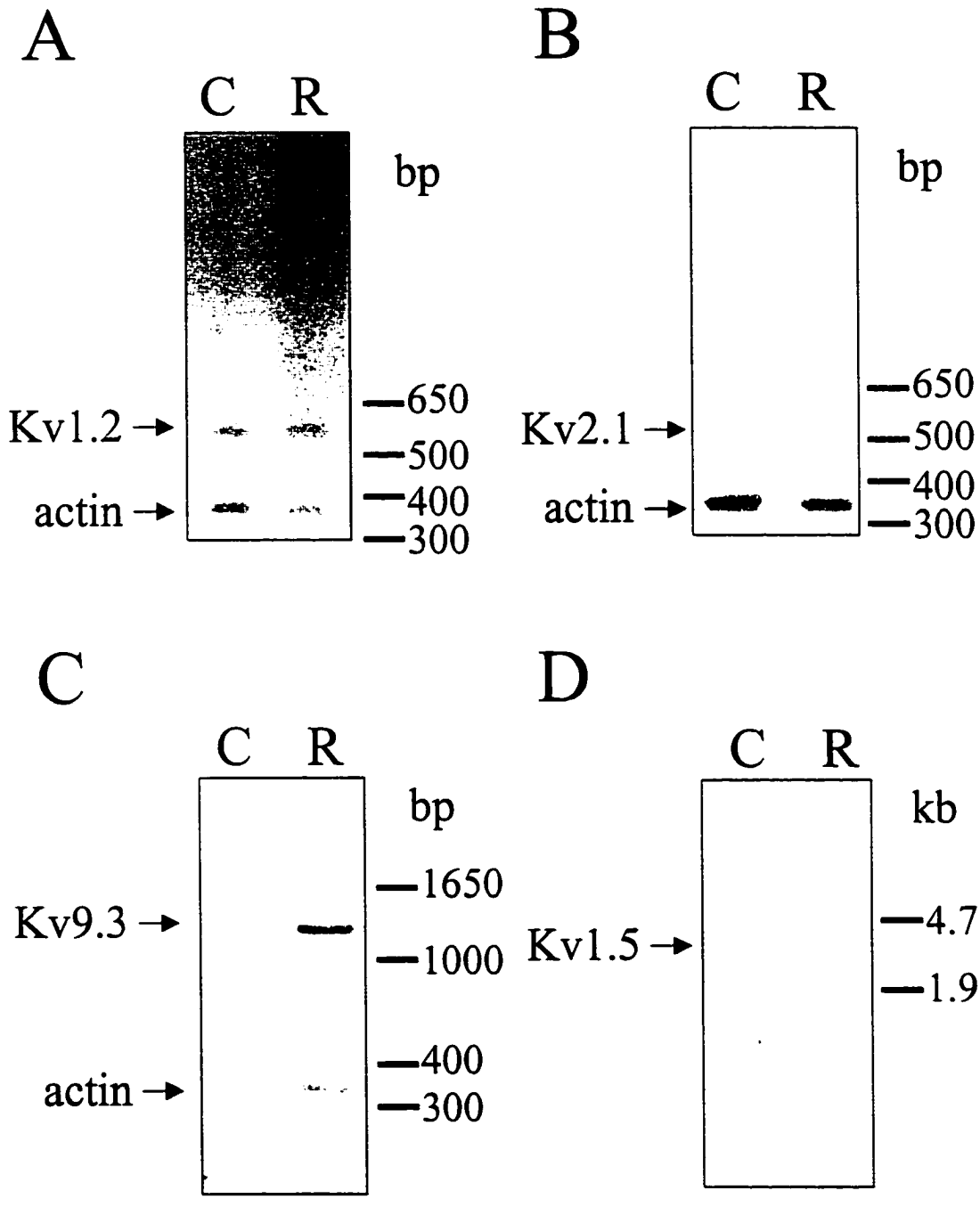

Figure 3.1. Detection of Kv α-subunit mRNA in C (conduit) and R (resistance) bovine pulmonary artery. A-C) RT-PCR amplification of Kv α-subunits and α-actin mRNA. Amplified products were displayed in acrylamide gel stained with ethidium bromide. All amplified Kv α-subunits are listed with fragment sizes in parentheses: A) Kv1.2 (620 bp), B) Kv2.1 (550 bp), C) Kv9.3 (1350 bp). D) Northern blot analysis of Kv1.5 mRNA. Each lane represents 10 μg of total RNA. Positions of the large and small rRNA subunits, approximately 4.7 and 1.9 kb, respectively, are indicated.

```
                  10         20         30         40         50
Coppock      1 MVFGEFFHRP GQDEELVNLN VGGFKQSVDQ STLLRFPHTR LGKLLTCHSE      50
Patel        1 MVFGEFFHRP GQDEELVNLN VGGFKQSVDQ STLLRFPHTR LGKLLTCHSE      50

                  60         70         80         90        100
Coppock     51 EAILELCDDY SVADKEYYFD RNPSLFRYVL NFYYTGKLHV MEELCVFSFC     100
Patel       51 EAILELCDDY SVADKEYYFD RNPSLFRYVL NFYYTGKLHV MEELCVFSFC     100

                 110        120        130        140        150
Coppock    101 QEIEYWGINE LFIDSCCSSR YQERKEESHE KDWDQKSNDV STDSSFEESS     150
Patel      101 QEIEYWGINE LFFDSCCSSR YQERKEESHE KDWDQKSNDV STDSSFEESS     150

                 160        170        180        190        200
Coppock    151 LFEKELEKFD ELRFGQLRKK IWIRMENPAY CLSAKLIAIS SLSVVLASIV     200
Patel      151 LFEKELEKFD ELRFGQLRKK IWIRMENPAY CLSAKLIAIS SLSVVLASIV     200

                 210        220        230        240        250
Coppock    201 AMCVHSMSGF QNEDGEVDDP VLEGVEIACI AWFTGELAIR LVAAPSQKKF     250
Patel      201 AMCVHSMSEF QNEDGEVDDP VLEGVEIACI AWFTGELAIR LVAAPSQKKF     250

                 260        270        280        290        300
Coppock    251 WKNPLNIIDF VSIIPFYATL AVDTKEEESE DIENMGKVVQ ILRLMRIFRI     300
Patel      251 WKNPLNIIDF VSIIPFYATL AVDTKEEESE DIENMGKVVQ ILRLMRIFRI     300

                 310        320        330        340        350
Coppock    301 LKLARHSVGL RSLGATLRHS YHEVGLLLLF LSVGISIFSV LIYSVEKDEL     350
Patel      301 LKLARHSVGL RSLGATLRHS YHEVGLLLLF LSVGISIFSV LIYSVEKDEL     350

                 360        370        380        390        400
Coppock    351 ASSLTSIPIC WWWATISMTT VGYGDTHPVT LAGKIIASTC IICGILVVAL     400
Patel      351 ASSLTSIPIC WWWATISMTT VGYGDTHPVT LAGKIIASTC IICGILVVAL     400

                 410        420        430        440        450
Coppock    401 PITIIFNKFS KYYQKQKDMD VDQCSEDPPE KCHELPYFNI RDVYAQQVHA     450
Patel      401 PITIIFNKFS KYYQKQKDMD VDQCSEDPPE KCHELPYFNI RDVYAQQVHA     450

                 460        470        480        490        500
Coppock    451 FITSLSSIGI VVSDPDSTDA SSVEDNEDAY NTASLENCTA K.........     500
Patel      451 FITSLSSIGI VVSDPDSTDA SSVEDNEDAY NTASLENCTA K.........     500
```

Figure 3.2. Comparison of current (Coppock) rat Kv9.3 amino acid sequence with the published rat Kv9.3 amino acid sequence (Patel et al, 1997). The two amino acid differences at positions 113 and 209 are highlighted in color.

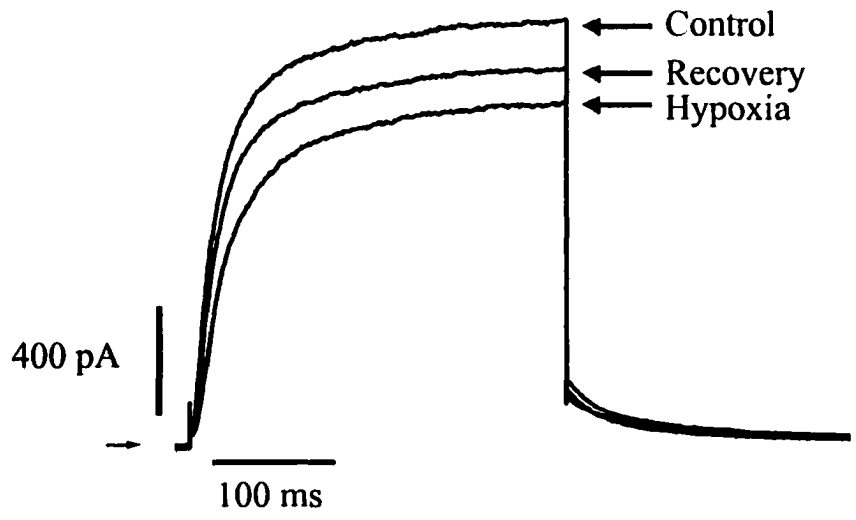

Figure 3.3. Effect of hypoxia on Kv2.1 current expressed in mouse L-cells. Representative current tracings elicited in response to step depolarization from -80 mV to 60 mV before, during and after 10 min of exposure to hypoxic solution. Voltage-clamp analysis performed by Dr. Joanne Hulme.

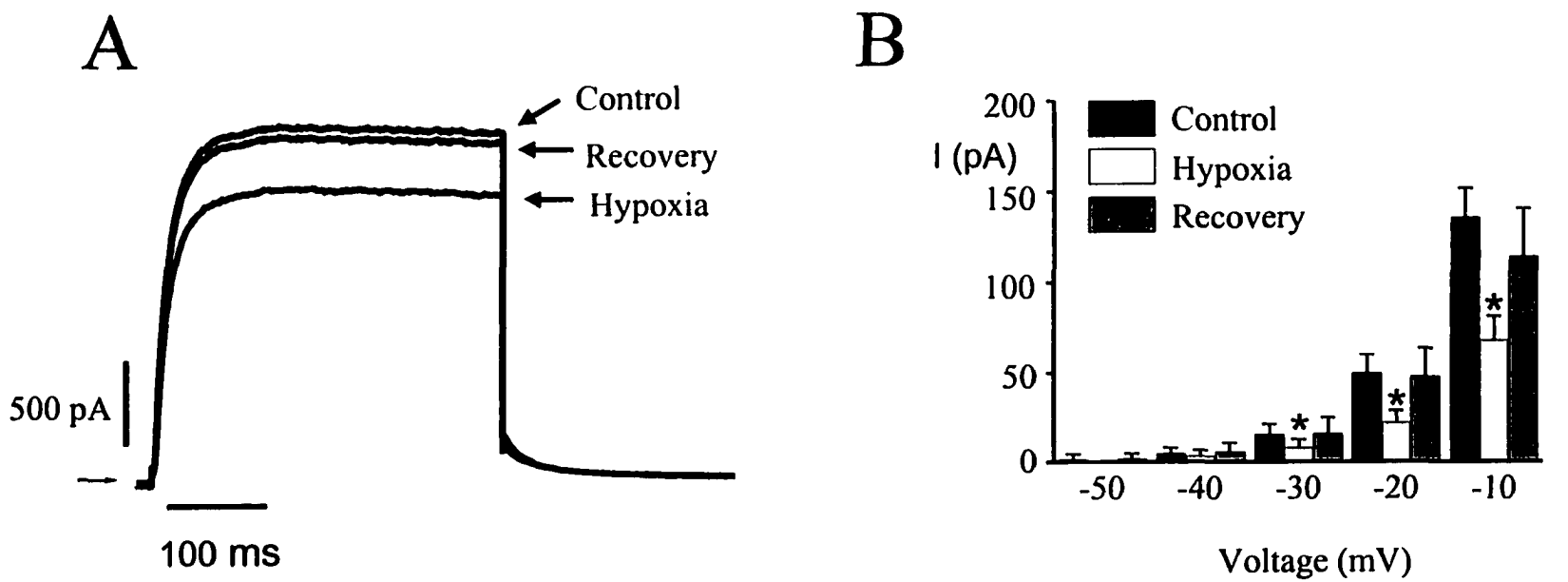

Figure 3.4. Effect of hypoxia on Kv2.1/Kv9.3 heteromeric channels expressed in mouse L-cells. A) Representative current tracings elicited in response to step depolarization from –80 mV to 60 mV before, during and after 10 min of exposure to hypoxic solution. B) Bar graph highlighting the effects of hypoxia on Kv2.1/Kv9.3 current at more negative potentials. Voltage-clamp analysis performed by Dr. Joanne Hulme. *Significantly different from control.

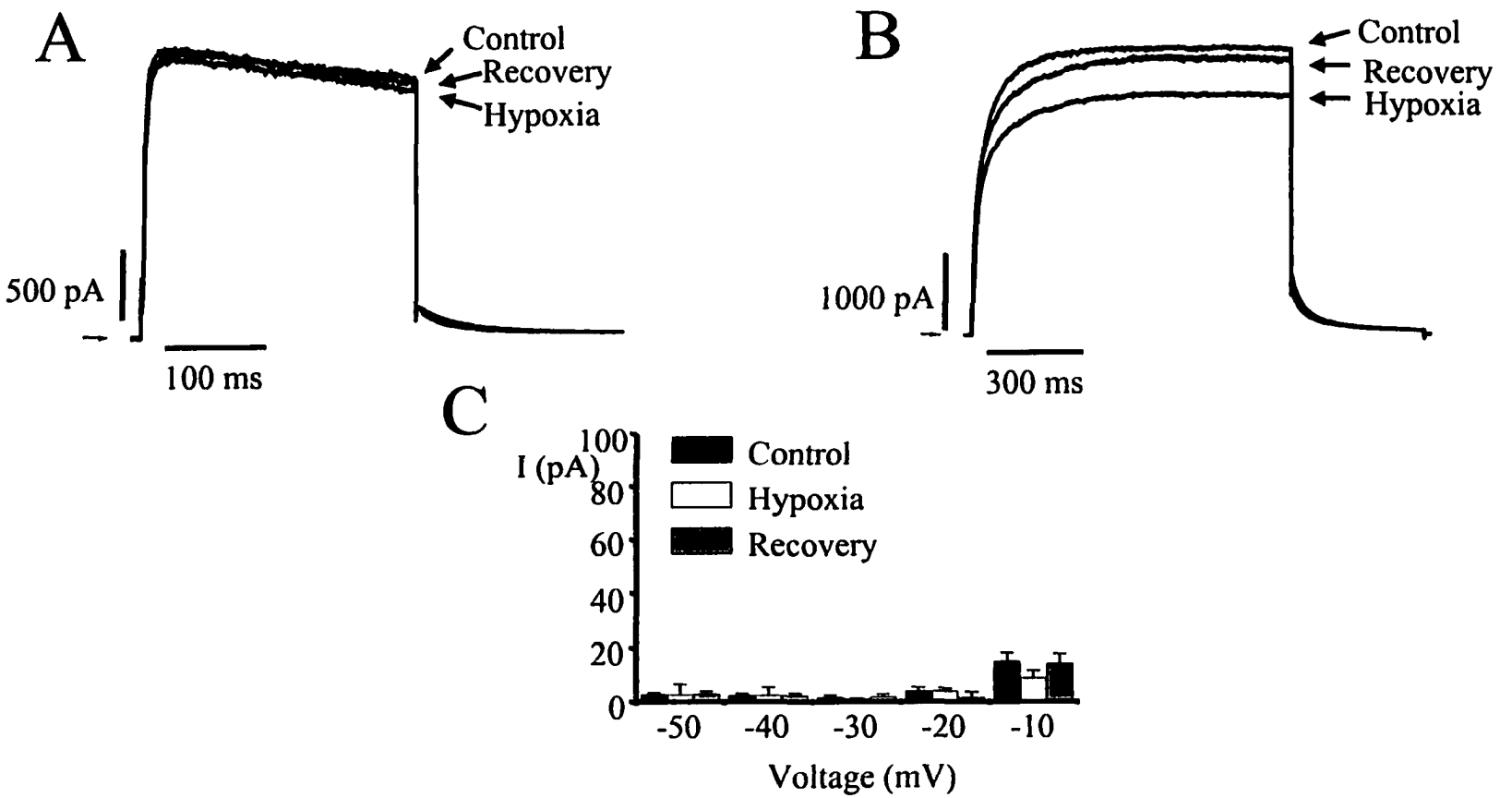

Figure 3.5. Effect of hypoxia on Kv1.5 and Kv1.2 current expressed in mouse L-cells. Representative current tracings of A) Kv1.5 and B) Kv1.2 currents elicited in response to step depolarization from –80 mV to 60 mV before, during and after 10 min of exposure to hypoxic solution. C) Bar graph highlighting the effects of hypoxia on Kv1.2 current at more negative potentials. Voltage-clamp analysis performed by Dr. Joanne Hulme.

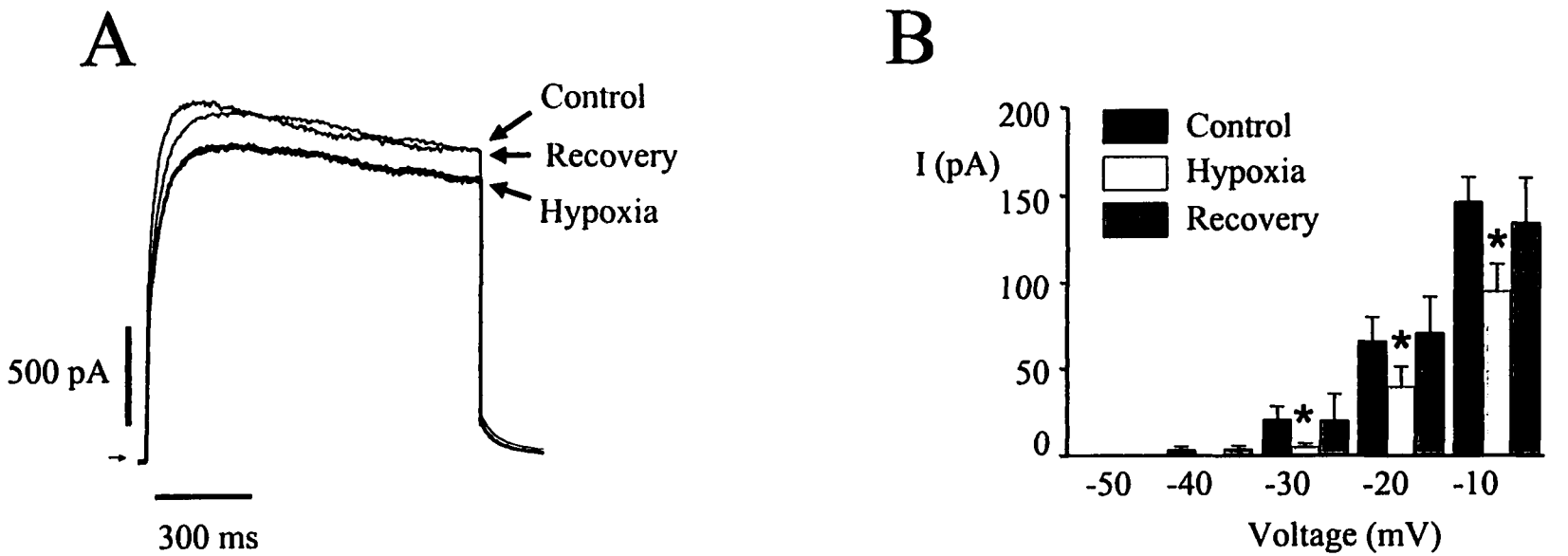

Figure 3.6. Effect of hypoxia on Kv1.2/Kv1.5 heteromeric channels expressed in mouse L-cells. A) Representative current tracings elicited in response to step depolarization from –80 mV to 60 mV before, during and after 10 min of exposure to hypoxic solution. B) Bar graph highlighting the effects of hypoxia on Kv1.2/Kv1.5 current at more negative potentials. Voltage-clamp analysis performed by Dr. Joanne Hulme. *Significantly different from control.

REFERENCES

1. Archer SL, Huang JM, Reeve HL, Hampl V, Tolarova S, Michelakis E, and Weir EK. Differential distribution of electrophysiologically distinct myocytes in conduit and resistance arteries determines their response to nitric oxide and hypoxia. *Circ Res* 78: 431-442, 1996.

2. Archer SL, Souil E, Dinh-Xuan AT, Schremmer B, Mercier JC, El Yaagoubi A, Nguyen-Huu L, Reeve HL, and Hampl V. Molecular identification of the role of voltage-gated K^+ channels, Kv1.5 and Kv2.1, in hypoxic pulmonary vasoconstriction and control of resting membrane potential in rat pulmonary artery myocytes. *J Clin Invest* 101: 2319-2330, 1998.

3. Ausubel FM, Brent R, Kingston RE, Moore DD, Seidman JG, Smith JA, and Struhl K. Preparation and analysis of RNA. Current Protocols in Molecular Biology - Volume 1. New York: Wiley. 1997, p. 4.2-4.3.

4. Conforti L, Bodi I, Nisbet JW, and Millhorn DE. O_2-sensitive K^+ channels: role of the Kv1.2 -subunit in mediating the hypoxic response. *J Physiol (Lond)* 524 (Pt 3): 783-793, 2000.

5. Conforti L and Millhorn DE. Selective inhibition of a slow-inactivating voltage-dependent K^+ channel in rat PC12 cells by hypoxia. *J Physiol (Lond)* 502 (Pt 2): 293-305, 1997.

6. Evans AM, Osipenko ON, and Gurney AM. Properties of a novel K^+ current that is active at resting potential in rabbit pulmonary artery smooth muscle cells. *J Physiol (Lond)* 496 (Pt 2): 407-420, 1996.

7. Gelband CH and Gelband H. Ca^{2+} release from intracellular stores is an initial step in hypoxic pulmonary vasoconstriction of rat pulmonary artery resistance vessels. *Circulation* 96: 3647-3654, 1997.

8. Grissmer S, Nguyen AN, Aiyar J, Hanson DC, Mather RJ, Gutman GA, Karmilowicz MJ, Auperin DD, and Chandy KG. Pharmacological characterization of five cloned voltage-gated K^+ channels, types Kv1.1, 1.2, 1.3, 1.5, and 3.1, stably expressed in mammalian cell lines. *Mol Pharmacol* 45: 1227-1234, 1994.

9. Hamill OP, Marty A, Neher E, Sakmann B, and Sigworth FJ. Improved patch-clamp techniques for high-resolution current recording from cells and cell-free membrane patches. *Pflugers Arch* 391: 85-100, 1981.

10. Hulme JT, Coppock EA, Felipe A, Martens JR, and Tamkun MM. Oxygen sensitivity of cloned voltage-gated K^+ channels expressed in the pulmonary vasculature. *Circ Res* 85: 489-497, 1999.

11. Michelakis ED, Archer SL, and Weir EK. Acute hypoxic pulmonary vasoconstriction: a model of oxygen sensing. *Physiol Res* 44: 361-367, 1995.

12. Osipenko ON, Evans AM, and Gurney AM. Regulation of the resting potential of rabbit pulmonary artery myocytes by a low threshold, O_2-sensing potassium current. *Br J Pharmacol* 120: 1461-1470, 1997.

13. Osipenko ON, Tate RJ, and Gurney AM. Potential role for kv3.1b channels as oxygen sensors. *Circ Res* 86: 534-540, 2000.

14. Patel AJ, Lazdunski M, and Honore E. Kv2.1/Kv9.3, a novel ATP-dependent delayed-rectifier K^+ channel in oxygen-sensitive pulmonary artery myocytes. *EMBO J* 16: 6615-6625, 1997.

15. Post JM, Gelband CH, and Hume JR. $[Ca^{2+}]_i$ inhibition of K^+ channels in canine pulmonary artery. Novel mechanism for hypoxia-induced membrane depolarization. *Circ Res* 77: 131-139, 1995.

16. Post JM, Hume JR, Archer SL, and Weir EK. Direct role for potassium channel inhibition in hypoxic pulmonary vasoconstriction. *Am J Physiol* 262: C882-C890, 1992.

17. Russell SN, Overturf KE, and Horowitz B. Heterotetramer formation and charybdotoxin sensitivity of two K^+ channels cloned from smooth muscle. *Am J Physiol* 267: C1729-C1733, 1994.

18. Snyders DJ, Tamkun MM, and Bennett PB. A rapidly activating and slowly inactivating potassium channel cloned from human heart. Functional analysis after stable mammalian cell culture expression. *J Gen Physiol* 101: 513-543, 1993.

19. Sobko A, Peretz A, Shirihai O, Etkin S, Cherepanova V, Dagan D, and Attali B. Heteromultimeric delayed-rectifier K^+ channels in schwann cells: developmental expression and role in cell proliferation. *J Neurosci* 18: 10398-10408, 1998.

20. Thompson BT and Hales CA. Hypoxic pulmonary hypertension: acute and chronic. *Heart Lung* 15: 457-465, 1986.

21. Wang J, Juhaszova M, Rubin LJ, and Yuan XJ. Hypoxia inhibits gene expression of voltage-gated K^+ channel alpha subunits in pulmonary artery smooth muscle cells. *J Clin Invest* 100: 2347-2353, 1997.

22. Weir EK and Archer SL. The mechanism of acute hypoxic pulmonary vasoconstriction: the tale of two channels. *FASEB J* 9: 183-189, 1995.

23. Yuan XJ. Voltage-gated K^+ currents regulate resting membrane potential and $[Ca^{2+}]_i$ in pulmonary arterial myocytes. *Circ Res* 77: 370-378, 1995.

24. Yuan XJ, Goldman WF, Tod ML, Rubin LJ, and Blaustein MP. Ionic currents in rat pulmonary and mesenteric arterial myocytes in primary culture and subculture. *Am J Physiol* 264: L107-L115, 1993.

25. Yuan XJ, Wang J, Juhaszova M, Golovina VA, and Rubin LJ. Molecular basis and function of voltage-gated K^+ channels in pulmonary arterial smooth muscle cells. *Am J Physiol* 274: L621-L635, 1998.

CHAPTER 4

IDENTIFICATION, LOCALIZATION AND DIFFERENTIAL EXPRESSION OF Kv α AND β SUBUNITS IN THE PULMONARY ARTERY

INTRODUCTION

Hypoxic pulmonary vasoconstriction (HPV) is confined to the small vessels of the pulmonary arterial circulation. Small resistance pulmonary arteries (3rd intrapulmonary artery or greater) constrict in response to hypoxia (2,13,19,26), while large, conduit pulmonary arteries (main pulmonary artery and right and left branches) usually do not respond, or dilate slightly (2,13,19). Hypoxia leads to membrane depolarization (13) an increase in intracellular Ca^{2+} (21) and contraction (13,21) of pulmonary arterial smooth muscle cells (PASMCs) isolated from resistance vessels, but has little or no effect on conduit PASMCs (13,21).

The hypoxia-induced membrane depolarization of resistance PASMCs is thought to occur via inhibition of voltage-gated K^+ (Kv) channels that are open at the resting membrane potential. Indeed, hypoxia has been shown to inhibit PASMC whole-cell Kv current (2,19,20), leading to membrane depolarization (2,20,25) and constriction of small pulmonary arteries (2). Therefore, much attention has been focused on identifying the Kv channel subunits involved in this response.

As previously mentioned in Chapters 2 and 3, several groups of investigators have studied the O_2-sensitivity of cloned Kv channels, expressed in heterologous expression systems, in order to help elucidate the molecular components of the PASMC O_2-sensitive Kv current. Kv2.1 and Kv2.1/Kv9.3 were found to be significantly inhibited by hypoxia in COS cells (17) and in L-cells (11). In contrast, Kv1.5 was found to be insensitive to hypoxia when expressed in L-cells (11), COS-7 cells (16) or MEL cells (16). On the other hand, Kv1.2 homomeric channels, and Kv1.2/Kv1.5 heteromeric channels, were found to be significantly inhibited by hypoxia in L-cells (11). Most recently, Kv3.1b was found to be significantly inhibited by hypoxia when expressed in L929 cells (16). Previous studies indicate that Kv1.2, Kv1.5, Kv2.1 and Kv3.1b α subunit proteins are expressed in PASMCs (3,11,16,17,27). Detection of Kv9.3 message has been reported in freshly dispersed (17) and cultured (27) PASMCs; however, protein expression has not been determined. A role for Kv β subunits in cellular O_2-sensing has been suggested (10); however, expression of Kv β subunit proteins in the pulmonary artery has not been determined.

Certainly, these studies have given us insight as to which Kv channel subunits are most likely to be involved in PASMC O_2-sensing. However, it is unknown if these proteins are expressed primarily in the resistance vessels, where HPV is thought to occur, or distributed evenly throughout the pulmonary vasculature. Intuitively, one would expect that those subunits that are involved in the physiological response of resistance pulmonary arteries to hypoxia, would be expressed more abundantly in resistance than in conduit PASMCs and, furthermore, that this differential expression could at least partially account for the differential responses of conduit and resistance pulmonary

arteries to hypoxia. Therefore, the primary objectives of the present study were to determine the expression and localization of Kv channel α and β subunits in smooth muscle cells of the pulmonary artery and to determine whether expression levels of these subunits varied between conduit and resistance PASMCs. Work by Archer and colleagues, in which PASMCs were separated into three distinct populations based on current density and whole-cell current pharmacology, suggests that there is K^+ channel heterogeneity within the vascular wall (2). Therefore, expression heterogeneity of Kv α and β subunits within the smooth muscle layer of a given blood vessel was also examined. A delayed-rectifier current with biophysical and pharmacological properties similar to those displayed by the expression of Kv1.5, Kv2.1, Kv2.1/Kv9.3, Kv1.2/Kv1.5 and Kv3.1b cDNAs in heterologous expression systems has been described for the O_2-sensitive current in resistance PASMCs. Therefore, we confined our study to those α subunits that make up these channels and to members of the Kvβ1 and Kvβ2 families. Specifically, immunoblotting with densitometry and/or immunohistochemistry were used to examine protein expression of Kv1.2, Kv1.5, Kv2.1, Kv3.1b, Kvβ1.1, Kvβ1.2, Kvβ1.3 and Kvβ2.1 subunits between bovine conduit and resistance PASMCs. As attempts at producing an antibody against Kv9.3 that worked in tissue was unsuccessful, Northern blot analysis to examine PASMC Kv9.3 mRNA expression between conduit and resistance vessels.

MATERIALS AND METHODS

Antibodies and Fluorophores

Anti-Kv2.1 rabbit polyclonal and anti-Kv1.2 mouse monoclonal antibodies were purchased from Upstate Biotechnology (Lake Placid, NY). Anti-Kv3.1b rabbit polyclonal antibody was purchased from Alomone Laboratories (Jerusalem, Israel). The following antibodies were kindly donated by Dr. James Trimmer (State University of New York at Stony Brook): anti-Kv1.2C rabbit polyclonal, anti-Kv1.5C mouse monoclonal, anti-Kvβ1.1N rabbit polyclonal, anti-Kvβ1.2N rabbit polyclonal and anti-Kvβ2.1 mouse monoclonal. Anti-Kv1.2 rabbit polyclonal (anti-Kv1.2-T (480)), anti-human-Kv1.5 rabbit polyclonal (anti-human-Kv1.5-T (649)), anti-bovine-Kv1.5 rabbit polyclonal (anti-bovine-Kv1.5-T (1495)), anti-Kv9.3 rabbit polyclonal (anti-Kv9.3-T (1125)), anti-Kvβ1.2 rabbit polyclonal (anti-Kvβ1.2-T (687)) and anti-Kvβ1.3 (anti-Kvβ1.3-T (1068)) polyclonal antibodies were produced and characterized in the Tamkun Laboratory. Anti-α smooth muscle actin mouse monoclonal and Cy3-conjugated anti-α smooth muscle actin mouse monoclonal antibodies were purchased from Sigma Chemical Co (St. Louis, MO). Horseradish peroxidase (HRP)-goat anti-mouse IgG (H+L) and HRP-goat anti-rabbit IgG (H+L) secondary antibodies were purchased from Zymed Laboratories (San Francisco, CA) and used for immunoblotting. Biotin-SP-conjugated goat anti-rabbit IgG (H+L) and Biotin-SP-conjugated goat anti-mouse IgG (H+L) secondary antibodies, and Cy3- and Cy5-conjugated Streptavidin were purchased from Jackson ImmunoResearch Laboratories (West Grove, PA) and used for immunostaining.

Transfection and Tissue Culture

The mouse L-cell lines stably expressing human Kv1.5 (22) and rat Kv2.1 (11) were used as previously described. L-cells were cultured in Dulbecco's modified Eagle's medium supplemented with 10% horse serum, 100 U/ml penicillin G, 0.1 mg/ml streptomycin and 0.25 mg/ml G418 at 37°C and 5% CO_2. Expression of Kv1.5 or Kv2.1 was induced by overnight incubation with 4 μmol/liter dexamthasone. Transient transfection was carried out for Kv1.2 and Kv9.3 as described in Chapter 3.

Isolation of Total RNA, RT-PCR and Northern Blot Analysis

Total RNA was isolated using a guanidinium thiocyanate method (4) as described in Chapter 3. Bovine Kv9.3 cDNA was obtained from resistance PASMC RNA using materials and methods described in Chapter 3. Northern blot analysis was performed as described in Chapter 3.

Cloning of Bovine Kv9.3

The bovine Kv9.3 α subunit was cloned and sequenced from bovine PASMC RNA in order to select peptides for antibody production. RT-PCR of Kv9.3 from bovine PASMC RNA was performed as described in Chapter 3. The bovine Kv9.3 α subunit could not be amplified directly with the same primers utilized for amplification of rat Kv9.3, therefore, an overlap PCR strategy and three rounds of PCR, were used to obtain the bovine sequence. First, a 1364 bp fragment was amplified from the 5' end using rat Kv9.3 primers corresponding to the following nucleotides (the adenine in the ATG start codon = +1): upper primer -1-17; lower primer 1343-1363. Second, a 607 bp fragment was amplified from the 3' end using rat Kv9.3 primers corresponding to the following

nucleotides (the adenine in the ATG start codon = +1): upper primer 860-877, lower primer 1467-1448. Finally, the PCR products from the first two reactions were combined with the two outside primers and a 1468 bp fragment was amplified. This cDNA was subcloned into PGEM7 for sequencing (the translated sequence is shown in Figure 4.1).

Production of Anti-Kv9.3-T Antibody

One region within the N-terminus and one region within the C-terminus of the bovine Kv9.3 channel were chosen for antibody production (Figure 4.1). These epitopes were predicted to be antigenic in the rabbit based on surface probability and antigenic index plots (MacDNasis). Furthermore, the regions selected were unique compared with other Kv channels. These two peptides, LFLDSCCSNRYQERKEENHEKDWDQKSNDV and VVSDPDSTDASSVEDNEDAY were produced, purified, conjugated to KLH and then used to immunize two rabbits each by the Colorado State University Macromolecular Resources Facility. The antisera were tested by immunofluorescent staining of Kv9.3-transfected L-cells and immunoblotting of GST/Kv9.3 fusion proteins as described below.

Production of Anti-Bovine Kv1.5-T Antibody

Three regions within the N-terminus of the bovine Kv1.5 channel reported in Genbank (8)were chosen for antibody production (Figure 4.2). These epitopes were predicted to be antigenic in the rabbit as the sequence shows some species variation between bovine and rabbit sequences. The following peptides were produced and purified by the Colorado State University Macromolecular Resources Facility: GGAMTVRGEEEARTT, PAPRRRSGGERG and

ADPGGRPAPPPRQELPQASPRPPEEEDGED. These peptides were conjugated to KLH and all three were used to immunize two rabbits. The antisera were tested by immunoblotting of bovine tissue with antisera alone and antisera plus peptide as described below.

Production of GST Fusion Proteins

The following fusion protein constructs were already available for use in the Tamkun laboratory: GST/Kv1.2, GST/Kv1.5 and GST/Kvβ1.2. Production of GST/Kv9.3 fusion proteins is described below. PCR primers were designed to amplify regions of Kv9.3 from which the antibodies were targeted. The first set of primers amplified nucleotides 301-536, while the second set of primers amplified nucleotides 1150-1449, of the bovine channel. The upper and lower primers were designed with *XbaI* and *XhoI* sites, respectively, along with additional nucleotides as needed maintain the reading frame when subloned into the pGEX-KG vector (Pharmacia, LKB Biotechnology; Piscataway, NJ). The amplified PCR products where digested with *XbaI* and *XhoI*, gel purified, ligated into the pGEX-KG vector and transformed into *Escherichia coli* (XL1-Blue) (Stratagene; La Jolla, CA) as previously described (7). Construct-containing bacteria were induced to produce GST protein containing the above mentioned Kv channel sequences as described below. Briefly, 500 ml cultures were grown overnight at 37°C, induced with 0.1 mmol/liter isopropylthio-B-D-galactoside (IPTG) (Sigma) and then incubated an additional 2-3 h. Bacterial cells were pelleted at 6000 rpm for 15 min (Beckman JLA 10.5 rotor) and resuspended in 15 ml of ice-cold PBS with 1 mmol/liter PMSF (Sigma) and 0.2 mg/ml lysozyme (Sigma). The suspension was placed on ice for 30 min followed by sonication with a microtip on setting 2.5 for 1.5

min. Triton X-100 was added to the sample so that it contained 1% Triton. The sample was centrifuged at 8,000 rpm at 4°C for 10 min (Beckman JA 25.5 rotor). Following the centrifugation, the supernatant was added to 0.5 ml of packed glutathione agarose beads (Sigma) and incubated for 1 h at room temperature. The beads were washed 3 times with approximately 50 ml of ice-cold phosphate buffered saline (PBS). The beads were transferred to a purification column (VWR), packed with 5-10 ml PBS and eluted with two 1 ml volumes of 50 mmol/liter Tris (pH 8)/5 mmol/liter reduced glutathione. Finally, GST fusion proteins were dialyzed against PBS and samples were fractionated by sodium dodecyl sulfate polyacrylamide gel electrophoresis (SDS-PAGE).

Immunofluorescence Staining of Transfected Tissue Culture Cells

Transfected cells were grown on gelatin-coated UV-sterilized glass cover slips (placed in 25 mm plastic tissue culture dishes) in standard culture medium. Expression of Kv1.5 or Kv2.1 channels was induced by overnight incubation with 4 μmol/liter dexamethasone. In order to obtain good cell surface expression, transient transfections were carried out for Kv1.2, Kv9.3 and Kv1.5/1.2 tandem cDNAs using approximately the same concentrations (corrected for dish size) of cDNA, lipofectamine and GFP, and approximately the same time periods, as used for the electrophysiological studies described in Chapter 3. The cells were incubated with the lipofectamine mixture for 6 to 8 h, following which, the mixture was removed and replaced with standard culture medium and the cells were incubated for an additional 36 to 48 h (during this time period, Kv2.1 expression was induced in order to study Kv2.1/Kv9.3 expression). After transfection, coverslips were removed from the tissue culture dishes and placed in Columbia staining jars. Cells were rinsed once with PBS and then fixed according to the

primary antibody they would be stained with. All fixation steps were performed for 2 min at room temperature under the following conditions: cells immunostained with Kv2.1 or Kv9.3-T antibodies were fixed with 4% paraformaldehyde, cells immunostained with the Kv1.2-T antibody were fixed with 100% acetone and cells immunostained with the anti-human-Kv1.5-T antibody were fixed with 100% methanol. After fixation, the coverslips were processed as previously described (14). The following wash and overnight blocking steps were performed in Columbia staining jars while avidin and biotin blocking steps, and the antibody and fluorochrome incubations, were performed in a humidity chamber. The cells were permeabilized with 0.5% CHAPS (3-[(3-cholamidopropyl)-dimethylammonio]-1-propane-sulfonate hydrate) in PBS with three solution changes, 10 min each. The coverslips were washed again with PBS (3 X 10 min) to remove CHAPS, and then blocked overnight at 4°C in PBS containing 10% goat serum and 5% nonfat dry milk (blotto). After the overnight block, the cells were incubated in primary antiserum diluted in PBS plus 10% goat serum and 0.5% CHAPS for 1 h at room temperature. For Kv1.2 and Kv1.5 immunostaining, coverslips were incubated with anti-Kv1.2-T or anti-human-Kv1.5-T diluted 1:500. For Kv2.1 and Kv9.3 immunostaining, coverslips were incubated with anti-Kv2.1 antibody diluted 1:200 or anti-Kv9.3-T antibody diluted 1:500. Following the primary antibody incubation, cells were washed 3 times for 10 min each with PBS plus 10% goat serum and 0.5% CHAPS, followed by a 10 minute wash with PBS alone. Endogenous avidin and biotin were blocked using an avidin/biotin blocking kit (Vector Laboratories; Burlingame, CA) according to the manufacturer's recommendations. The coverslips were incubated with the appropriate biotin-conjugated goat anti-rabbit (or mouse) IgG diluted 1:200 in PBS

plus 1.5% blotto for 30 min at room temperature. The cells were washed (3 X 10 min) with PBS plus 0.5% CHAPS and incubated with Cy3-conjugated strepavidin diluted 1:500 in PBS containing 0.5% CHAPS and 1% BSA for 45 min at room temperature. The coverslips were washed a final time with PBS plus 0.5% CHAPS, mounted on glass slides with Aqua Poly/Mount (Polysciences, Warrington, PA) and allowed to dry overnight before microscopic examination. Samples were analyzed using a Nikon E800 microscope equipped with standard epifluorescence and a Princeton Instruments CCD camera using a Sony Interline 1300 X 1030, 12 bit chip.

Immunostaining of Pulmonary Artery Tissue Sections

Lungs obtained from freshly slaughtered cattle were immediately placed in ice-cold PBS. As soon as possible (approximately 1 h later), the following bovine pulmonary arteries (PAs) were exposed by dissection, carefully removed from the lungs, and rinsed with ice-cold PBS (pH 7.5): main conduit (main conduit PA before it branches, external diameter ~ 25 mm), 2nd intralobar (2nd branch off of the main intralobar PA, external diameter ~ 8 mm), 3rd intralobar (3rd branch off of the main intralobar PA, external diameter ~ 3 mm) and 4th intralobar (4th branch off of the main intralobar PA, external diameter ~ 1.5 mm). Tissue sections were immersed in 30% sucrose in PBS for 1 h, placed in cryomolds, embedded in Tissue Tek (Sakura Finetechnical; Tokyo, Japan), and quickly frozen on a slab of dry ice. Cryosections measuring 10 μm in thickness were collected on gelatin-coated coverslips, dried for 5 to 10 min at room temperature, treated with 0.5% CHAPS in PBS and then processed with the antibodies and analyzed as described above for immunofluorescence of transfected cells. Anti-Kvβ1.2-T antiserum was diluted 1:500 and used as described above.

Immunogen block of tissue staining was performed to demonstrate antibody specificity. Staining was performed as described above, except that cryosections were stained with antiserum that had been preincubated overnight at 4°C with 40 nmol/liter (for Kv1.2 and Kv1.5 immunogen block) or 1 μmol/liter (for Kvβ1.2 immunogen block) of either glutathione transferase (GST) or the appropriate GST fusion protein construct, as previously described (11).

Preparation of PASMC Membranes

Lungs obtained from freshly slaughtered cattle were immediately placed in ice-cold PBS. As soon as possible, the following PAs were carefully exposed, removed from the lungs and placed in fresh ice-cold PBS: Conduit (main conduit PA before it branches, external diameter 25-30 mm), 2nd intralobar (2nd branch off of the main intralobar PA, external diameter 5-10 mm), 3rd intralobar (3rd branch off of the main intralobar PA, 3-5 mm), 4th intralobar (4th branch off of the main intralobar PA, external diameter 1-2 mm). Resistance PAs were defined as pooled 3rd and 4th intralobar PAs. The pulmonary arteries were dissected free of adventitia, cut open longitudinally, and then gently scraped with a cotton swab to remove the endothelium. Approximately 2-5 g of each of the resultant PASMC tissue was cut into small pieces and homogenized with a polytron homogenizer in 30-40 ml 0.32M sucrose/5 mM Na_2HPO_4 with the following protease inhibitors: benzamidine 0.31 mg/ml, N-ethylmaleamide 0.62 mg/ml, bacitracin 1 mg/ml (Sigma), pepstatin 1 μg/ml, leupeptin 1 μg/ml and pefablock 0.07 μg/ml (Boehringer Mannheim, Germany). The tissue was homogenized on ice at high speed with first a large, and then a small, diameter probe for 60 sec each. The homogenate was centrifuged at 4°C for 10 min at 3,000 rpm (Beckman JA 25.5 rotor) to remove large debris and

nuclei. The supernatant was filtered through one layer of gauze and centrifuged at 4°C for 1 h at 12,000 rpm (Beckman JA 25.5) in order to pellet the membranes. The resultant pellet was resuspended in an appropriate volume of ice-cold PBS (approximately 200-400 µl) and stored at –80°C.

Western Blotting

PASMC membrane proteins were fractionated by SDS-PAGE and transferred overnight to nitrocellulose membrane (Schleicher & Schuell, Dassel, Germany) using the standard Laemmli method (5). Briefly, 4X sodium dodecyl sulfate (SDS) sample buffer was added to the membrane sample to a final concentration of 1XSDS and samples were adjusted with additional 1XSDS as needed in order to achieve a similar α smooth muscle actin signal between samples. Samples were boiled for five min and then run at 125 v on a 7.5%, 10% or 12% polyacrylamide gel using a minigel system (Bio-Rad). Proteins were transferred onto nitrocellulose membrane overnight at 40 V using a mini-trans-blot cell (Bio-Rad). After transfer, membranes were stained with Ponceau S solution (Sigma) (in order to visualize the quality of the transfer), rinsed with deionized water and incubated for 1 h at room temperature in solution 1A (S1A) (50 mM Tris (pH 7.5), 150 mM NaCl, 0.1% Tween-20, 5% nonfat dry milk) in order to block non-antigenic sites. The blots were then incubated in S1A at room temperature for 2 h with one of the following primary antibodies: Kv1.2-T polyclonal (1:500), Kv1.2C polyclonal (1 µg/ml), Kv1.2 monoclonal (0.5 µg/ml), Kv1.5C monoclonal (1 µg/ml), Kv2.1 polyclonal (1:500), Kv3.1b polyclonal (1 µg/ml), Kv9.3-T polyclonal (1:1500), Kvβ1.1N polyclonal (1 µg/ml), Kvβ1.2N polyclonal (1 µg/ml), Kvβ1.3-T polyclonal (1:500), Kvβ2.1

monoclonal (1 μg/ml) or α smooth muscle actin (1:50,000). The blots were washed 3 times for 15 min each with solution 3A (S3A) (50 mM Tris (pH 7.5), 500 mM NaCl, 0.1% Tween-20) and then incubated for 1 h in S1A containing a 1:3000 dilution of HRP-conjugated goat anti-rabbit IgG or goat anti-mouse IgG. The blots were washed 3 times for 15 min each with S3A and detection was achieved with an enhanced chemiluminescence kit (ECL) (NEN Life Science; Boston, MA) per manufacture's instructions. For blots incubated with anti-human or anti-bovine Kv1.5, a modified version of the above protocol was used. Briefly, blots were incubated overnight at 4°C in solution 1B (S1B) (50 mM Tris (pH 7.5), 150 mM NaCl, 10% goat serum (Gibco)). Following the blocking step, all subsequent steps were performed at room temperature. The blots were incubated in solution 2B (S2B) (50 mM Tris (pH 7.5), 150 mM NaCl, 5% goat serum, 0.05% Tween-20) containing a 1:500 (anti-human) or a 1:1000 (anti-bovine) dilution of anti-Kv1.5-T for 2.5 h. The blots were washed twice for 15 min in solution 3B (50 mM Tris (pH 7.5), 500 mM NaCl, 5% NaCl, 0.05% Tween-20) and incubated for 1 h in S2B containing a 1:5000 dilution of HRP-conjugated goat anti-rabbit IgG. The blots were washed sequentially for 15 min each in S1B, S2B and S3B and detection was achieved with an ECL kit per manufacture's directions.

Immunogen block of the Western blot channel bands was performed to demonstrate antibody specificity. Western blots were performed as described above, except that for GST-blocks, identical blots were incubated with antiserum that had been preincubated overnight at 4°C with 4 nmol/liter (for anti-Kv9.3-T Western blots) or 40 nmol/L (for anti-Kv1.2-T Western blots) of either GST or the appropriate GST fusion protein construct. For peptide blocks (anti-bovine-Kv1.5-T), identical blots were

incubated with antiserum that had been preincubated overnight at 4°C with 1 μmol/liter of each of the peptides used to generate the antibody or antiserum that was preincubated in the same solution (S2B) minus the peptides.

Immunoprecipitation

Rat brain and bovine PASMC membranes (approximately 10 times the amount used to generate a Western blot signal) were solubilized in 1 ml Tris buffered saline (10 mM Tris, (pH 8.0) 0.15 M NaCl) plus 1% Triton X-100, 60 mM Octyl-glucoside (Fisher) and 1 mmol/liter Pefablock (Boehringer Mannheim) on ice for 45 min. The samples were centrifuged at 12,000-14,000 g at 4°C for 15 min (IEC 851 rotor). Following centrifugation, the supernatant was transferred to a clean tube and incubated with 1-10 μl of the primary antibody overnight at 4°C. The following day, 50 μl of packed protein A-sepharose beads (Sigma) were added to the tubes and incubated an additional 3 h at 4°C. The samples were centrifuged for 10 sec and the supernatant was aspirated. The beads were washed 3 times with 1 ml buffer A (0.5% w/v Triton X-100, 150 mM NaCl, 50 mM Tris-Cl (pH 7.5), 1 mM EDTA) followed by 1 wash with 1 ml 1% Triton X-100. The beads were boiled for 5 min with 50 μl 1 X SDS, centrifuged and the supernatants transferred to a new tube and then separated by SDS-PAGE (25 μl per lane).

Quantification of Western Blot Signals

Nitrocellulose blots were exposed to X-ray film for multiple time periods (generally ranging between 5 sec and 5 min) in order to detect saturation. Non-saturated films were scanned into Adobe Photoshop® and densitometry was used to quantify the immunoblot product (NIH Image, Scion, Frederick, MD). In order to compare channel

expression between conduit and resistance PASMC membranes, the average intensity of the channel signal was multiplied by the number of pixels in that area and then corrected for the α smooth muscle actin signal present in the same lane (calculated the same way).

Statistical Analysis

A paired t test was used to assess differences in channel expression between conduit and resistance PASMCs. $P<0.05$ was considered statistically significant.

RESULTS PART 1 – ANTIBODY CHARACTERIZATION

Anti-Kv9.3-T Antibody Recognizes the GST/Kv9.3 N-terminus Fusion Protein and Kv9.3-Transfected L-Cells

Polyclonal antisera from the rabbits injected with the Kv9.3 peptides were assayed for Kv9.3 subunit recognition. Antisera from the rabbits injected with the N-terminus Kv9.3 peptide (Anti-Kv9.3-T) recognize the N-terminus GST/Kv9.3 fusion protein (Figure 4.3). After preincubation with GST alone, the antibody recognizes a band of approximately 36 kDa (Figure 4.3 A), the predicted molecular weight of the fusion protein. This band is absent in the GST-only lane and is absent after antibody preincubation with the GST/Kv9.3 N-terminus fusion protein (Figure 4.3 B). Furthermore, anti-Kv9.3-T recognizes non-denatured Kv9.3 in transfected L-cells (Figure 4.4). Because Kv9.3 does not form a functional channel when expressed alone, as expected, all channel expression was intracellular (panels D & F). As it is likely that Kv9.3 forms a heteromeric channel when expressed with Kv2.1 *in vivo*, we also immunostained cells cotransfected with Kv2.1 and Kv9.3 cDNAs in order to determine if the epitope was still available and the antibody was able to recognize cell surface

channel. As illustrated Figure 4.4, anti-Kv9.3-T immunostained Kv2.1/Kv9.3 transfected cells (panels J-L) but not cells transfected with Kv2.1 alone (panels G-I). Furthermore, anti-Kv9.3-T appeared to recognize cell surface expression of the heteromeric channel (compare panels F and L for cell surface expression).

Anti-Bovine Kv1.5-T Antibody Recognizes Bovine Kv1.5 Protein

Polyclonal antisera from the rabbits injected with the bovine Kv1.5 N-terminus peptides were assayed for Kv1.5 subunit recognition. Anti-bovine Kv1.5-T antibody recognizes bovine Kv1.5 protein in aorta and conduit and resistance PASMCs (Figure 4.5). The anti-bovine Kv1.5-T antibody recognizes a band of approximately 70 kDa (Figure 4.5 A), which is blocked by preincubation with the peptide sequences from which the antibody was generated (Figure 4.5 B). The molecular weight of the Kv1.5 peptide is consistent with previous reports in PASMCs (3,27). A strong, approximately 70 kDa, band was also detected with this antibody in rat heart, rat aorta and L-cells expressing rat Kv1.5 (data not shown).

Anti-Kv1.2-T Antibody Recognizes GST/Kv1.2 Fusion Protein and Kv1.2-Transfected L-Cells

The anti-Kv1.2-T antibody was characterized before use in bovine pulmonary arterial tissue. Anti-Kv1.2-T binds to the thrombin cleaved GST/Kv1.2 proteins and Kv1.2 expressing L-cell membranes (Figure 4.6). After preincubation with GST, the antibody recognizes a band at approximately 10 kDa (the predicted molecular weight of the Kv1.2 fragment is approximately 9 kDa) in the Kv1.2/GST lane, but not in the GST-only lane (Figure 4.6 A). This band is no longer present after antibody preincubation with the GST/Kv1.2 fusion protein from which the antibody was generated (Figure 4.6

B). Furthermore, anti-Kv1.2-T binds to a band of approximately 58 kDa in transfected cells (Figure 4.6 C) which is blocked after preincubation with the GST/Kv1.2 fusion protein (Figure 4.6 D). Transfected L-cells were immunostained with anti-Kv1.2-T in order to determine if this antibody could recognize non-denatured Kv1.2. As illustrated Figure 4.7, anti-Kv1.2-T recognized Kv1.2 expressed as a homomeric channel (panels C & D) and as a heteromeric channel with Kv1.5 (panels E & F), but did not immunostain mock-transfected cells (panels A & B). It should be noted that consistently more channel got to the cell surface in the Kv1.5/1.2 tandem-transfected cells than cells transfected with Kv1.2 alone (compare panels F & D).

RESULTS PART 2 – EXPRESSION AND LOCALIZATION OF Kv α AND β SUBUNITS WITHIN THE PULMONARY ARTERY

Expression of Kv2.1 in Bovine PASMCs

Kv2.1 was detected in bovine PASMCs via Western blot analysis. The Kv2.1 antibody recognized a single band of approximately 110 kDa in transfected L-cells and conduit and resistance PASMC membranes (Figure 4.8). The molecular weight of the Kv2.1 subunit is consistent with previous reports in freshly dissociated rat resistance PASMCs (3) and combined primary cultures of rat conduit and intrapulmonary PASMCs (27). The Kv2.1 antibody recognized cell surface channel in L-cells stably transfected with Kv2.1 (Figure 4.9) and in rat hippocampal neurons (Figure 4.10); however, it did not recognize Kv2.1 channel expressed in bovine pulmonary artery sections (Figure 4.10). Multiple conditions and antibodies were tried, but no Kv2.1 signal was detected in the bovine pulmonary artery. Potentially, the Kv2.1 antibody epitope could be masked if Kv2.1 was expressed as a heterotetramer, with Kv9.3 (rather than a homotetramer), and

that could be the reason for the failed PASMC immunostaining. However, anti-Kv2.1 recognized cell surface channel in mouse L-cells whether or not Kv9.3 was coexpressed with Kv2.1 (Figure 4.9 E-G), suggesting that something other than the Kv9.3 α subunit was masking this epitope in bovine PASMC tissue. In support of this observation, although Kv2.1 was easily immunoprecipitated from whole rat brain extracts, it could not be immunoprecipitated from PASMC lystates (data not shown).

Expression of Kv9.3 in Bovine PASMCs

Although the Kv9.3-T antibody was able to recognize Kv9.3 protein via immunobloting of the GST/Kv9.3 N-terminus fusion protein (Figure 4.3) and immunostaining of Kv9.3-transfected L-cells (Figure 4.4), clear, consistent results could not be obtained in tissue preparations. Western blot analysis of rat brain and bovine conduit and resistance PASMC membranes with anti-Kv9.3-T yielded many immunoblot bands around the predicted molecular weight; however, it could not be determined if any of these bands represented Kv9.3. Furthermore, immunostaining of bovine conduit and resistance pulmonary arteries with the Kv9.3 antibody did not yield a significant signal above background, although Kv9.3 message was detected via PCR (Figure 3.1) and Northern blot analysis (Figure 4.11). Therefore, Northern blot analysis was utilized to assess Kv9.3 expression in bovine conduit and resistance PASMCs. A strong signal of approximately 3.2 kb, consistent with previous reports in rat lung (17), was evident in bovine resistance PASMCs, rat lung and rat brain; however, very little signal was detected in bovine conduit PASMCs (Figure 4.11) although α actin controls showed that the mRNA was intact (data not shown).

Heteromeric Formation of Kv2.1/Kv9.3 Channels in Bovine PASMCs

Due to the limitations of the Kv channel antibodies, heteromeric assembly of Kv2.1/Kv9.3 could not be assessed. While anti-Kv2.1 worked extremely well for immunoblotting and immunoprecipitation from rat brain, Kv2.1 could not be immunoprecipitated from bovine conduit or resistance PASMCs (data not shown). Furthermore, the Kv9.3 antibody did not work for immunoprecipitation or immunoblotting of PASMC membranes. In both cases, the most likely explanation is that the antibody epitopes are simply blocked in vascular tissue.

Expression of Kv1.2 in Bovine PASMCs

In contrast to Kv2.1 and Kv9.3, Kv1.2 was detected in bovine PASMCs via immunohistochemistry. Binding of anti-Kv1.2-T to bovine resistance pulmonary arteries (Figure 4.12 A & B) was unaffected by preincubation with GST (panels C & D); however, it was almost completely eliminated after preincubation with the channel-containing fusion protein (panels E & F). Furthermore, Kv1.2 channel expression was observed to be localized to individual PASMCs in both conduit and resistance pulmonary arteries (Figure 4.13). Panels A-C and D-F show DIC, α smooth muscle actin immunostaining (to stain for smooth muscle cells), and Kv1.2 immunostaining in conduit and resistance pulmonary arteries, respectively. Intensity of the Kv1.2 immunostaining appeared to be fairly equal at the cellular level throughout the vessel wall in both conduit and resistance pulmonary arteries.

Although Kv1.2 was detected in bovine conduit and resistance pulmonary arteries via immunohistochemistry, Kv1.2 expression could not be detected via immunoblotting of bovine PASMC membranes. Three different Kv1.2 antibodies recognized rat or

bovine brain Kv1.2 channel immunoblot bands; however, a clear Kv1.2 channel signal from bovine conduit or resistance PASMC membranes could not be obtained (Figure 4.14). The 80 kDa band in rat brain produced by incubation with the anti-Kv1.2-T antibody (Figure 4.14 A) was completely blocked after antibody preincubation with the GST/Kv1.2 fusion protein from which the antibody was generated (Figure 4.14 B). There were no distinct Kv1.2 channel signals in bovine conduit or resistance PASMC membranes after incubation with anti-Kv1.2-T polyclonal (Figure 4.14 A), anti-Kv1.2C polyclonal (Figure 4.14 C) or anti-Kv1.2 monoclonal (Figure 4.14 D) antibodies. This was not due to a species difference in amino acids at the region of these epitopes as sequence alignment of bovine and rat Kv1.2 revealed 100% homology in these regions (data not shown). Furthermore, all three antibodies recognized bovine Kv1.2 from bovine brain membranes (data shown for anti-Kv1.2C polyclonal only, Figure 4.14 C). The simplest explanation is that there is not much Kv1.2 channel protein expressed in pulmonary vascular smooth muscle relative to brain and that the signal to noise ratio in the PASMC lanes was too low.

Expression of Kv1.5 in Bovine PASMCs

Kv1.5 was detected in bovine PASMCs via Western blot analysis and immunohistochemistry. As shown previously in Figure 4.5, anti-bovine-Kv1.5-T antibody recognized a single band of approximately 70 kDa in bovine conduit and resistance PASMC membranes. Kv1.5C monoclonal antibody recognized a similar 70 kDa band in bovine conduit and resistance PASMCs, bovine ventricle, rat heart and L-cells transfected with rat Kv1.5 cDNA (Figure 4.15). The bovine Kv1.5 PASMC band is

consistent with previous studies which reported an approximately 65 kDa band in freshly dispersed (3), and acute primary cultures (27), of rat PASMCs.

Before using the Kv1.5 antibody for immunohistochemistry of bovine tissue, we first worked out the experimental conditions in transfected L-cells. Anti-human-Kv1.5-T antibody recognized Kv1.5 expressed as a homomeric channel (panels C & D) and as a heteromeric channel with Kv1.2 (panels G & H), but did not immunostain non-transfected (panels A & B) or mock-transfected (panels E & F) L-cells. Anti-human-Kv1.5-T also recognized Kv1.5 in bovine conduit and resistance pulmonary arteries (Figure 4.17 & Figure 4.18). Kv1.5 antibody binding to bovine resistance pulmonary arteries (Figure 4.17 panels A & B) was unaffected by preincubation with GST (panels C & D); however, it was reduced after preincubation with the channel containing fusion protein (panels E & F). Furthermore, Kv1.5 channel expression was observed to be localized to individual PASMCs and to the endothelial layer in both conduit and resistance pulmonary arteries (Figure 4.18), consistent with previous reports in rat lung sections (3). Panels A-C and D-F show DIC, α smooth muscle actin immunostaining and Kv1.5 immunostaining in conduit and resistance pulmonary arteries, respectively. The intensity of the Kv1.5 immunostaining did not appear to differ between smooth muscle cells within the vascular wall of a given blood vessel; however, the intensity of staining of resistance PASMCs appeared to be slightly greater than in conduit PASMCs. These differences will be addressed in Results Part 3.

Heteromeric Formation of Kv1.2/Kv1.5 Channels in Bovine PASMCs

Due to the limitations of the Kv channel antibodies available, heteromeric assembly of Kv1.2/Kv1.5 in PASMCs could not be examined. Although the

Kv1.2/Kv1.5 heteromeric channel could be immunoprecipitated from tandem Kv1.5/1.2 transfected L-cells with the anti-human Kv1.5-T and anti-Kv1.2-T antibodies (data not shown), Kv1.2/Kv1.5 heteromeric assembly could not be detected in bovine PASMCs. It is possible that the heteromeric channel is not expressed in PASMCs. Alternatively, the Kv1.2/Kv1.5 heteromeric channel could be expressed at low levels *in vivo* in PASMCs and its expression was not detected simply because of the inefficiency of the immunoprecipitation and Western blot experiments.

Expression of Kv3.1b in Bovine PASMCs

Kv3.1b was detected in bovine PASMC membranes via Western blot analysis. Anti-Kv3.1b recognized a band of approximately 70 kDa in both conduit and resistance bovine PASMCs (Figure 4.19 A), which was almost completely blocked by antibody preincubation with the Kv3.1b peptide from which the antibody was generated (Figure 4.19 B). PASMC Kv3.1b ran at a lower molecular weight than bovine brain or rat brain, which ran at approximately 90 kDa (Figure 4.19 A); however, it is consistent with the predicted molecular weight of approximately 66 kDa. Interestingly, there appeared to be more Kv3.1b expressed in resistance than in conduit PASMCs. A 51 kDa band, which was also blocked after preincubation with the Kv3.1b peptide, was noted in both the conduit and resistance PASMC lanes. It is likely that the 51 kDa band represents a proteolysis product since it is blocked by the peptide and it parallels the increase of the 66 kDa band from conduit to resistance PASMCs. Unfortunately, the anti-Kv3.1b antibody did not provide consistent immunostaining above background in bovine pulmonary artery tissue sections, therefore, detection of Kv3.1b protein was limited toWestern blot analysis.

Expression of Kv β Subunits in Bovine PASMCs

Kvβ1.1, Kvβ1.2 and Kvβ1.3, but not Kvβ2.1 were detected in bovine conduit and resistance PASMC membranes via Western blot analysis (Figure 4.20). Anti-Kvβ1.1N antibody recognized a single prominent band of approximately 49 kDa that was stronger in resistance than in conduit PASMC membranes (Figure 4.20 A). Kvβ1.1 polypeptide ran higher in PASMCs than its predicted molecular weight of approximately 40 kDa and instead ran closer to the 44 kDa band reported in transfected COS 1 cells (15). It is possible that Kvβ1.1, generally considered to be a neuronal channel, came from nerve endings in the smooth muscle wall. However, this is unlikely due to the large amount of protein that was detected in the PASMC lanes. Furthermore, we also Kvβ1.1 mRNA was detected via RT-PCR of PASMC RNA (data not shown) and it is unlikely that mRNA would be present in these nerve endings.

Anti-Kvβ1.2N recognized a prominent band of approximately 38 kDa in conduit and resistance PASMC membranes (Figure 4.20 B), which corresponds closely with its predicted molecular weight. Like Kvβ1.1, the intensity of this band seemed to be greater in resistance than in conduit PASMC membranes.

Anti-Kvβ1.3-T recognized a single prominent band of approximately 70 kDa in conduit and resistance PASMC membranes (Figure 3.20 C). This band was also more intense in resistance than in conduit PASMC membranes, although the lanes contained approximately equal amounts of PASMC membranes. PASMC Kvβ1.3 ran at a much higher molecular weight than its predicted size of about 40 kDa. However, a single band of approximately 62 kDa was evident in cells transfected with Kvβ1.3, suggesting that

the larger, 70 kDa band in PASMCs, most likely represents Kvβ1.3 expression (Figure 4.20 C).

Anti-Kvβ2.1 gave a strong band of approximately 40 kDa in bovine brain; however, a signal was not detected in conduit, 2nd intralobar, or 3rd and 4th resistance intralobar PASMCs, even after extended exposures (Figure 4.20 D). Therefore, it is likely that Kvβ2.1 is not expressed, or is expressed in limited quantities, in the bovine pulmonary artery.

While the anti-Kvβ1.1 and anti-Kvβ1.3 antibodies failed to stain bovine pulmonary artery sections, Kvβ1.2 was detected in bovine PASMCs via immunohistochemistry. Kvβ1.2-T antibody binding to bovine resistance pulmonary arteries (Figure 4.21 panels A & B) was unaffected by preincubation with GST (panels C & D); however, it was almost completely eliminated after preincubation with the channel containing fusion protein (panels E & F). Furthermore, Kvβ1.2 channel expression was localized to individual PASMCs in both conduit and resistance pulmonary arteries (Figure 4.22). Panels A-C and D-F show DIC, α smooth muscle actin immunostaining and Kvβ1.2 immunostaining in conduit and resistance pulmonary arteries, respectively. The intensity of Kvβ1.2 immunostaining seems to be greater in resistance than in conduit pulmonary arteries. This increased expression appears to be due to increased expression at the cellular level.

Archer and coworkers reported expression heterogeneity within the wall of a given pulmonary arterial blood vessel (2), therefore, pulmonary artery tissue sections were examined for evidence of this type of differential K^+ channel expression. No evidence of expression heterogeneity was found within the smooth muscle layer of a

given blood vessel for any of the Kv channel subunits examined. While the intensity of Kvβ1.2 immunostaining appeared to be greater in individual PASMCs from resistance vessels than from conduit vessels, there did not seem to be any difference in intensity of immunostaining between pulmonary arterial smooth muscle cells of a given-sized vessel.

RESULTS PART 3 – DIFFERENTIAL EXPRESSION OF Kv α AND β SUBUNITS IN CONDUIT AND RESISTANCE PULMONARY ARTERIES

Differential Expression of Kv α Subunits in the Pulmonary Artery

Kv1.2, Kv1.5, Kv2.1, Kv3.1b and Kv9.3 α subunits have all been hypothesized to be molecular components of the O_2-sensitive K^+ current in resistance PASMCs. Therefore, expression levels of these subunits were examined between conduit and resistance PASMCs with the assumption that those subunits involved in the differential response of conduit and resistance pulmonary arteries to hypoxia would be differentially expressed between these vessels. Protein expression of Kv1.5, Kv2.1 and Kv3.1b between conduit and resistance PASMCs was examined quantitatively via Western blot analysis and densitometry. Representative immunoblots demonstrating Kv1.5, Kv2.1 and Kv3.1b expression in PASMC membranes from conduit PAs, 2nd intralobar PAs and 3rd and 4th intralobar resistance PAs are shown in Figure 4.23. Kv1.5 expression appeared to be fairly equal to slightly greater in the 3rd and 4th intralobar resistance PASMCs than in conduit PASMCs (Figure 4.23 A). Kv2.1 expression appeared to be similar between conduit and 3rd and 4th resistance PASMCs (Figure 4.23 B). On the other hand, Kv3.1b expression was dramatically greater in 3rd and 4th intralobar resistance PASMCs compared to that of conduit PASMCs and even 2nd intralobar PASMCs (Figure 4.23 C). Only after over-exposure of the resistance lane was a Kv3.1b signal detected in the

conduit lane. Protein expression was also examined quantitatively between conduit PASMCs and pooled 3rd and 4th resistance PASMCs (Figure 4.24). Kv1.5 expression levels were significantly greater in resistance than in conduit PASMCs, though the difference was not that large (approximately 1.5 times greater in resistance) (Figure 4.24 A). Kv2.1 expression levels were not significantly different between conduit and resistance PASMCs (Figure 4.24 B). On the other hand, expression levels of Kv3.1b were dramatically greater in resistance than in conduit PASMCs (approximately 12 times greater in resistance) (Figure 4.24 C). As Kv1.2 expression could not be assessed via Western analysis, Kv1.2 expression, along with Kv1.5 expression, was examined qualitatively, between conduit and resistance pulmonary arteries, via immunohistochemistry.

Figures 4.25 and 4.26 show expression of Kv1.2 and Kv1.5 α subunits, respectively, in conduit, 2nd intralobar and 3rd and 4th resistance intralobar pulmonary arteries via immunohistochemistry. The intensity of the Kv1.2 immunostaining at the level of a single myocyte appeared to be fairly equal between conduit and resistance PASMCs (Figure 4.25). The intensity of Kv1.5 immunostaining appeared to be fairly equal between, or modestly greater in, resistance than in conduit pulmonary arteries (Figure 4.26). A small increase in individual myocyte Kv1.5 expression agrees with the Western blot data of Figure 4.23.

Protein expression of Kv9.3 could not be assessed, therefore, expression of Kv9.3 mRNA was compared between conduit and resistance PASMCs via Northern blot analysis. A band of approximately 3.2 kb was detected in resistance PASMCs while little

or no Kv9.3 expression was detected in conduit PASMCs, although the α smooth muscle actin control signal was equal or greater in conduit PASMCs (Figure 4.27).

Differential Expression of Kv β Subunits in the Pulmonary Artery

It is possible that Kvβ subunits play a role in PASMC O_2-sensing. If this hypothesis is correct, it is likely that Kvβ subunit expression is greater in resistance than in conduit PASMCs. In this study, expression of Kvβ1.1, Kvβ1.2 and Kvβ1.3 were compared between conduit and resistance PASMCs via Western blot analysis and densitometry (Figures 4.28 and 4.29). Representative immunoblots demonstrating Kvβ1.1, Kvβ1.2 and Kvβ1.3 expression in PASMCs from conduit PAs, 2nd intralobar PAs and 3rd and 4th intralobar resistance PAs are shown in Figure 4.28. Kvβ1.1 was dramatically greater in 3rd and 4th intralobar resistance PASMCs than in conduit PASMCs (Figure 4.28 A). Kvβ1.2 expression appeared to increase from conduit to 3rd and 4th intralobar resistance PAs (Figure 4.28 B). Kvβ1.3 expression appeared to be greater in PASMCs isolated from 4th intralobar PAs than in PASMCs isolated from conduit PAs; however, there seemed to be little difference in Kvβ1.3 expression between 3rd intralobar and conduit PASMCs (Figure 4.28 C). When examined quantitatively, subunit expression of Kvβ1.1, Kvβ1.2 and Kvβ1.3 was found to be significantly greater (approximately 6.1, 3.6 and 2.9 times respectively) in resistance than in conduit PASMCs (Figure 4.29).

Protein expression of Kvβ1.2 was also examined in conduit PAs and 2nd, 3rd and 4th intralobar PAs via immunohistochemistry (Figure 4.30). Consistent with the Western blot data, Kvβ1.2 immunostaining intensity, at the level of the single myocyte, was

observed to be greater in resistance than in conduit PASMCs (compare panels F & H with panels B & D).

DISCUSSION

It has been hypothesized that the contrasting vasoactive response to hypoxia between conduit and resistance pulmonary arteries is due to differential PASMC K^+ channel expression (1,2). Indeed, the electrophysiological and pharmacological profile of the PASMC K^+ current depends on whether the smooth muscle cells that were examined were isolated from large or small pulmonary arteries (1,2). Archer et al classified these smooth muscle cells into three distinct populations based on current density and whole-cell current pharmacology (2). Pulmonary arterial smooth muscle cells in which the whole-cell current was significantly inhibited by TEA, with little effect from 4-AP, named K_{Ca} cells, were found predominately in the conduit vessels. While cells that were significantly inhibited by 4-AP, with little effect from TEA, named K_{DR} cells, were found predominately in resistance vessels. Cells in which TEA and 4-AP were approximately equally effective at inhibiting the outward K+ current, named mixed cells, were found throughout the pulmonary vasculature. With the recent molecular identification of several pulmonary arterial Kv channels, the question arises as to whether the diverse hypoxic response of conduit and resistance pulmonary arteries is due to the differential expression of O_2-sensitive Kv channels.

Expression of Kv Channel α Subunits in the Pulmonary Artery

Kv2.1 has been shown to be O_2-sensitive in COS cells (17) and L-cells (11). Furthermore, Kv2.1 meets the biophysical and pharmacological characteristics of the O_2-

sensitive K^+ current in resistance PASMCs (delayed-rectifier that is CTX-insensitive). Therefore, the Kv2.1 channel is a good candidate for the pulmonary arterial O_2-sensitive K^+ current. In the present study, Kv2.1 expression levels between conduit and resistance PASMCs were found to be similar (Figures 4.23 and 4.24). This is interesting, as one would think that if the Kv2.1 channel were responsible for the pulmonary arterial O_2-sensitive K^+ current then more Kv2.1 channel would be expressed in resistance than in conduit PASMCs. However, while some previous studies found Kv2.1 to be O_2-sensitive, others have found it to be O_2-insensitive (6). Furthermore, in the studies in which Kv2.1 was found to be O_2-sensitive, it did not activate in the voltage range of the PASMC resting membrane potential. Therefore, it is unlikely that Kv2.1 *homomeric* channels account for the pulmonary arterial O_2-sensitive K^+ current (11,17). On the other hand, Kv2.1 has been shown to form a heteromeric channel with Kv9.3 that is significantly inhibited by hypoxia in the voltage range of the PASMC resting membrane potential (11,17). In the current study, we found Kv9.3 message to be more abundant in resistance than in conduit PASMCs (Figure 4.27). This result supports the hypothesis that the Kv2.1/Kv9.3 *heteromeric* channel is an important component of the pulmonary arterial O_2-sensitive K^+ current of resistance PASMCs. Because Kv9.3 expression increases from conduit to resistance pulmonary arteries, while Kv2.1 expression stays fairly constant, it is possible that in the conduit pulmonary artery, Kv2.1 is primarily expressed as a homomeric channel which is insensitive to hypoxia at physiological membrane potentials, while in the resistance pulmonary artery, Kv2.1 is primarily expressed as a heteromeric channel with Kv9.3, which is significantly inhibited by hypoxia at physiologically relevant membrane potentials. Unfortunately, this possibility

could not be explored as neither subunit could be immunoprecipitated from PASMC membranes. Neither the Kv2.1, nor the Kv9.3, antibodies worked for pulmonary artery immunostaining, therefore, it was not surprising that the immunoprecipitation experiments failed. Nonetheless, multiple immunoprecipitation experimental conditions were tried. Although Kv9.3 could not be immunoprecipitated under any of these experimental conditions, Kv2.1 was easily immunoprecipitated from both transfected cells and rat brain. Further experiments will be necessary to explore the possibility of differential expression of Kv2.1/Kv9.3 heteromeric channels in the pulmonary artery.

Kv1.2 channels have been shown to be O_2-sensitive in mouse L-cells (11) and in *Xenopus* oocytes (6) but not when expressed in B82 cells (16). Additionally, Kv1.2 is thought to underlie the CTX- and hypoxia- sensitive current in PC12 cells (a model for O_2-sensing in the carotid body) (6,28). In the current study, Kv1.2 protein was detected in both conduit and resistance PASMCs. Furthermore, expression levels of Kv1.2 between conduit and resistance pulmonary arteries were found to be fairly similar (Figure 4.25). Although Kv1.2 has been reported to be O_2-sensitive in some expression systems, it does not activate in the voltage range of the PASMC resting membrane potential (11). Furthermore, Kv1.2 channels do not fit the pharmacological profile of the PASMC O_2-sensitive K^+ current in that they are sensitive to CTX (I.C. $50 \leq 50$ nM) (9). These results, taken together with the results of the present study that Kv1.2 is not differentially expressed between conduit and resistance PASMCs, imply, that at least, Kv1.2 *homomeric* channels are not likely to underlie O_2-sensitive K^+ current of resistance PASMCs.

Kv1.5 has been suggested to be an important component of the pulmonary arterial O_2-sensitive K^+ current (3). Indeed, the Kv1.5 channel fits the biophysical and pharmacological profile of this current. However, Kv1.5 channels are not inhibited by hypoxia when expressed in L-cells (11), COS-7 cells (16) or MEL cells (16). Data from the present study suggest that Kv1.5 expression is modestly greater in resistance than in conduit PASMCs (Figures 4.23, 4.24 and 4.25). Qualitative experiments using immunohistochemistry and quantitative experiments using immunoblot analysis with densitometry were consistent with each other. While the difference in Kv1.5 protein expression between conduit and resistance PASMCs was found to be significantly different, one has to question whether this difference (1.5 times greater in resistance than in conduit PASMCs) is very meaningful from a physiological perspective. Certainly the results from heterologous expression systems suggest that the Kv1.5 *homomeric* channel is not likely to be responsible for the O_2-sensitive K^+ current of resistance PASMCs. However, it is not known if Kv1.5 is expressed as a homomeric channel and/or a heteromeric channel *in vivo*.

When coexpressed, Kv1.2 and Kv1.5 α subunits can assemble to form a functional heteromeric channel with biophysical and pharmacological properties consistent with the pulmonary arterial O_2-sensitive K^+ current (11). Furthermore, when expressed in L-cells whole-cell current from the Kv1.2/Kv1.5 *heteromeric* channel is significantly inhibited by hypoxia in the voltage range of the PASMC resting membrane potential (11). If this channel was responsible for the O_2-sensitive K^+ current in resistance PASMCs, it seems likely that Kv1.2/Kv1.5 heteromeric channel expression would be greater in resistance than in conduit PASMCs. Data from the present study

indicate that Kv1.2 expression levels are similar between conduit and resistance PASMCs while Kv1.5 expression levels are slightly greater in resistance PASMCs. It is possible that Kv1.2/Kv1.5 heteromeric channels are differentially expressed between conduit and resistance PASMCs; however, these proteins could not be coimmunoprecipitated from PASMCs. Therefore, it could not be determined if Kv1.2/Kv1.5 heteromeric channels are expressed in the pulmonary artery and, if so, whether or not the expression of heteromeric channels differs between conduit and resistance PASMCs. As with the Kv2.1/Kv9.3 experiments, multiple experimental conditions were tried, and even a new antibody was produced and characterized; however, these experiments did not work in the pulmonary vasculature. Antibodies against both channels immunoprecipitated their respective subunits from transfected cells, and multiple Kv1.2 antibodies immunoprecipitated the Kv1.2 subunit from rat brain; these subunits did not immunoprecipitate from conduit or resistance PASMC membranes. Additional experiments are needed to explore the possibility of Kv1.2/Kv1.5 heteromeric channel formation in pulmonary arteries.

In the present study, we report differential expression of Kv3.1b between conduit and resistance pulmonary arteries via Western blot analysis. Kv3.1b expression is approximately 12 times greater in resistance than in conduit PASMCs (Figure 4.24). This is consistent with observation that Kv3.1b current is significantly inhibited by hypoxia when expressed in transfected L929 cells (16). Furthermore, Kv3.1b expression had previously been demonstrated in freshly dissociated rat resistance PASMCs via immunocytochemistry (16). In the current study, Kv3.1b expression was examined via Western blot analysis. At 70 kDa, PASMC Kv3.1b ran at a lower molecular weight than

that of Kv3.1b in rat brain or bovine brain (which ran at approximately 90 kDa); however, it is consistent with its predicted protein core molecular weight of approximately 66 kDa. The dramatic difference in Kv3.1b expression between conduit and resistance pulmonary arteries, coupled with the hypoxic inhibition of this current, suggest that Kv3.1b is likely to be an important molecular component of the O_2-sensitive K^+ current of resistance PASMCs. However, Kv3.1b homomeric channels are not active at the PASMC resting membrane potential (16) and, therefore, it is not likely that Kv3.1b alone, as a homotetramer, could account for the O_2-sensitive K^+ current of resistance PASMCs. Rather, Kv3.1b would have to be expressed as a heterotetramer with another α subunit, or with a β subunit, which shifts the activation potential in a more hyperpolarized direction *in vivo* in order to account for the physiological response of PASMCs to hypoxia.

Results from the present study demonstrating that Kv2.1 and Kv1.2 expression levels are similar between conduit and resistance PASMCs while Kv9.3 expression is greater in resistance PASMCs contradict those of Patel et al who used RT-PCR to compare Kv channel subunit expression between isolated conduit PASMCs and primary cultured resistance PASMCs (17). They reported greater expression levels of Kv2.1 and Kv1.2 in conduit than in resistance PASMCs while Kv9.3 expression was similar. They were unable to detect Kv1.5 message in conduit or resistance PASMCs, although several groups have detected Kv1.5 protein in PASMCs (3,11,27). Because mRNA expression does not necessarily accurately reflect protein expression, results from experiments where protein levels were examined more accurately reflect the levels of protein expressed *in vivo*. The discrepancies regarding Kv9.3 message expression, however, likely reflect the

conditions of the experiment. For example, Patel et al compared freshly dispersed conduit PASMCs with primary cultured resistance PASMCs. It is possible that the culturing of the resistance PASMCs caused a decrease in channel expression. On the other hand, our differences may simply reflect a species difference between bovine and rat PASMCs. In fact, cattle have been reported to be hypersensitive to hypoxia while rats are moderate responders (23).

Expression of Kv Channel β Subunits in the Pulmonary Artery

As Kv β subunits usually produce inactivation, and the outward K^+ current from smooth muscle cells in the pulmonary artery is slowing inactivating, or non-inactivating, Kv β subunits were easily overlooked in the search for the molecular components of the pulmonary arterial O_2-sensitive K^+ current. Recently, however, it was shown that PKA phosphorylation can remove β-induced inactivation (12). Therefore, the presence of Kv β subunits in the pulmonary artery doesn't necessarily lead to K^+ channel inactivation, but may instead represent on the of the many other functions of the Kv β subunit. For instance, recently added to the growing list of possible Kv β subunit functions, is that of a cellular O_2-sensor (10). In the present study we found Kv β subunit expression to be significantly greater in resistance than in conduit PASMCs (Figures 4.28 and 4.29). This result is consistent with a role for the Kv β subunit in O_2-sensing (10). Indeed, when the conserved core of the Kvβ2.1 subunit was crystallized, bound NADPH was detected in its crystal structure, further supporting a role for the Kv β subunit in O_2-sensing (10). Very recently, in fact, Kv β subunits have been shown to confer O_2-sensitivity onto certain Kv α subunits in a heterologous expression system (18).

mRNA for multiple Kv β subunits had been detected previously in PASMCs via RT-PCR of primary cultured rat PASMCs (27); however protein expression of Kv β subunits had not been confirmed. In the current study we report expression of Kvβ1.1, Kvβ1.2, and Kvβ1.3, but not Kvβ2.1, proteins in conduit and resistance PASMCs (Figure 4.20). These results using immunoblotting of bovine PASMCs both confirm and contradict the results of Yuan and coworkers, who, using RT-PCR of rat primary cultured PASMCs, detected mRNA expression of Kvβ2.1 (27).

We found Kvβ1.1 to run at a higher molecular weight than the predicted molecular mass of approximately 40 kDa; however, at approximately 49 kDa, this band is similar to that reported in transfected COS 1 cells (15). Although Kvβ1.1 is generally considered to be a neuronal channel, it is likely that the majority of protein detected in the pulmonary arterial smooth muscle layer came from the smooth muscle cells. The fact that a very strong Western blot signal was obtained, and that Kvβ1.1 mRNA was detected from the pulmonary arterial smooth muscle layer, supports the expression of Kvβ1.1 in PASMCs. Furthermore, Kvβ1.1 mRNA has been detected by other investigators in acute primary cultures of rat PASMCs (27) and in smooth muscle cells of the mesenteric artery (24).

Results from the present study indicate that the Kvβ1.2 polypeptide is approximately 38 kDa in bovine conduit and resistance PASMCs, which is consistent with its predicted molecular weight. Furthermore, Kvβ1.2 expression was confirmed in bovine conduit and resistance pulmonary arteries via immunohistochemistry, and found it to be localized to the smooth muscle layer. Kvβ1.2 expression appeared to be fairly evenly distributed throughout the smooth muscle layer of a given pulmonary artery

section; however, Kvβ1.2 expression was greater in individual smooth muscle cells from the resistance pulmonary artery than in individual smooth muscle cells from the conduit pulmonary artery.

In the present study, expression of Kvβ1.3 was also demonstrated in bovine conduit and resistance PASMCs. Anti-Kvβ1.3-T binds to an immunoblot band of approximately 70 kDa in PASMC membranes, which is considerably larger than the predicted molecular weight of approximately 40 kDa. To address this issue, Western blot analysis of Kvβ1.3-transfected and non-transfected cells was performed. A single band of approximately 62 kDa, which was absent in non-transfected cells lane, was detected in the transfected cell lane. Therefore, it is likely that the 70 kDa band in PASMC membranes represents Kvβ1.3. However, we are unable to explain why Kvβ1.3 runs at such a high molecular weight in transfected L-cells and PASMC membranes.

Kvβ2.1 was not detected in conduit, 2nd intralobar, or 3rd and 4th intralobar resistance PASMCs, although a strong band of approximately 40 kDa (which corresponds closely to the reported molecular weight of Kvβ2.1 in rat brain (15)), was detected in bovine brain. This is in contrast to the results of Yuan et al who reported mRNA expression of Kvβ2.1 in primary cultured rat PASMCs via RT-PCR. Although RT-PCR provides information about gene expression, it does not confirm the presence of an encoded protein. The lack of a Kvβ2.1 signal does not necessarily exclude the possibility of PASMC Kvβ2.1 expression; however, even after extended exposures, no channel was detected. In addition, Kvβ2.1 was easily detected via Western blot of rat and bovine brain membrane proteins. Therefore, if Kvβ2.1 protein is expressed in PASMCs it is

likely that it is in relatively small quantities. Alternatively, it is possible that bovine PASMCs do not express Kvβ2.1, while rat PASMCs do.

In the present study we demonstrate that expression levels of Kvβ1.1, Kvβ1.2 and Kvβ1.3 subunits are approximately 6, 3.5 and 3 times greater, respectively, in resistance than in conduit PASMCs (Figures 4.28 and 4.29). Furthermore the Kvβ1.2 result was confirmed qualitatively via immunohistochemistry, which shows that Kvβ1.2 expression dramatically increases from the conduit to the 4th intralobar pulmonary artery (Figure 4.30). This is interesting in light of the fact that resistance pulmonary arteries constrict in response to hypoxia while conduit pulmonary arteries do not (26) and that Kvβ1.2 confers O_2-sensitivity to Kvα4.2 (18). Therefore, it is possible that Kv β subunit expression in the pulmonary artery is at least partially responsible for the differential effects of hypoxia on conduit and resistance pulmonary arteries.

Study Limitations

This study was limited by the efficiency of the Kv channel antibodies available to us. Although the majority of these antibodies were useful in transfected cells and in rat/bovine brain, many of them did not work well in PASMC tissue (see Table 4.1). Staining levels above background could not be obtained with two different antibodies for Kv2.1 in bovine (or rat) PASMC, although cell surface staining was obtained in both transfected L-cells and rat hippocampal neurons, and very strong immunoblot signals were generated in bovine PASMCs. The lack of staining could be due to heteromeric channel formation of Kv2.1 and Kv9.3 in PASMCs such that the epitope in the heteromeric channel was blocked, while it was available in the homomeric channel. However, there was no difference in the cell surface staining pattern of Kv2.1 in cells

transfected with both Kv2.1 and Kv9.3, or cells transfected with Kv2.1 alone (Figure 4.9). Therefore, it is likely that the epitope is masked by other cellular components, such as the cytoskeleton, in the pulmonary artery. However, Archer and coworkers have reported Kv2.1 expression via immunohistochemistry of rat lungs (3). We are unable to explain the discrepancies in our findings and those of the Archer group.

Kv9.3 protein expression could not be determined; therefore, differential expression of Kv9.3 protein between conduit and resistance PASMCs, and heteromeric assembly of Kv2.1/Kv9.3 in PASMCs, could not be examined. There are no commercially available antibodies for Kv9.3, therefore, we produced and characterized an antibody against the N-terminus of the bovine channel. This antibody recognized the GST/Kv9.3 N-terminus fusion protein, and immunostained Kv9.3-transfected cells, but did not give clear, consistent results in whole tissue for either immunoblotting or immunohistochemistry. Therefore, Kv9.3 expression in the pulmonary vasculature could not be assessed directly.

Kv1.2 expression could not be determined via immunoblot. Therefore, Kv1.2/Kv1.5 heteromeric channel expression in resistance PASMCs could not be examined. Other investigators have reported expression of Kv1.2 via immunoblot of freshly dispersed resistance PASMCs (3), and of primary cultured PASMCs (27); however, consistent Kv1.2 immunoblot bands in bovine PASMC membranes were not obtained due to a low signal to noise ratio. These antibodies were able to recognize the bovine channel, however, as all three Kv1.2 antibodies recognized Kv1.2 in bovine brain. Although Kv1.2 expression was not detected via immunoblot analysis, it is most likely

that Kv1.2 is expressed in bovine PASMCs based on the intense immunostaining of PASMCs.

Summary

In summary, this study provides a molecular map for the expression of Kv channel subunits that have been hypothesized to contribute to the O_2-sensitive K^+ current in the pulmonary artery and demonstrates that some of these subunits are differentially expressed between conduit and resistance PASMCs (see Table 4.2). Specifically, in this study, we confirmed the presence of Kv1.2, Kv1.5, Kv2.1 and Kv3.1b and demonstrated the presence of Kvβ1.1, Kvβ1.2, Kvβ1.3, but not Kvβ2.1, channel proteins in PASMCs. Most importantly, however, in this study we demonstrated that expression levels of Kv3.1b and all three Kvβ subunits is dramatically increased from the main conduit pulmonary artery to the small resistance pulmonary arteries where HPV is thought to occur. The expression level of Kv1.5 protein was found to be modestly greater in resistance than in conduit PASMCs while expression levels of both Kv1.2 and Kv2.1 channel proteins were found to be similar between conduit and resistance PASMCs. Furthermore, mRNA expression of Kv9.3 was found to be qualitatively greater in resistance than in conduit PASMCs. As hypoxia significantly depresses Kv channel current in resistance PASMCs, but not in conduit PASMCs (2), it seems logical that the expression of O_2-sensitive Kv channels would be greater in resistance rather than conduit PASMCs. Comparisons of these molecular data and that of previous studies of native current in PASMCs and of the O_2-sensitivity of cloned channels allow us to make tentative hypotheses about the involvement of Kv3.1b and Kv9.3 α subunits and Kv β subunits in the physiological response of resistance PASMCs to hypoxia. Although

much progress has been made in determining the molecular components of the O_2-sensitive K^+ current in PASMCs, ultimately, future work should lead to the "knock-out" of individual subunits through the use of antisense techniques and transgenic mouse models, in order to determine an individual subunit's involvement in the O_2-sensitive current of resistance PASMCs.

Table 4.1. Summary of antibodies tested

	Western Blot		*Immunostaining*		
Antibodies	***Brain***	***Transfected Cells***	***PA SMCs***	***Transfected Cells***	***PA SMCS***
1.2 (480)	Yes	Yes	No	Yes	Yes
1.2C p (Trimmer)	Yes	Yes	No		
1.2 m (Upstate)	Yes	Yes	No		
1.5 (649)	No	Yes	No	Yes	Yes
1.5 (1495)	Yes?		Yes		Yes?
1.5 m (Trimmer)	?	Yes	Yes, but weak	No	
2.1 p (Upstate)	Yes	Yes	Yes	Yes	No
2.1 m (Upstate)	Yes	Yes	Yes	Yes	No
9.3 (1125)	No	Yes (GST)	No	Yes	No
9.3 (1124)	No		No	Yes	No
3.1b (Alomone)	Yes		Yes		No
Pan β (F-5)	Yes	Yes	Yes	No	
β1.1N p (Trimmer)	Yes		Yes		No
β1.1N m (Trimmer)	No		No		No
β1.2 (687)	No		No		Yes
β1.2N p (Trimmer)	Yes		Yes		No
β1.2N m (Trimmer)					No
β1.3 (1068)	Yes	Yes	Yes		No
β2.1 (689)	Yes	Yes	No	No	No
β2.1 m (Trimmer)	Yes	Yes	No		No

Yes/No/? indicates if antibody gave consistent signal above background. Blanks indicate antibody was not tested.

Table 4.2. Summary of Kv channel expression in conduit vs. resistance pulmonary arteries

Channel Subunit	*Fold Difference Between Conduit and Resistance Pulmonary Arteries*
Kv1.2	R~C*
Kv1.5	1.5
Kv2.1	1
Kv3.1	12
Kv9.3	R>C**
Kvβ1.1	6
Kvβ1.2	3.5
Kvβ1.3	3

Differences were assessed quantitatively via Western blot analysis unless otherwise indicated.

*Estimated qualitatively via immunohistochemical analysis

**Estimated qualitatively via Northern blot analysis

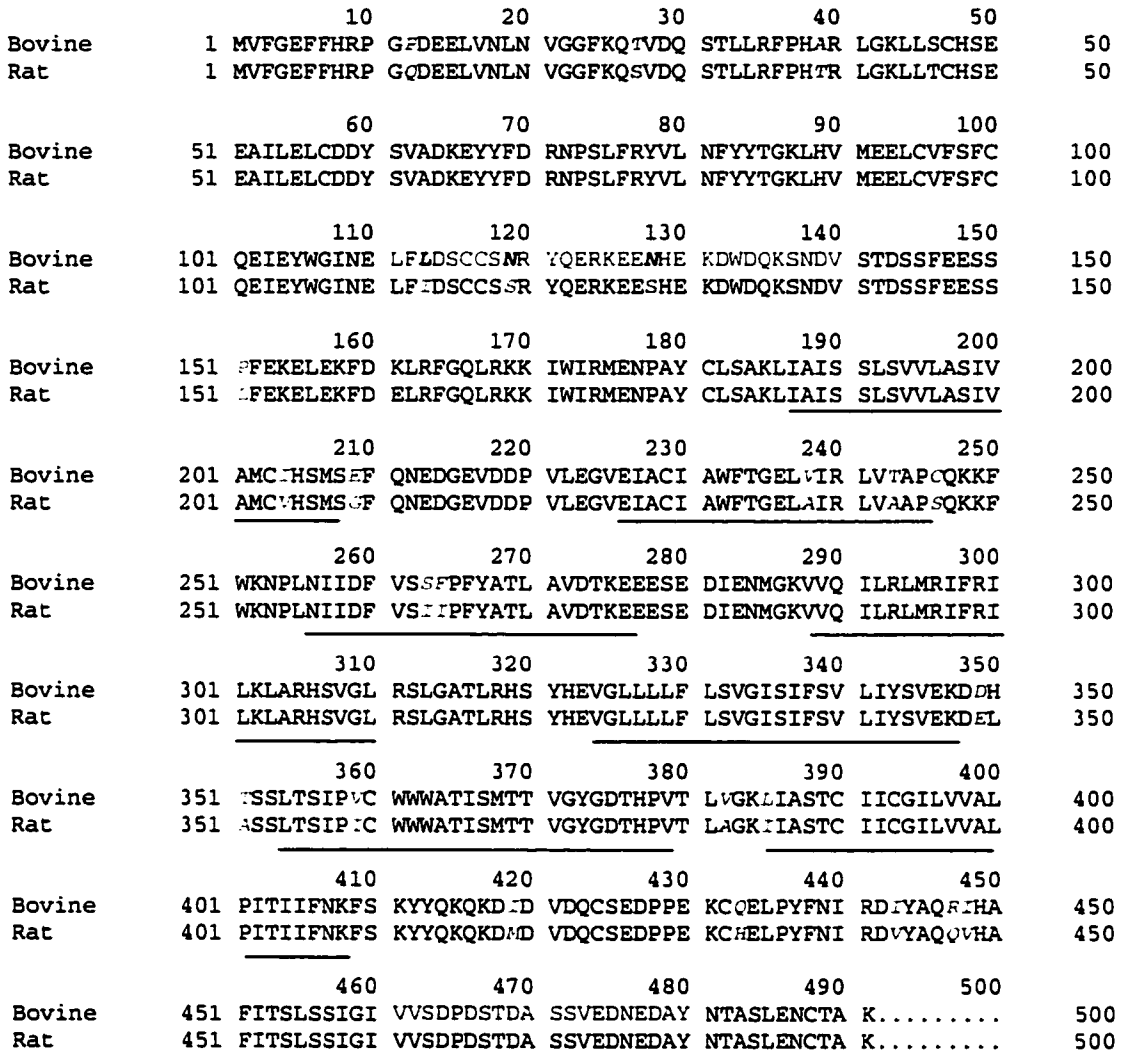

Figure 4.1. Amino acid sequence alignment of Bovine Kv9.3 with Rat Kv9.3. Amino acid sequence differences are highlighted in gray. Red and blue lettering indicate peptide sequences used for antibody production. Green and red underlining indicate approximate sequences of transmembrane segments S1-S6 and pore sequence, respectively.

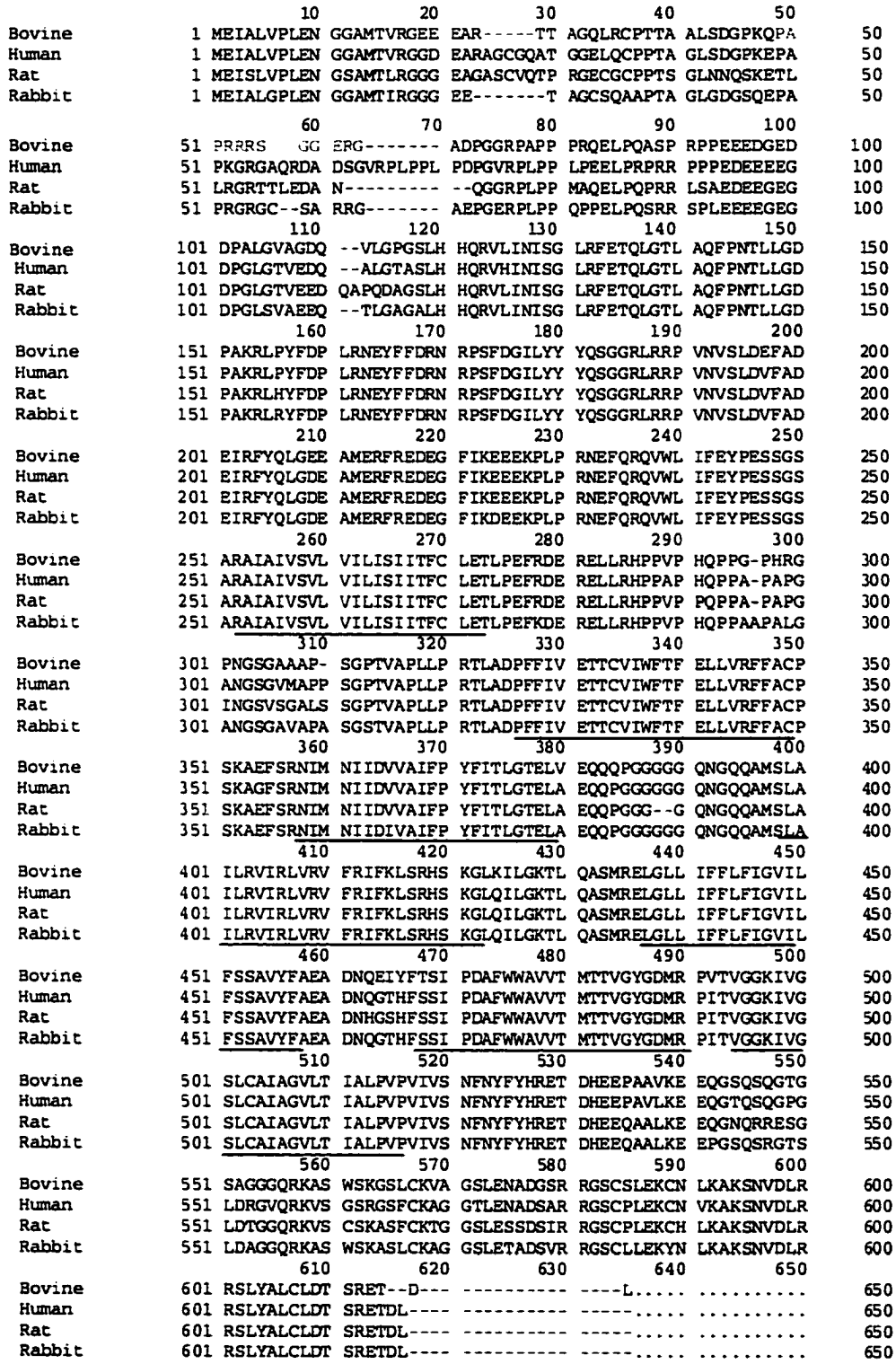

Figure 4.2. Amino acid sequence alignment of bovine, human, rat and rabbit Kv1.5 α subunits. Red, blue and green lettering indicate peptide sequences used for antibody production. Green and red underlining indicate approxi mate sequences of transmembrane segments S1-S6 and pore sequence, respectively.

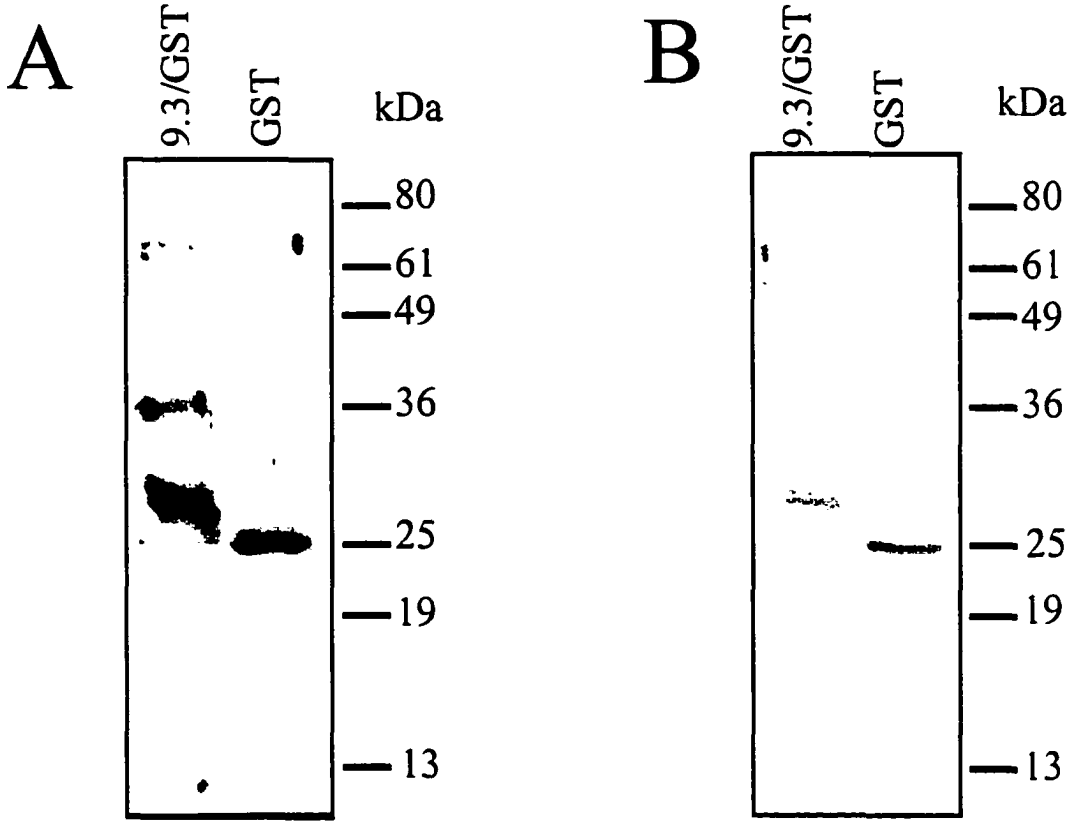

Figure 4.3. Western blot analysis of GST/Kv9.3 N-terminus fusion protein. Kv9.3-T antibody binding after preincubation with 4 nmol/liter GST (A) or GST/Kv9.3 (B) fusion proteins.

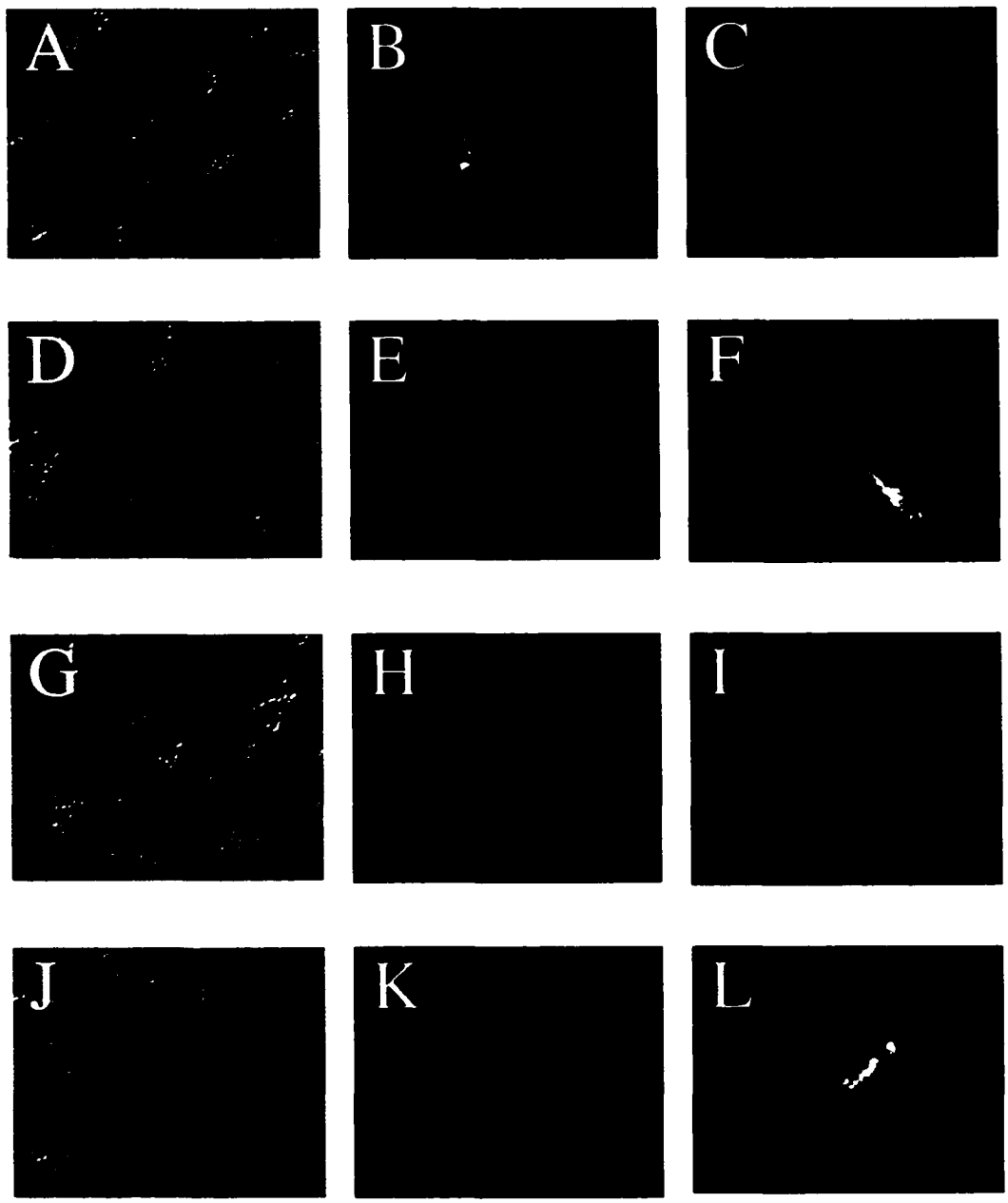

Figure 4.4. Kv9.3 immunostaining of transfected L-cells. Panels show DIC image, GFP image and binding of anti-Kv9.3-T antibody (Cy3 image), respectively, in mock-transfected (A-C), Kv9.3-transfected (D-F), Kv2.1-transfected (G-I) and, Kv9.3- and Kv2.1-transfected (J-L) L-cells. GFP color illustrates transfected cells. Exposure conditions for panels C, F, I and L were identical. Calibration bar illustrated in the first panel of each series.

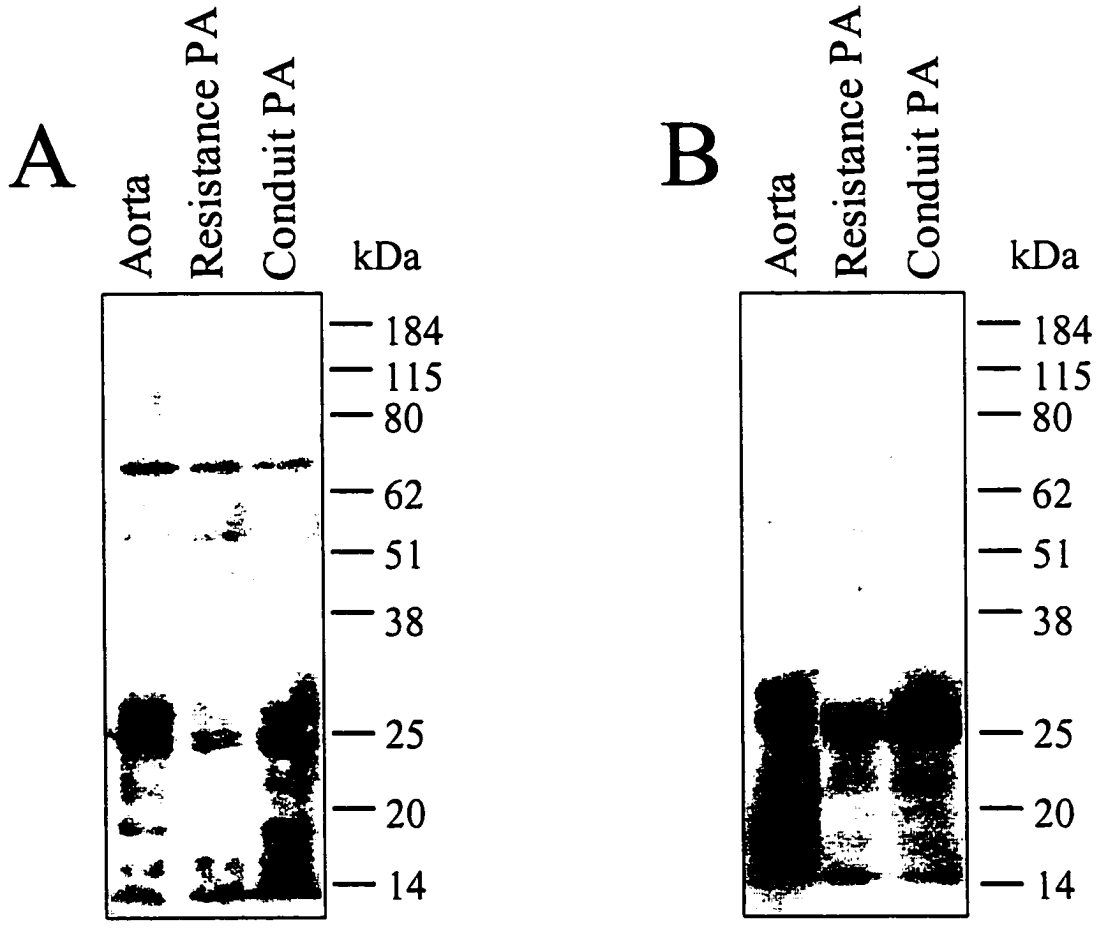

Figure 4.5. Kv1.5 Western blot analysis and corresponding peptide block. A) Anti-bovine-Kv1.5-T antibody binding of bovine aorta, resistance PA and conduit PA. B) Anti-bovine-Kv1.5-T antibody binding after overnight incubation with 1 μmol/liter of each of the Kv1.5 peptides from which the antibody was made.

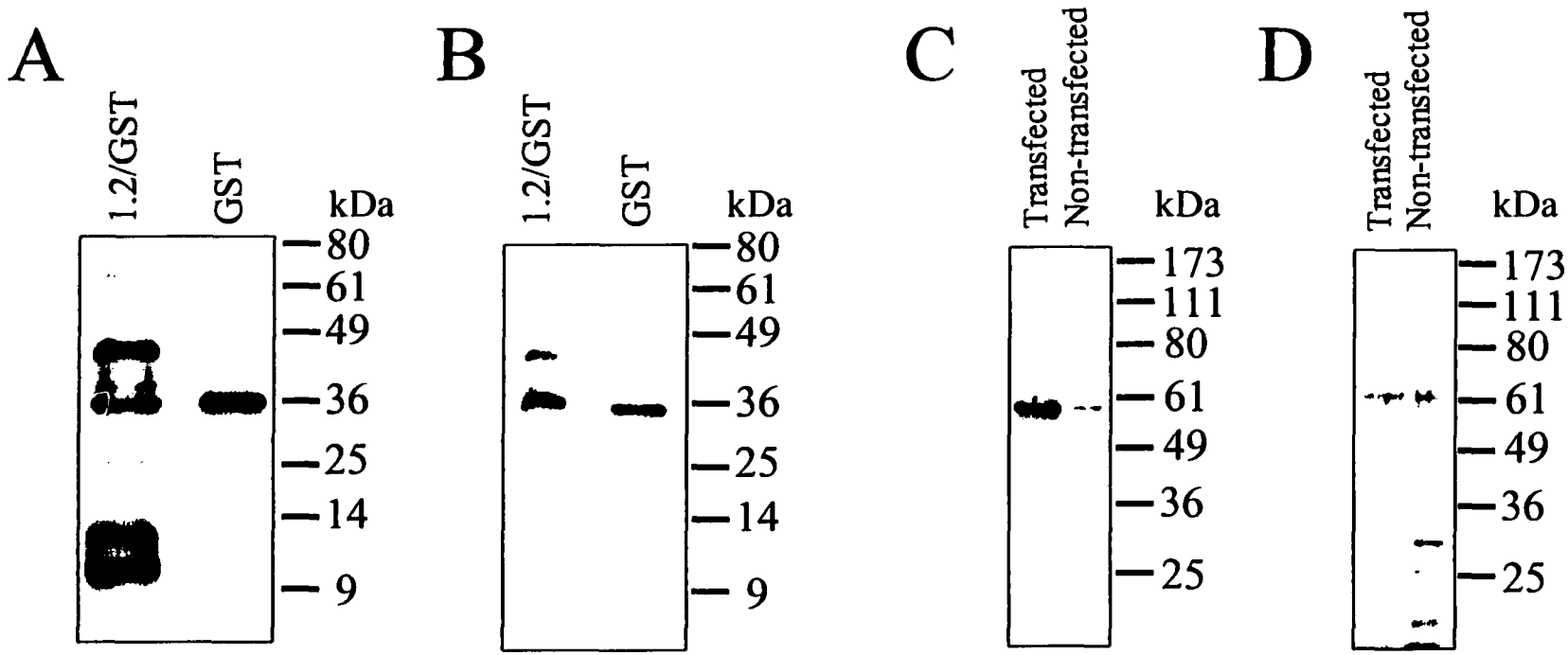

Figure 4.6. Western blot analysis of Kv1.2 and corresponding GST block. Panels A and B illustrate binding of anti-Kv1.2-T fusion protein antibody to the thrombin cleaved GST/Kv1.2 and GST proteins after preincubation with 40 nmol/liter GST (A) or GST/Kv1.2 (B). Panels C and D illustrate binding of the anti-GST-Kv1.2-T fusion protein antibody in transfected or non-transfected L-cell membranes after pre-incubation with GST (C) or GST/Kv1.2 (D).

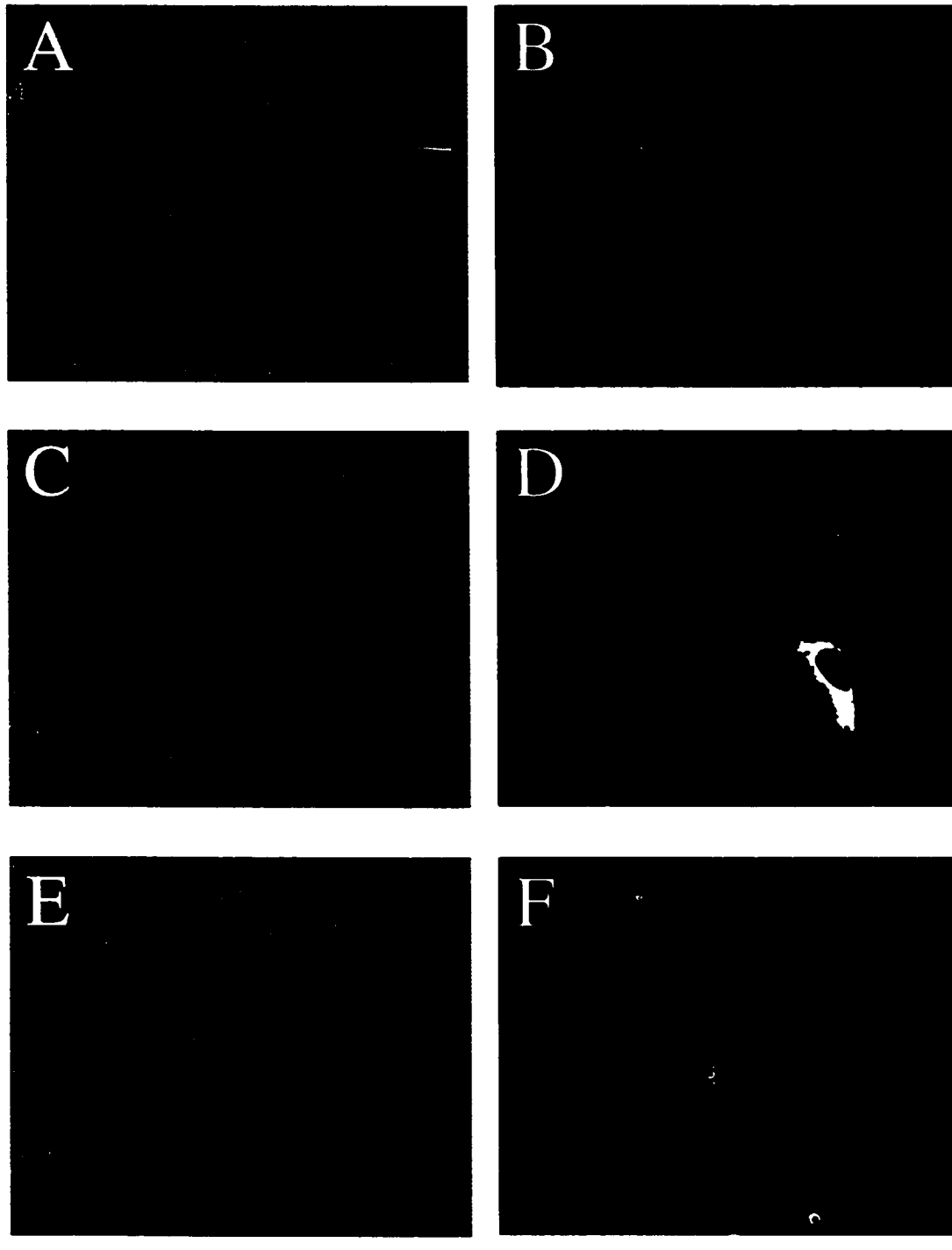

Figure 4.7. Kv1.2 immunostaining of transfected cells. Panels show DIC image and binding of anti-Kv1.2-T antibody (Cy3 image), respectively, in mock-transfected (A-B), Kv1.2-transfected (C-D), and Kv1.5/1.2 tandem-transfected (E-F) L-cells. Exposure conditions for B, D and F were identical. Calibration bar illustrated in first panel.

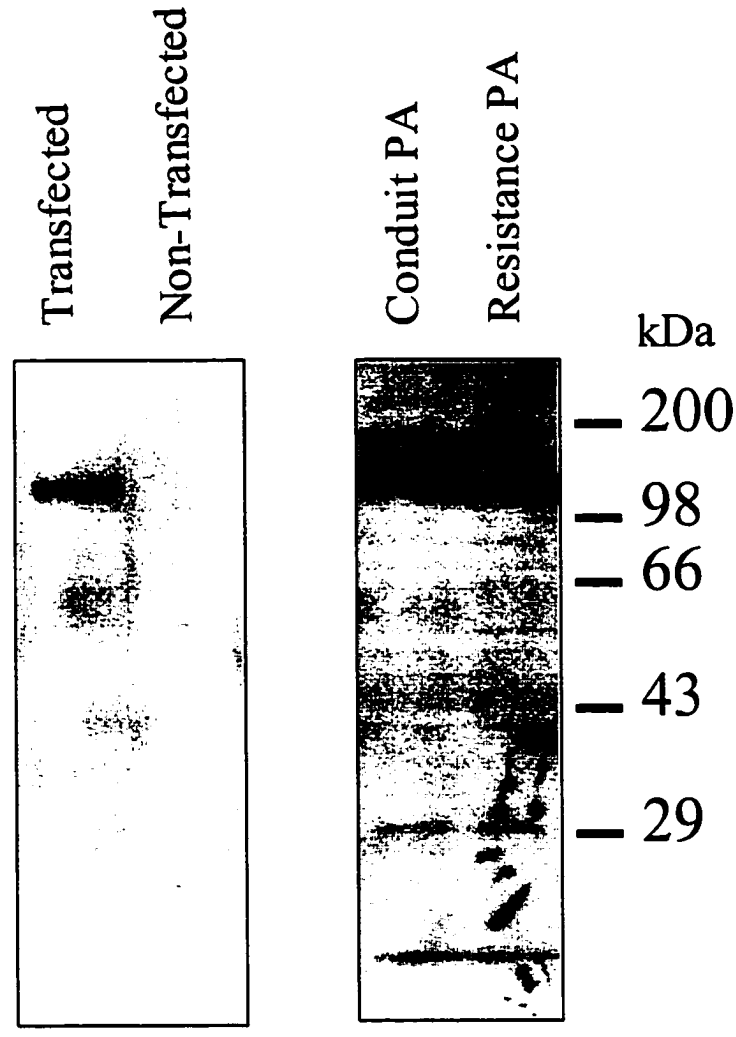

Figure 4.8. Western blot analysis of Kv2.1 expression in bovine conduit and resistance PASMCs. Immunoblot shows binding of anti-Kv2.1 antibody to an approximately 110 kDa band in transfected L-cells and bovine conduit and resistance PASMC membranes.

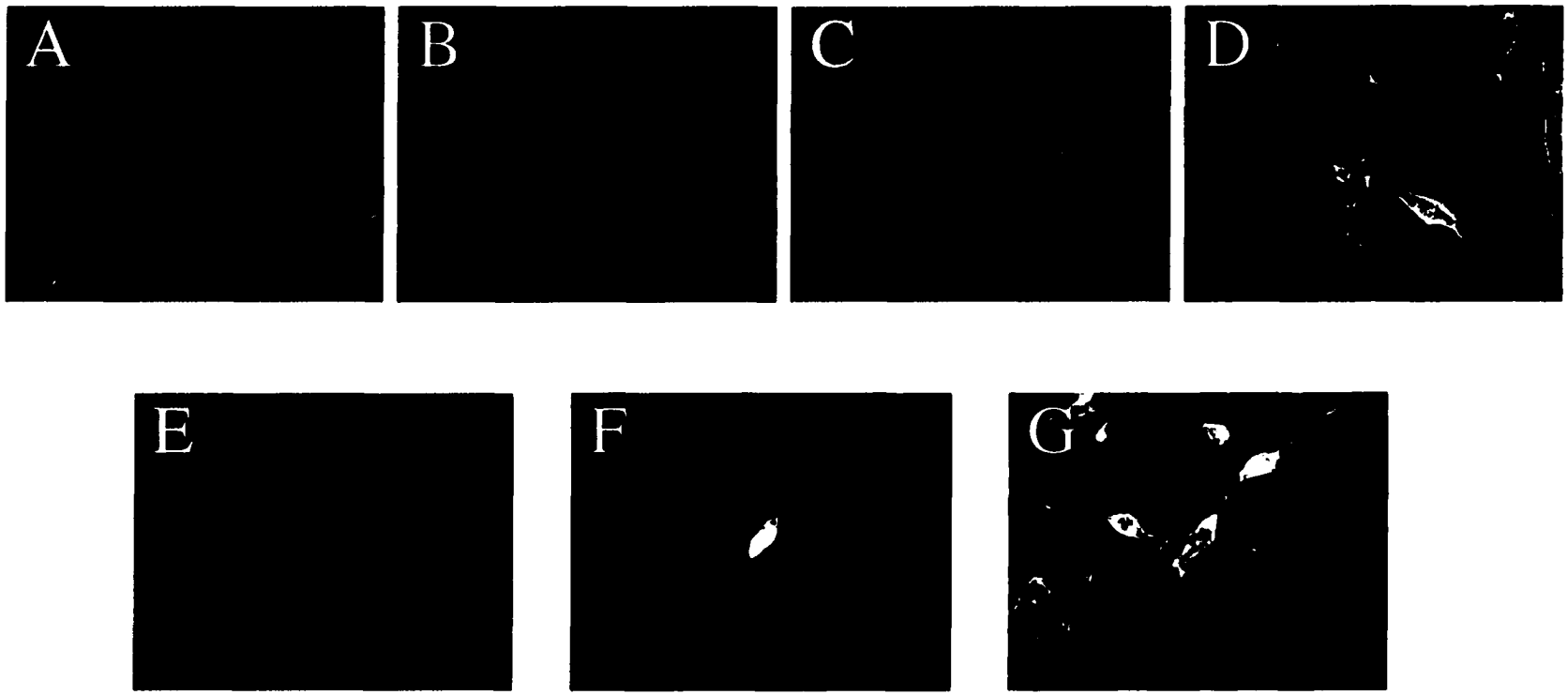

Figure 4.9. Kv2.1 immunostaining of transfected L-cells. Panels A-D show DIC image and binding anti-Kv2.1 antibody (Cy3 image), respectively, in non-transfected (A-B) and Kv2.1-transfected (C-D) L-cells. Panels E-F show DIC image, GFP image and binding of anti-Kv2.1 antibody (Cy3 image), respectively, in Kv2.1- and Kv9.3-transfected L-cells. GFP color illustrates cells likely to express Kv9.3. Exposure conditions for panels B, D and G were identical. Calibration bar illustrated in first panel.

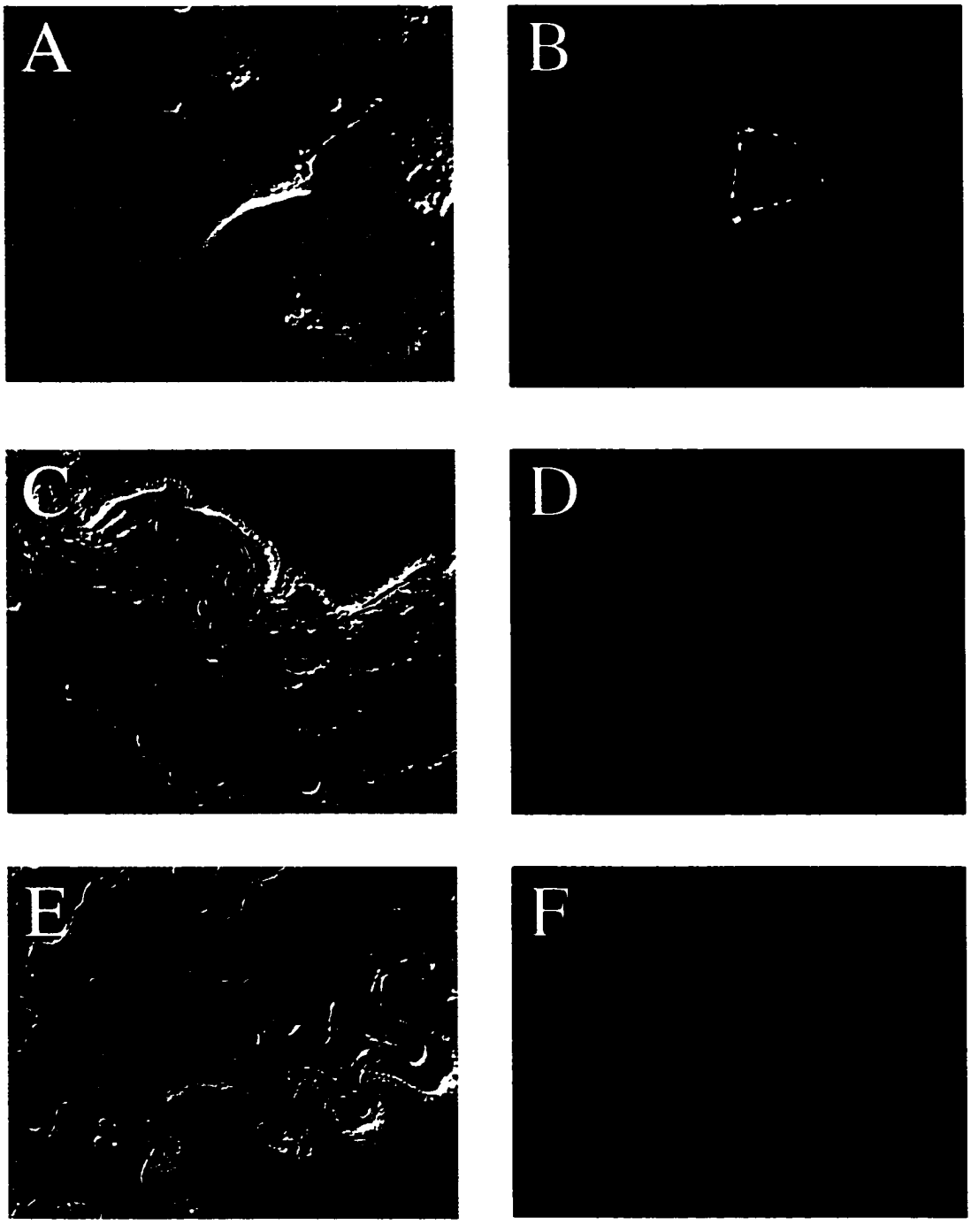

Figure 4.10. Immunolocalization of Kv2.1 in tissue. Panels A-D show DIC image and binding of anti-Kv2.1 antibody (Cy3 image), respectively, in rat hippocampal neuron (A-B) and bovine resistance pulmonary artery (C-D). DIC image and no primary antibody (Cy3 image) in bovine resistance pulmonary artery is shown as a control (panels E-F). Exposure conditions were identical for panels D and F. Calibration bars illustrated in first panel of each series. Panels A and B courtesy of Dr. Jeff Martens Ph.D.

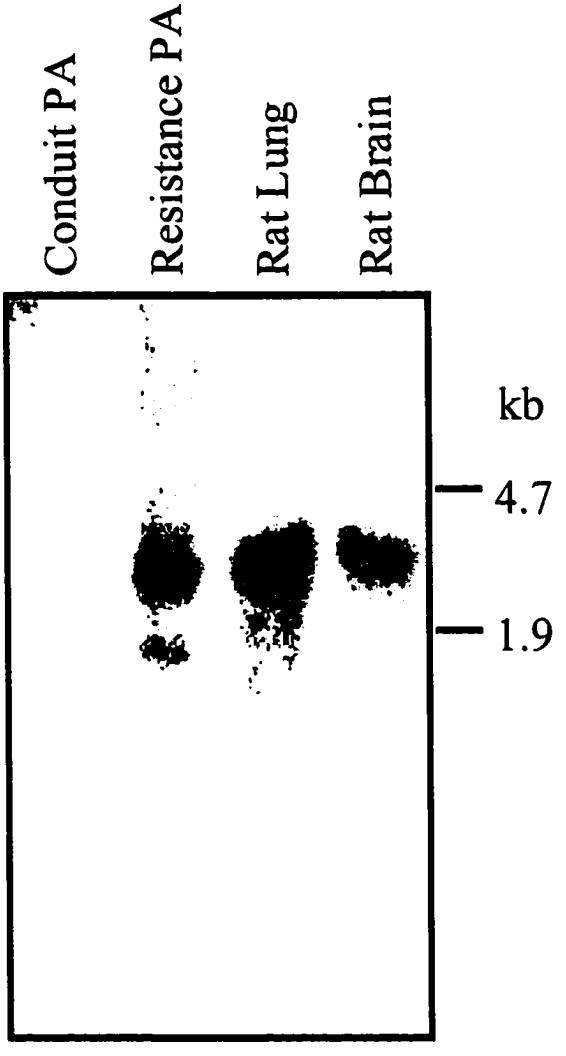

Figure 4.11. Northern blot analysis of Kv9.3 mRNA expression in bovine conduit and resistance PASMCs, rat lung and rat brain. Positions of the large and small rRNA subunits, approximately 4.7 and 1.9 kb, respectively, are indicated.

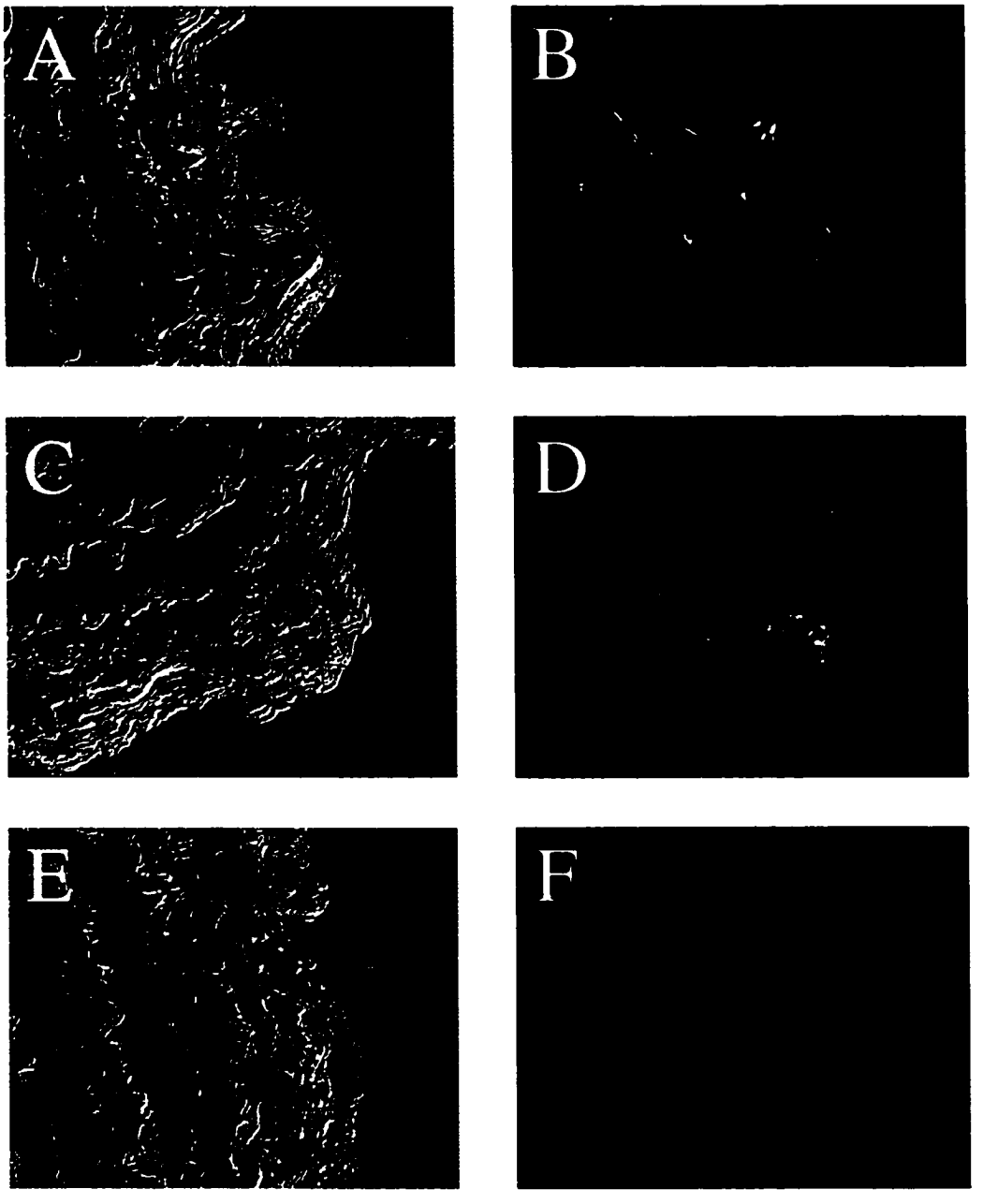

Figure 4.12. Immunolocalization of Kv1.2 α subunit in bovine resistance pulmonary arteries. Panels show DIC image and binding of anti-Kv1.2-T antibody (Cy3 image), respectively, in pulmonary resistance vessels (3rd intrapulmonary) incubated with anti-Kv1.2-T antibody alone (A-B), after preincubation with 40 nmol/liter GST(C-D) or after pre-incubation with 40 nmol/liter GST/Kv1.2 (E-F) fusion proteins. Exposure conditions for B, D and F were identical. Calibration bar illustrated in panel A.

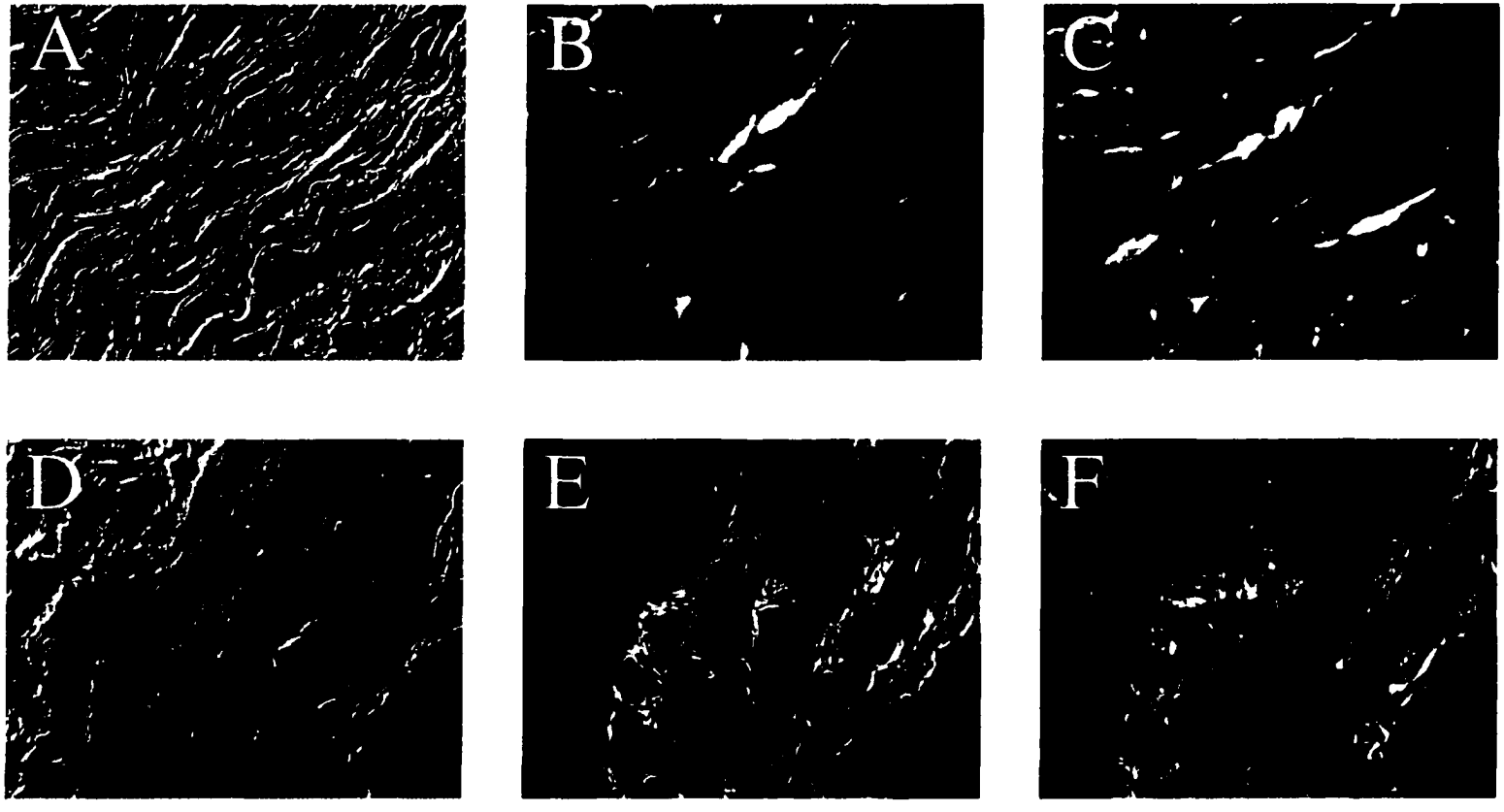

Figure 4.13. Immunolocalization of Kv1.2 α subunit and α-smooth muscle actin in bovine conduit and resistance pulmonary arteries. Panels show DIC image, binding of anti-α smooth muscle actin antibody (Cy3 image) and binding of anti-Kv1.2-T antibody (Cy5 image), respectively, in bovine conduit (A-C) and resistance (4^{th} intralobar) (D-F) pulmonary arteries. Exposure conditions for C and F were identical. Calibration bar illustrated in panel A.

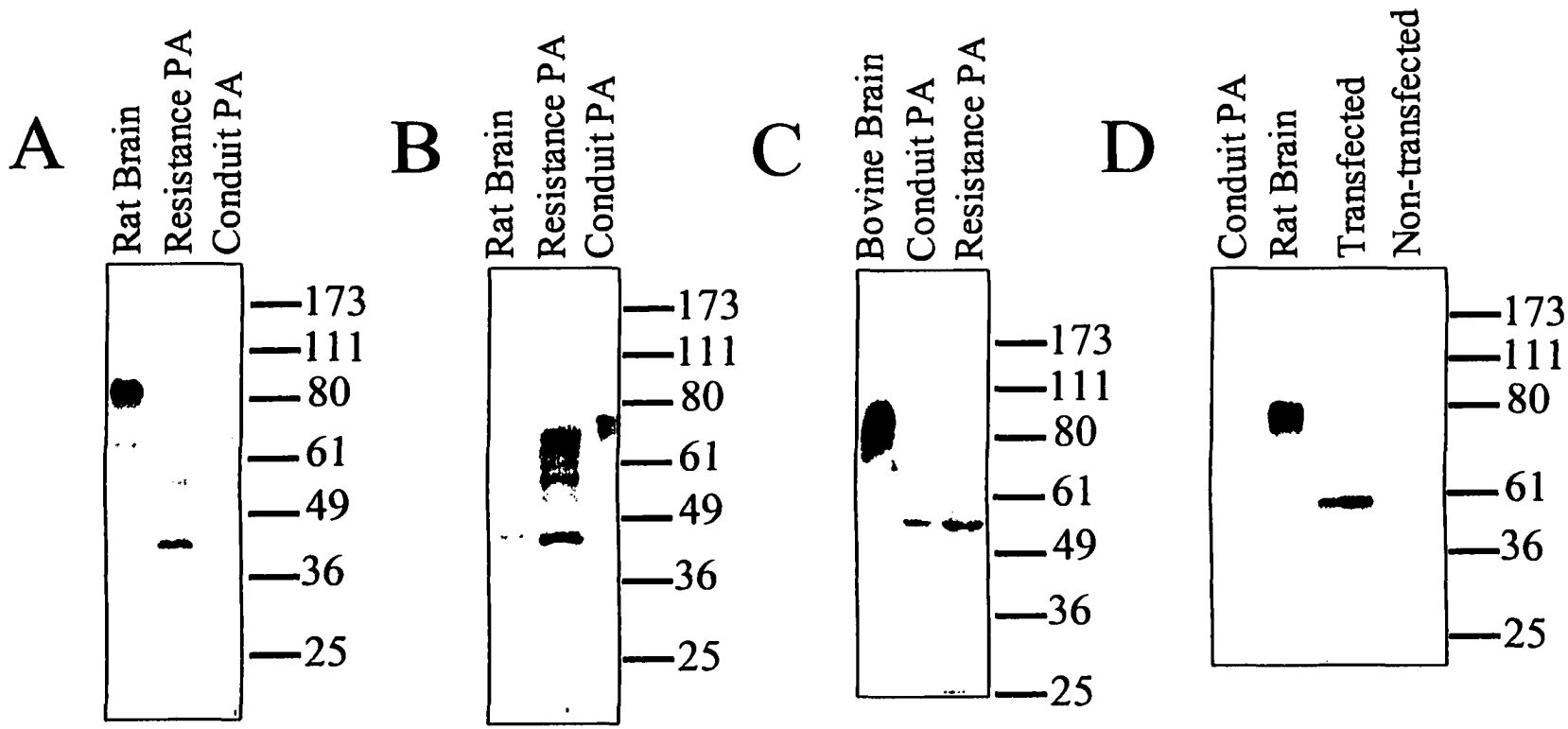

Figure 4.14. Western blot analysis of Kv1.2 protein expression in rat brain and bovine conduit and resistance PASMCs. Panels A and B show binding of anti-Kv1.2-T fusion protein antibody to rat brain and bovine conduit and resistance PASMC membranes after preincubation with 40 nmol/liter GST (A) or GST/Kv1.2 (B) fusion proteins. Panels C and D illustrate binding of anti-Kv1.2C polyclonal antibody (C) and anti-Kv1.2 monoclonal antibody (D) to bovine brain, rat brain, mouse *L*-cell and bovine conduit and resistance PASMC membranes.

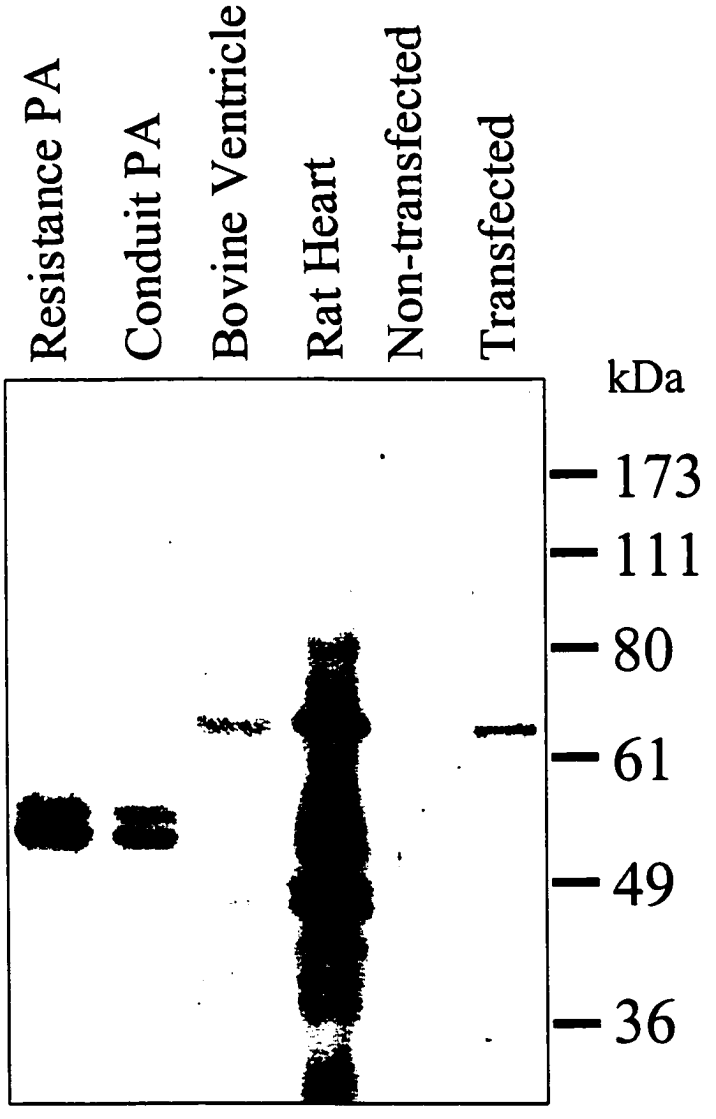

Figure 4.15. Western blot analysis of Kv1.5 protein expression in bovine conduit and resistance PASMCs. Immunoblot shows binding of anti-Kv1.5C monoclonal antibody to a band of approximately 70 kDa in bovine conduit and resistance PASMC and ventricular membranes, rat heart membranes and mouse L-cell membranes.

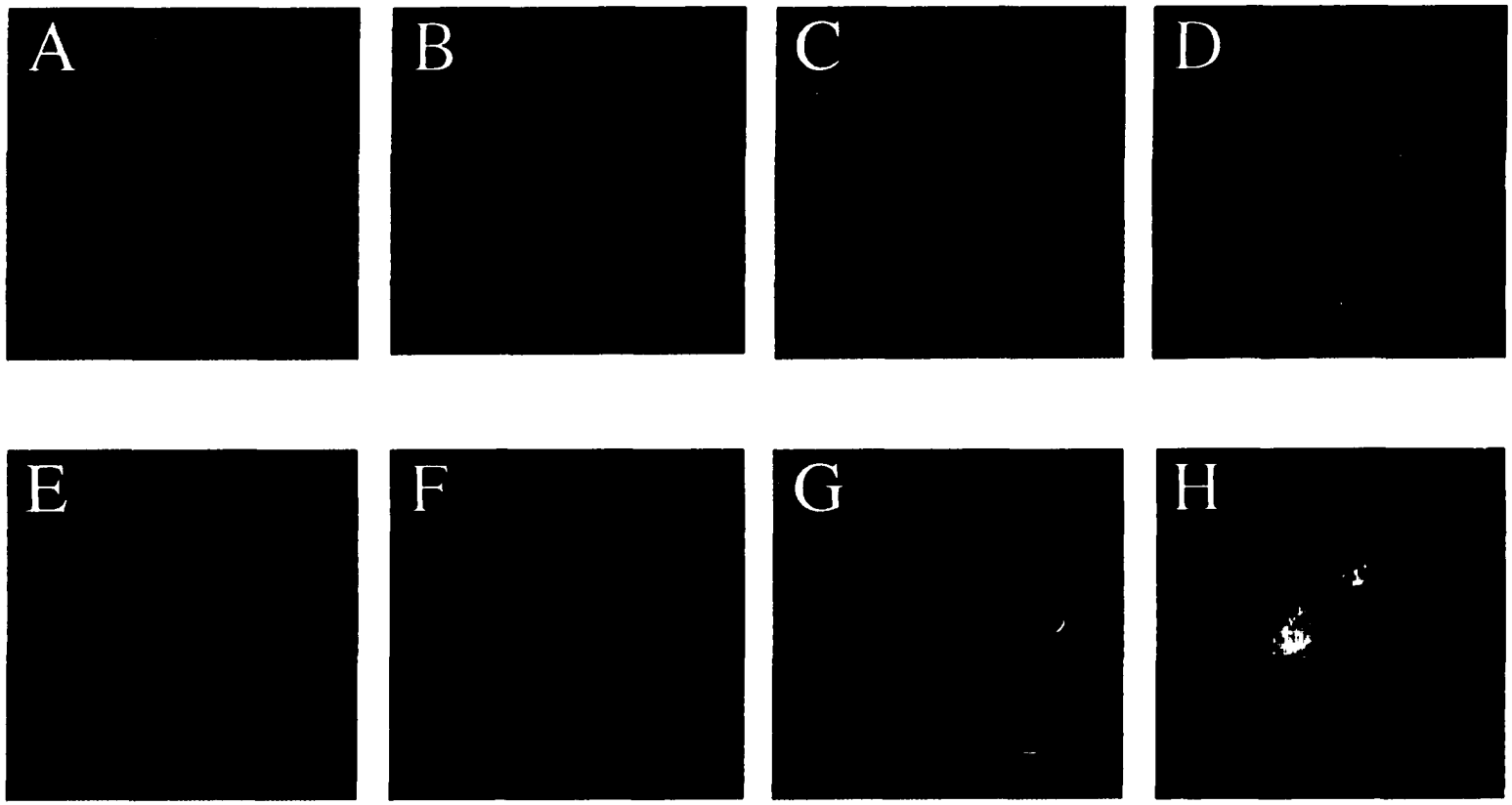

Figure 4.16. Kv1.5 immunostaining of transfected L-cells. Panels show DIC image and binding of anti-human-Kv1.5-T antibody (Cy3 image), respectively, in non-transfected (A-B), Kv1.5-transfected (C-D), mock-transfected (E-F) and Kv1.5/1.2 tandem-transfected (G-H) L-cells. Exposure conditions for B and D and for F and H were identical. Calibration bar illustrated in panel A.

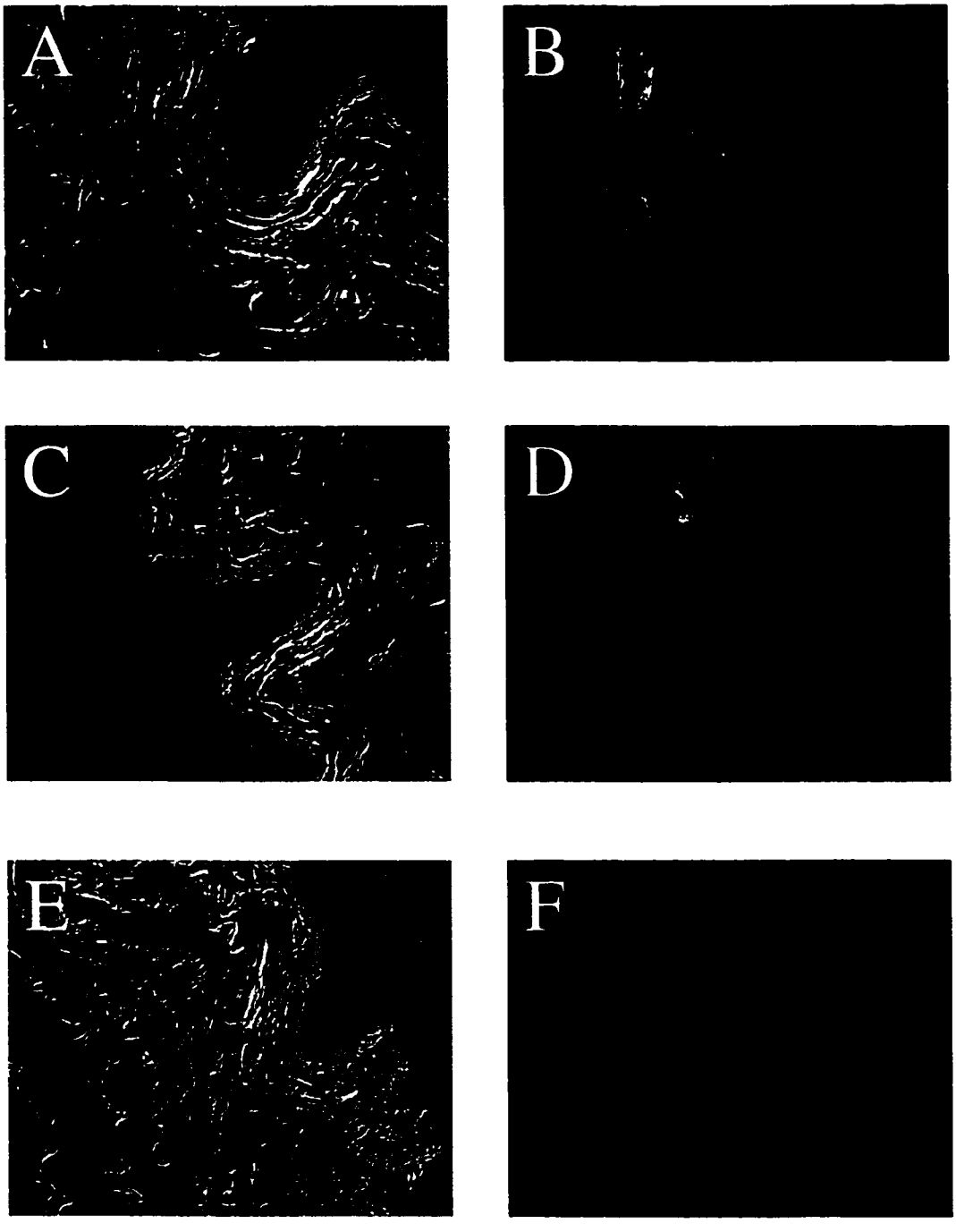

Figure 4.17. Immunolocalization of Kv1.5 α subunit in bovine resistance pulmonary arteries. Panels show DIC image and binding of anti-human-Kv1.5-T antibody (Cy3 image), respectively, in pulmonary resistance vessels (3rd intrapulmonary) incubated with anti-human-Kv1.5-T antibody alone (A-B), after preincubation with 40 nmol/liter GST (C-D) or after pre-incubation with 40 nmol/liter GST/Kv1.5 (E-F) fusion proteins. Exposure conditions for B, D and F were identical. Calibration bar illustrated in panel A.

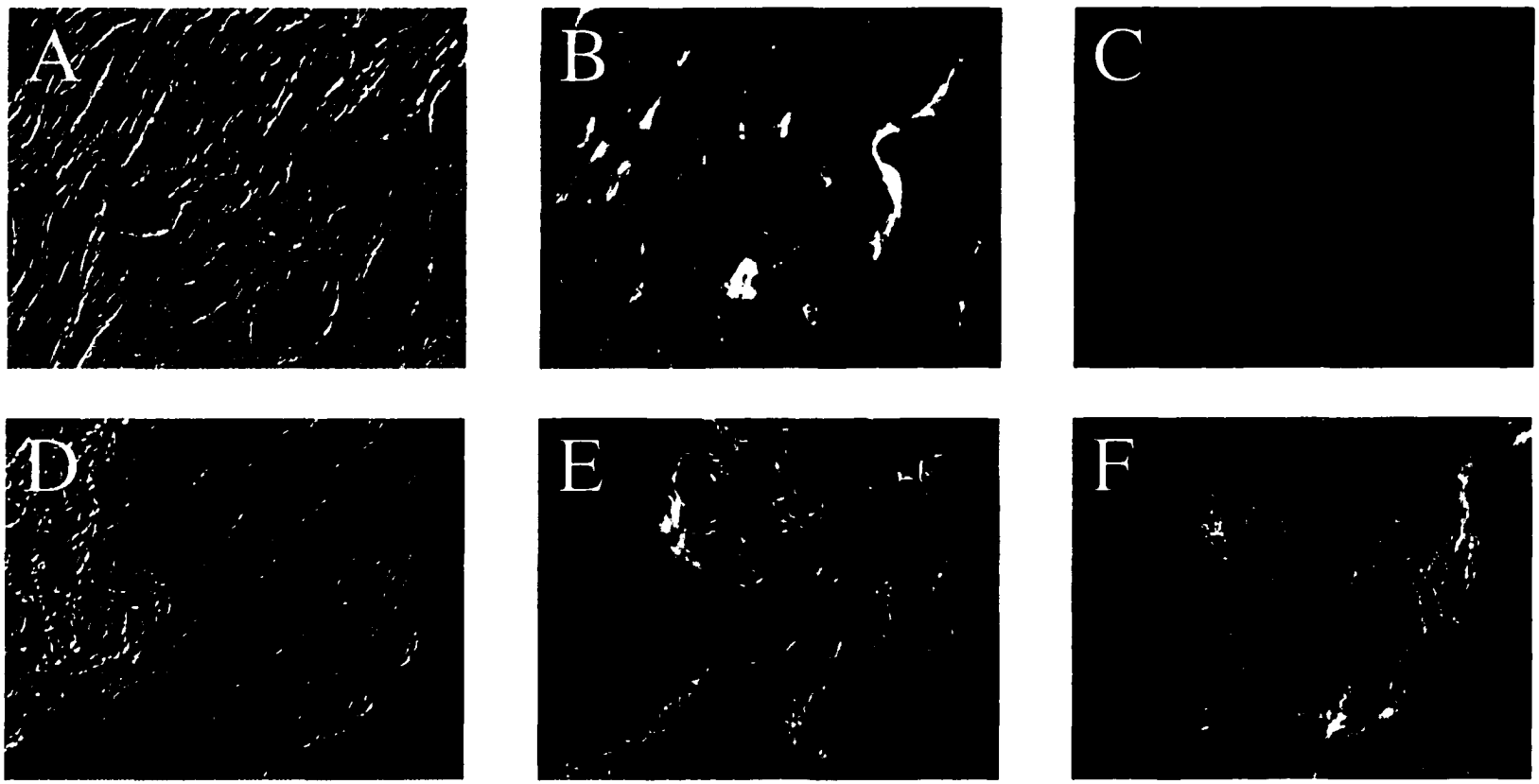

Figure 4.18. Immunolocalization of Kv1.5 α subunit and α smooth muscle actin in bovine conduit and resistance pulmonary arteries. Panels show DIC image, binding of anti-α smooth muscle actin antibody (Cy3 image) and binding of anti-human-Kv1.5-T antibody (Cy5 image), respectively, in bovine conduit (A-C) and resistance (4^{th} intralobar) (D-F) pulmonary arteries. Exposure conditions for C and F were identical. Calibration bar illustrated in panel A.

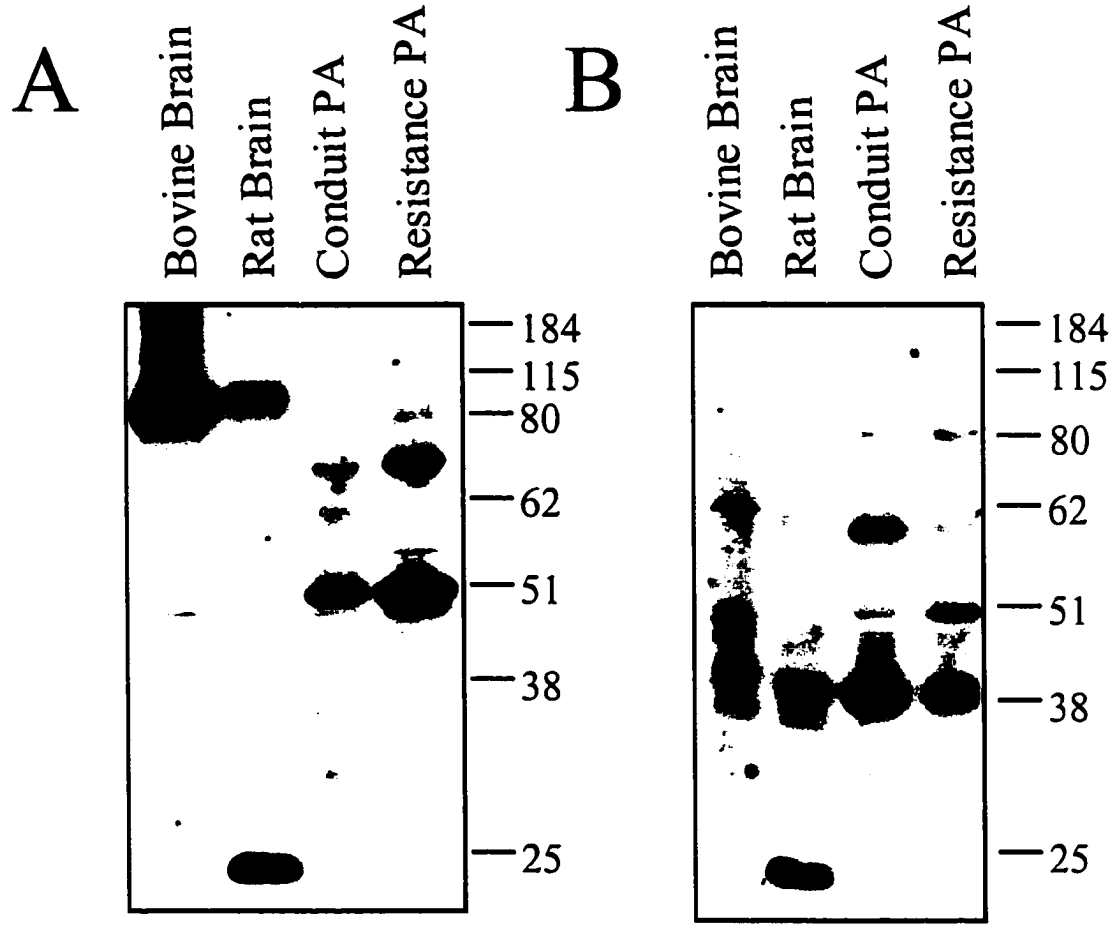

Figure 4.19. Western blot analysis of Kv3.1b protein expression in bovine conduit and resistance PASMCs. Panels A and B show binding of anti-Kv3.1b alone (A) and after preincubation with 1 μmol/liter Kv3.1b peptide (B).

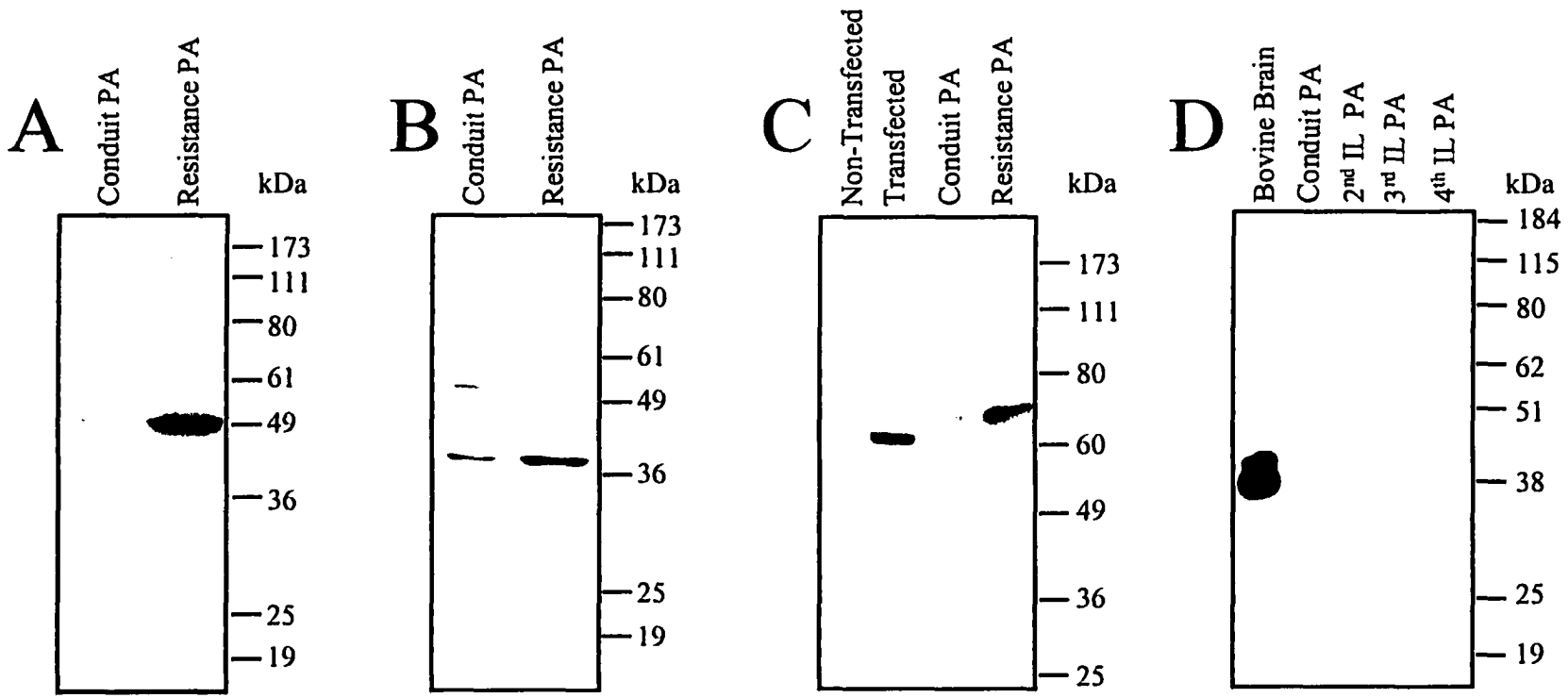

Figure 4.20. Western blot analysis of Kv β subunit expression in bovine conduit and resistance PASMCs. Immunoblots illustrate antibody binding of anti-Kvβ1.1N polyclonal antibody (A), anti-Kvβ1.2N polyclonal antibody (B), anti-Kvβ1.3-T polyclonal antibody (C) and anti-Kvβ2.1 monoclonal antibody (D). 2nd I.L., 3rd I.L.and 4th I.L. refer to the 2nd, 3rd and 4th branches of the intra-lobar pulmonary artery, respectively.

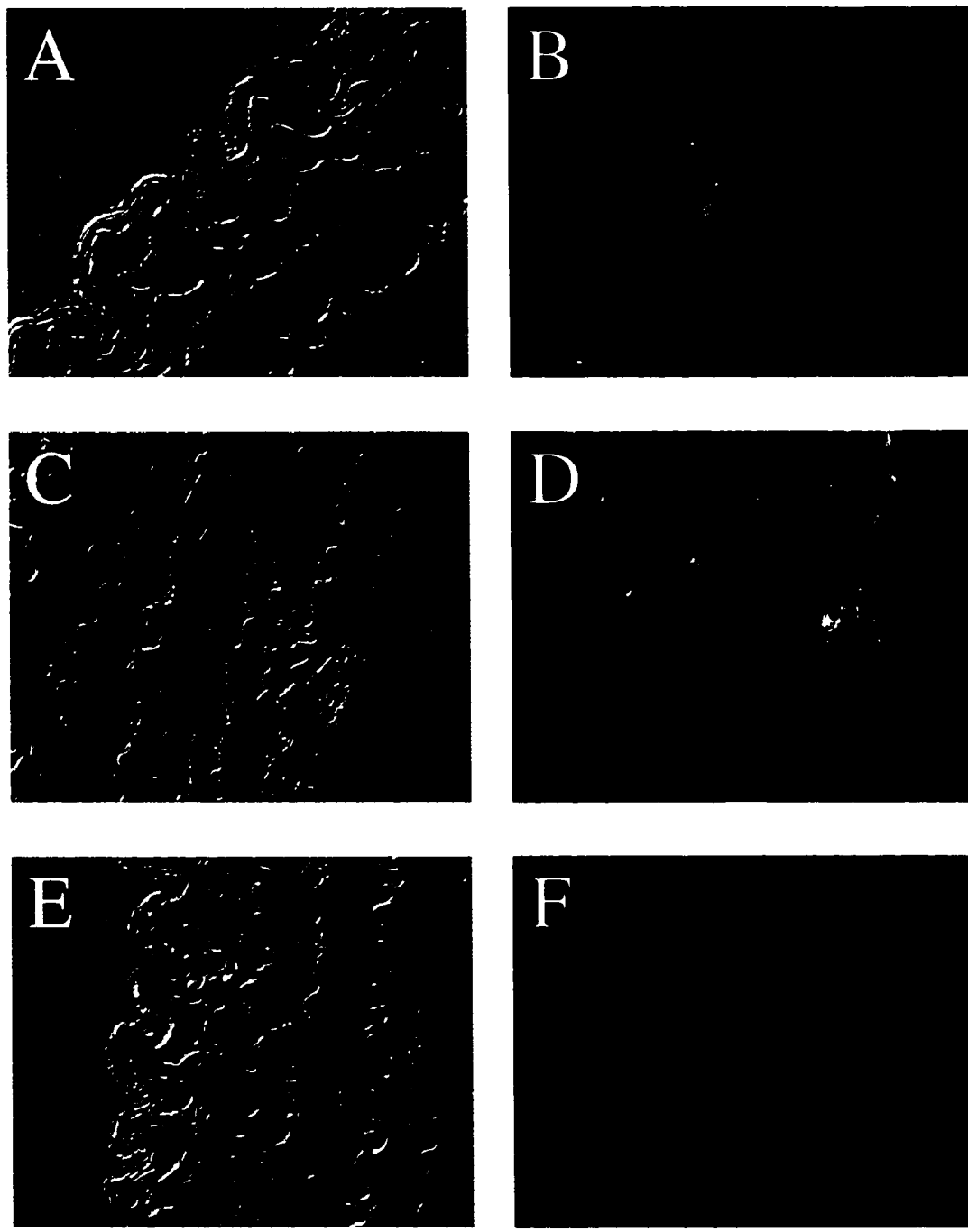

Figure 4.21. Immunolocalization of Kvβ1.2 in bovine resistance pulmonary arteries. Panels show DIC image and binding of anti-Kvβ1.2-T antibody (Cy3 image), respectively, in pulmonary resistance vessels (3rd intrapulmonary) incubated with anti-Kvβ1.2-T antibody alone (A-B), after preincubation with 1 μmol/liter GST (C-D) or after pre-incubation with 1 μmol/liter GST/Kvβ1.2 (E-F) fusion proteins. Exposure conditions for B, D and F were identical. Calibration bar illustrated in panel A.

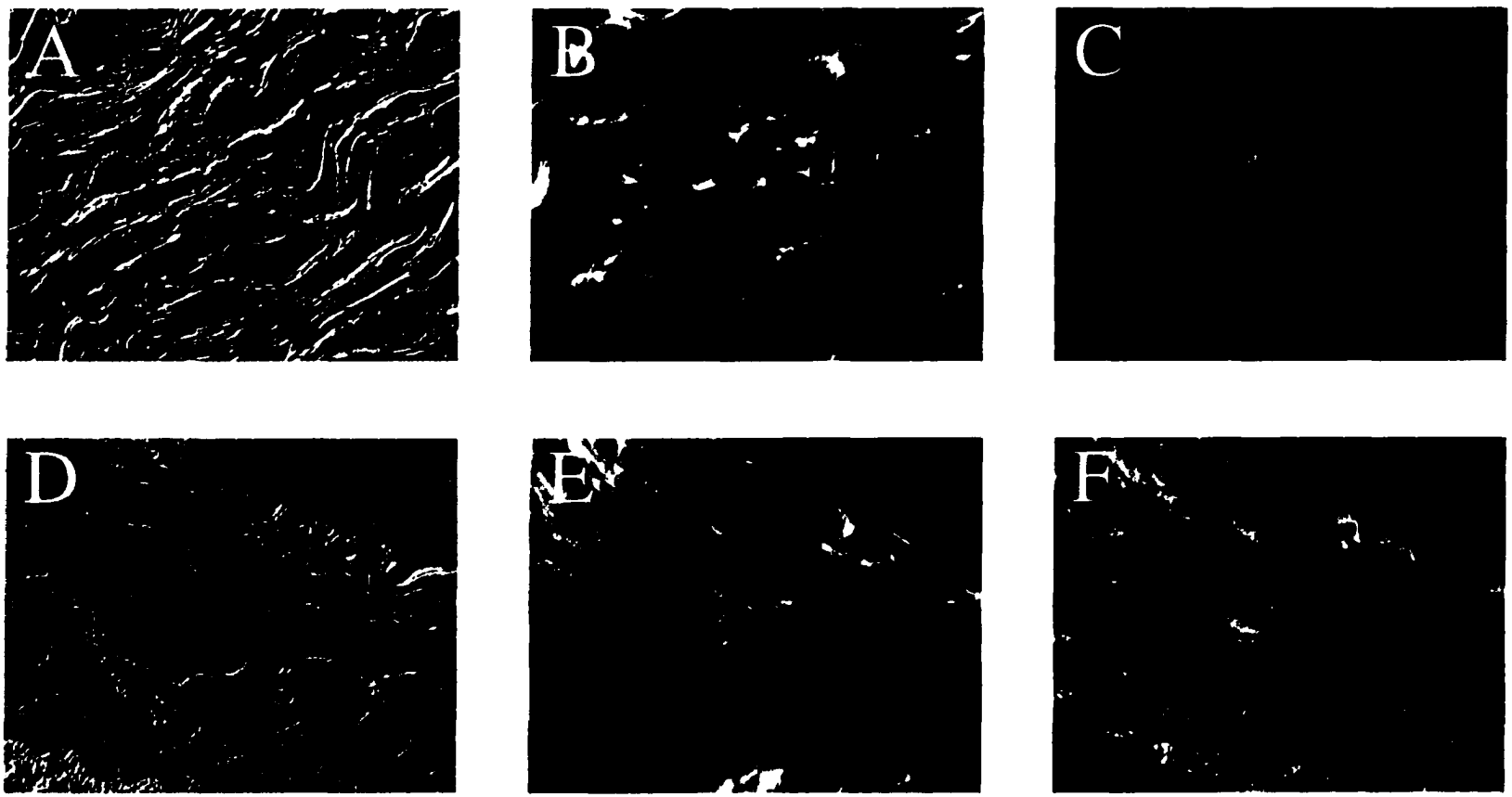

Figure 4.22. Immunolocalization of Kvβ1.2 and α smooth muscle actin in bovine conduit and resistance pulmonary arteries. Panels show DIC image, binding of anti-α smooth muscle actin antibody (Cy3 image) and binding of anti-Kvβ1.2-T antibody (Cy5 image), respectively, in bovine conduit (A-C) and resistance (4th intralobar) (D-F)pulmonary arteries. Exposure conditions for C and F were identical. Calibration bar illustrated in panel A.

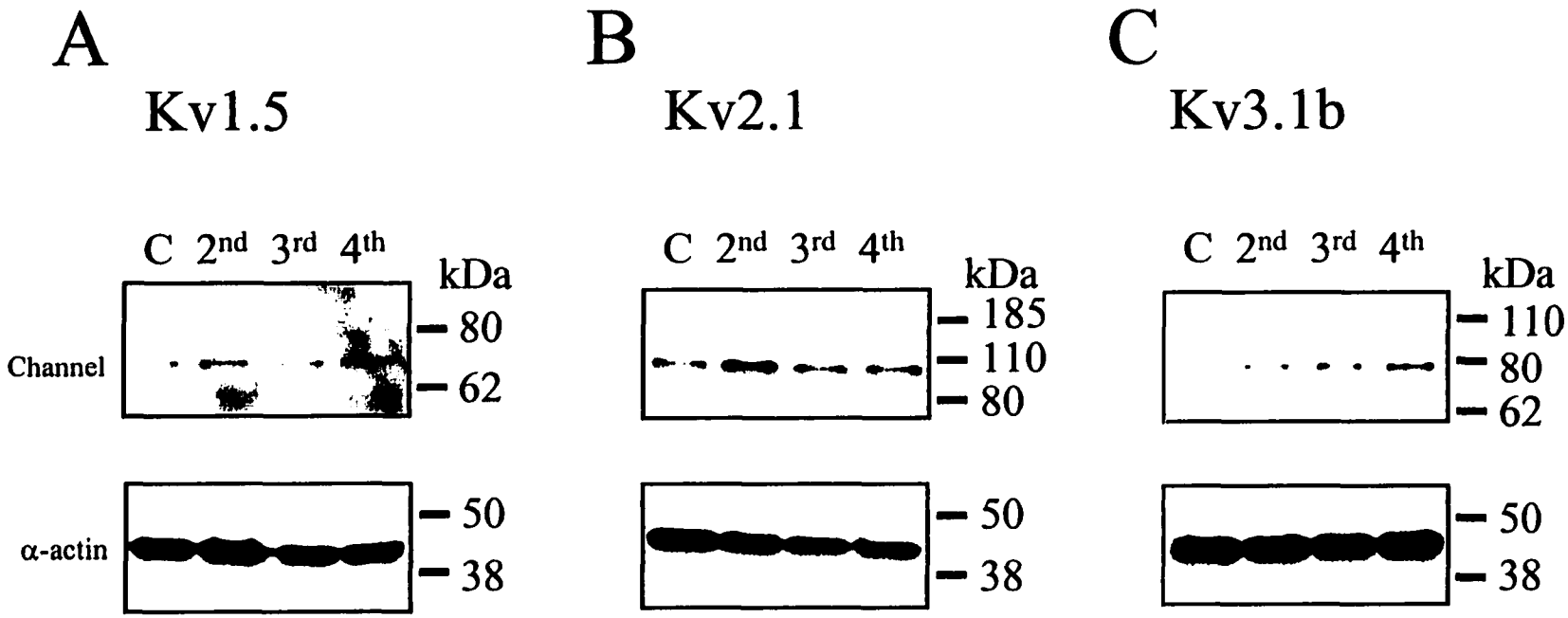

Figure 4.23. Western blot analysis of Kv α subunit expression in the pulmonary artery. Panels illustrate Kv1.5 (A), Kv2.1 (B) and Kv3.1b (C) expression in bovine conduit (C), 2nd intralobar, and 3rd and 4th resistance intralobar pulmonary artery smooth muscle cell membranes. Immunoblots were incubated with antibodies against Kv1.5, Kv2.1 or Kv3.1b and then stripped and reprobed with anti-α smooth muscle actin antibody in order to identify differences in PASMC loading between samples. Data shown are representative of 3 or more independent samples.

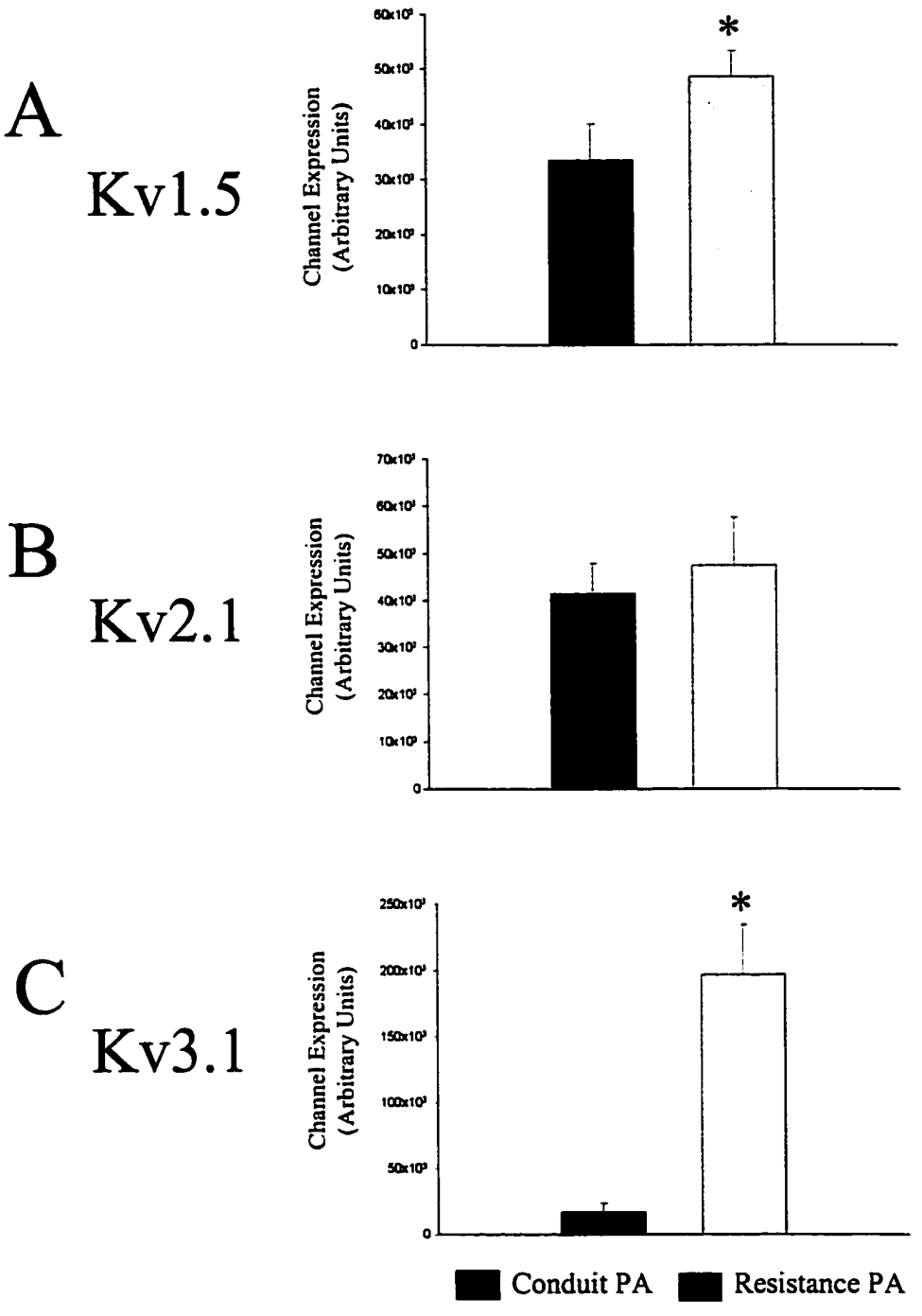

Figure 4.24. Bar graph highlighting the differences in Kv α subunit expression between bovine conduit and resistance (3rd and 4th pooled) PASMCs. Panels illustrate protein expression, as measured in arbitrary units corrected for smooth muscle α-actin, for: Kv1.5 (A), Kv2.1 (B) and Kv3.1b (C) as determined via Western blot analysis and densitometry. Sample sizes are as follows: Kv1.5 (n=5, 2 animals), Kv2.1 (n=4, 3 animals) and Kv3.1b (n=5, 3 animals) . *Significant difference, $p<0.5$.

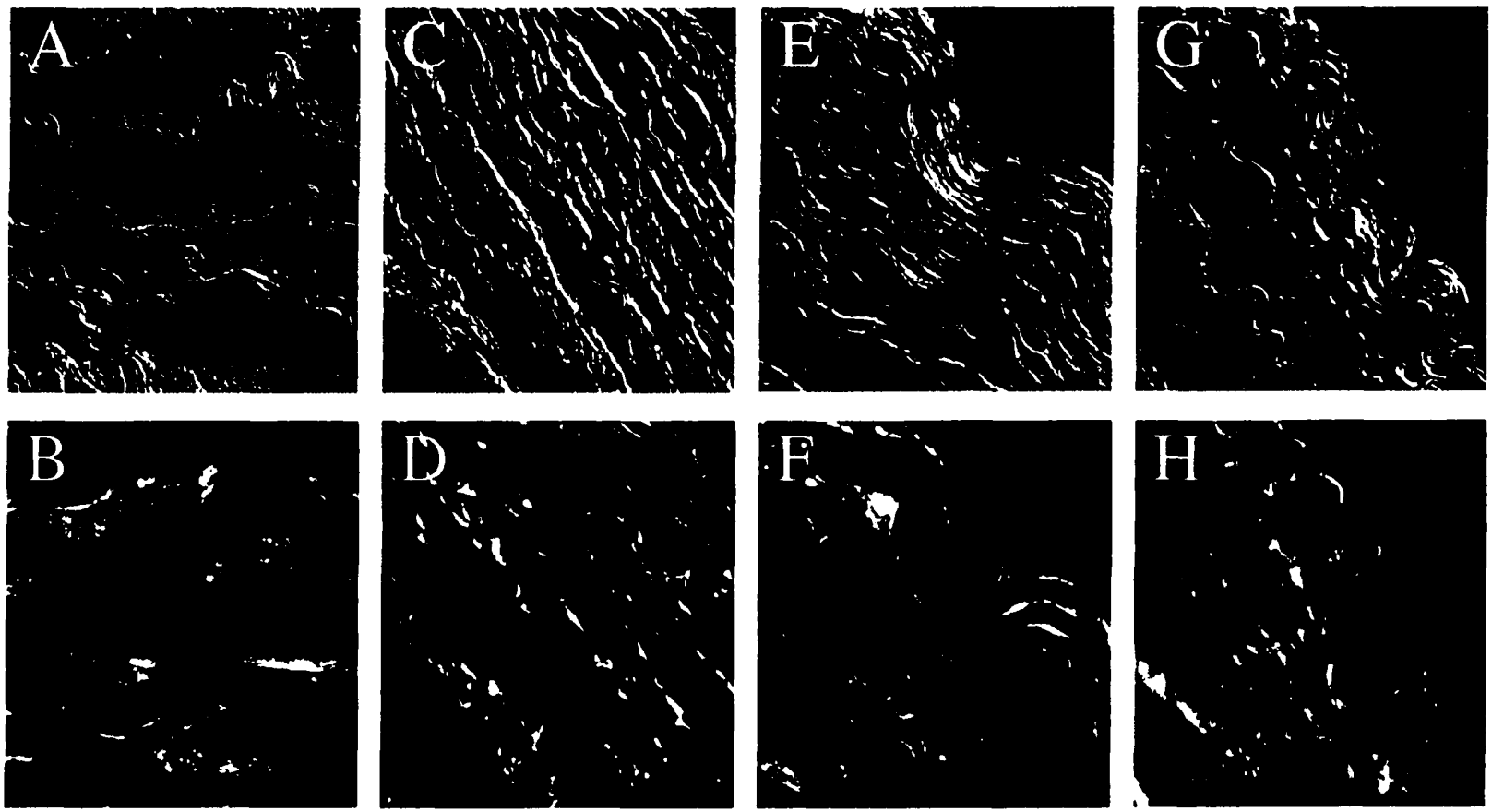

Figure 4.25. Immunolocalization of Kv1.2 α subunit in the bovine pulmonary artery. Panels show DIC image and binding of anti-Kv1.2-T antibody (Cy3 image), respectively, in bovine conduit (A-B), 2nd intralobar (C-D), 3rd intralobar (E-F) and 4th intralobar (G-H) pulmonary arteries. Exposure conditions for B, D, F and H were identical. Calibration bar illustrated in panel A.

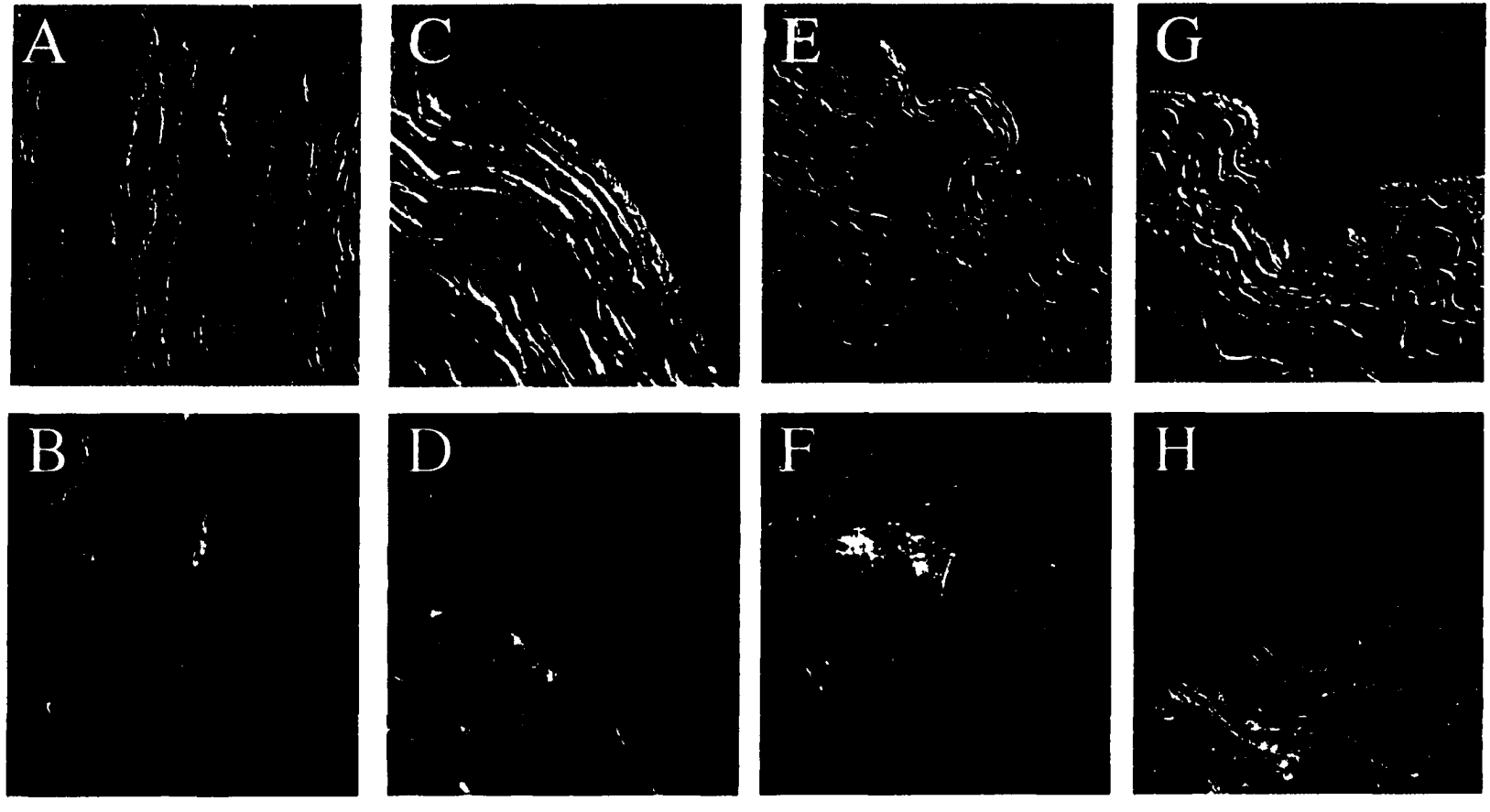

Figure 4.26. Immunolocalization of Kv1.5 α subunit in the bovine pulmonary artery. Panels show DIC image and binding of anti-human-Kv1.5-T antibody (Cy3 image), respectively, in bovine conduit (A-B), 2nd intralobar (C-D), 3rd intralobar (E-F) and 4th intralobar (G-H) pulmonary arteries. Exposure conditions for B, D, F and H were identical. Calibration bar illustrated in panel A.

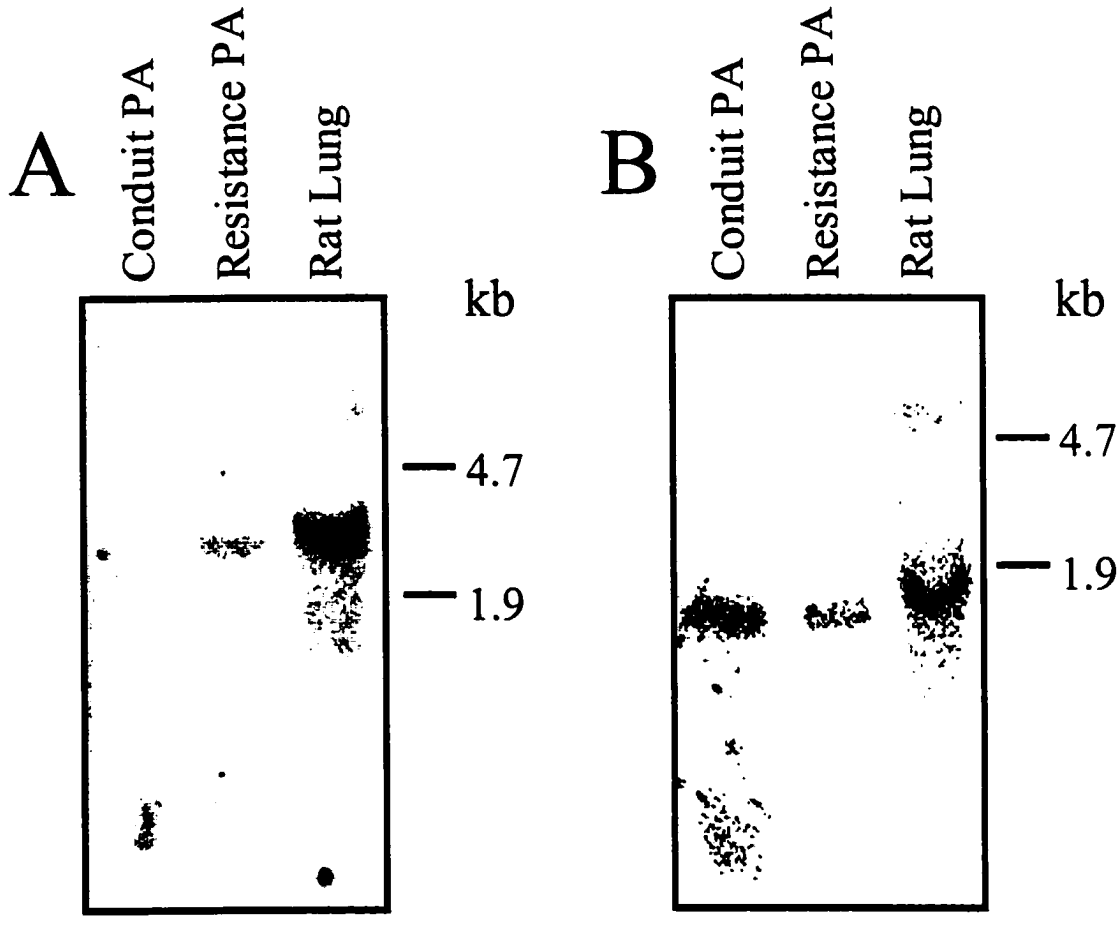

Figure 4.27. Northern blot analysis of Kv9.3 mRNA expression in the pulmonary artery. A) Kv9.3 expression in bovine conduit and resistance PASMCs. B) Same blot as in A reprobed with smooth muscle α-actin to ensure integrity of the RNA and to access possible differences in PASMC loading between groups. Positions of the large and small rRNA subunits, approximately 4.7 and 1.9 kb, respectively, are indicated.

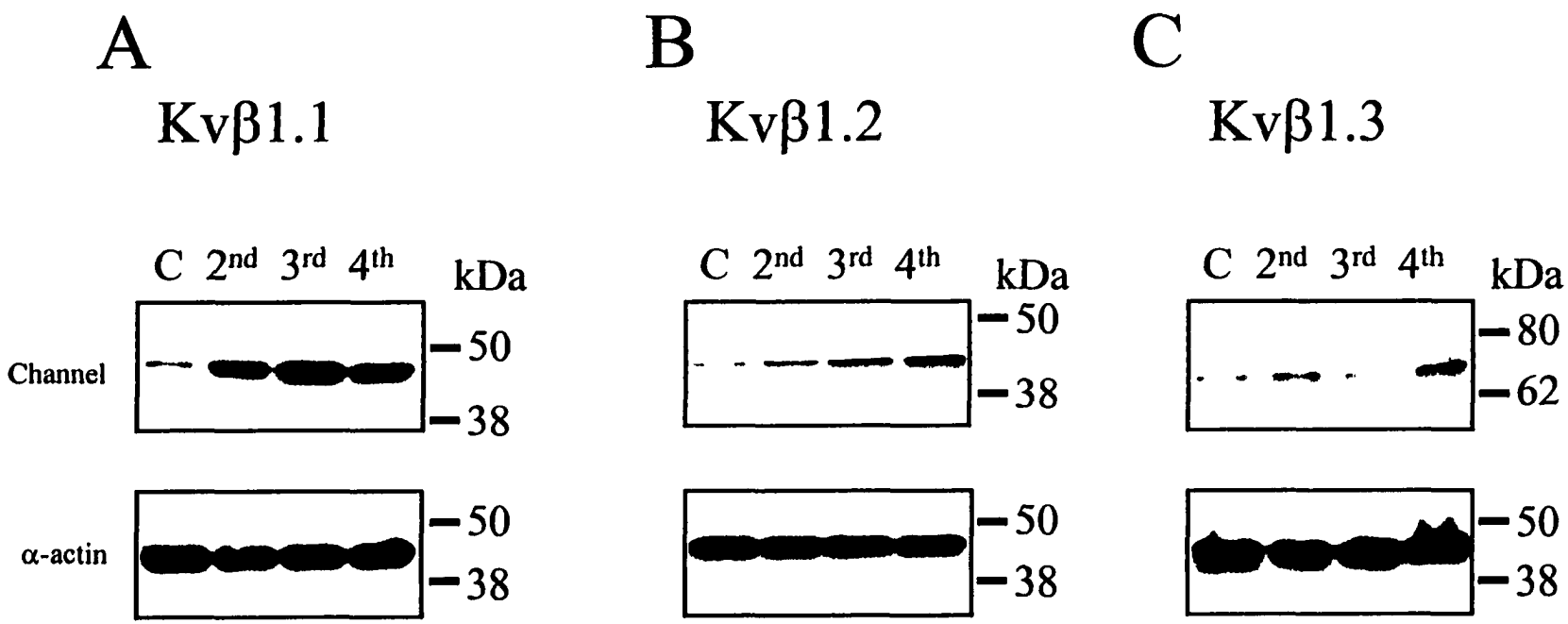

Figure 4.28. Western blot analysis of Kv β subunit expression in the pulmonary artery. Panels illustrate Kvβ1.1 (A), Kvβ1.2 (B) and Kvβ1.3 (C) expression in bovine conduit (C), 2nd intralobar, and 3rd and 4th resistance intralobar pulmonary artery smooth muscle cell membranes. Immunoblots were incubated with antibodies against Kvβ1.1, Kvβ1.2 or Kvβ1.3 and then stripped and reprobed with anti-α smooth muscle cell actin antibody in order to identify differences in PASMC loading between samples. Data shown are representative of 3 or more independent samples.

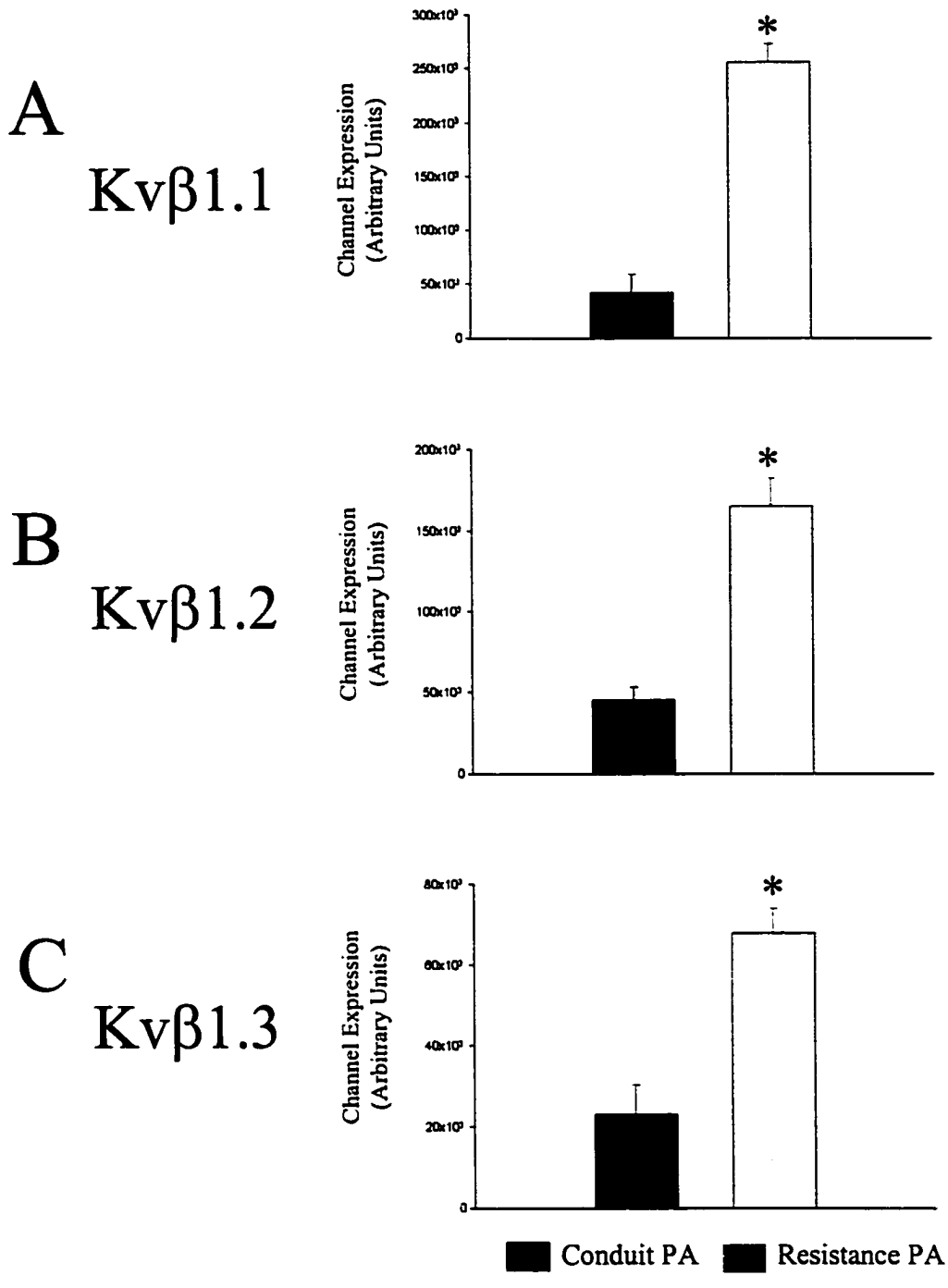

Figure 4.29. Bar graph highlighting the differences in Kv β subunit expression between bovine conduit and resistance (3rd and 4th pooled) PASMCs. Panels illustrate protein expression, as measured in arbitrary units corrected for smooth muscle α-actin, for Kvβ1.1 (A), Kvβ1.2 (B) and Kvβ1.3 (C) as determined via Western blot analysis and densitometry. Sample sizes are as follows: Kvβ1.1 (n=3, 3 animals), Kvβ1.2 (n=6, 4 animals) and Kvβ1.3 (n=3, 3 animals) *Significant difference, $p<0.5$.

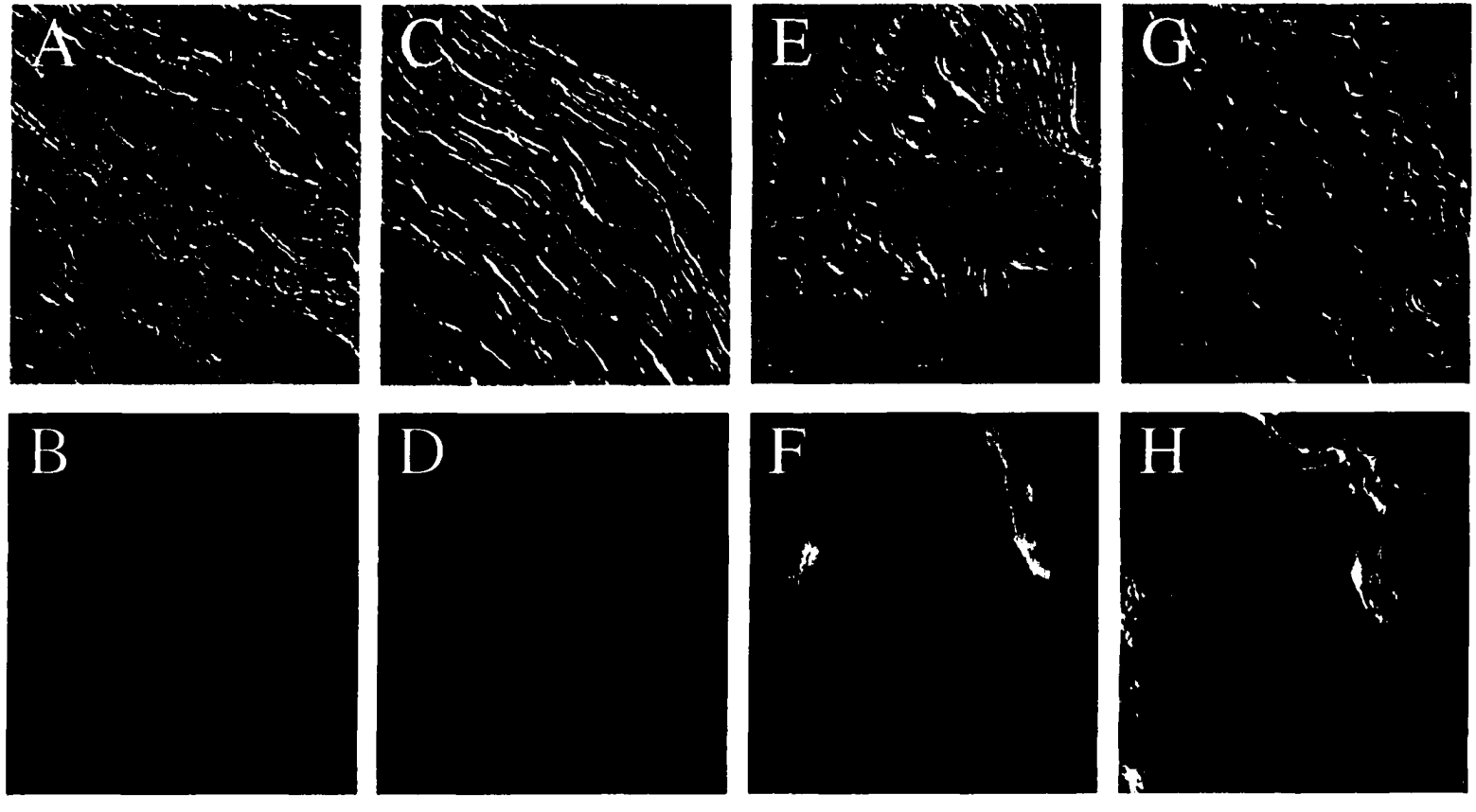

Figure 4.30. Immunolocalization of Kvβ1.2 subunit in the bovine pulmonary artery. Panels show DIC image and binding of anti-Kvβ1.2-T antibody (Cy3 image), respectively, in bovine conduit (A-B), 2nd intralobar (C-D), 3rd intralobar (E-F) and 4th intralobar (G-H) pulmonary arteries. Exposure conditions for B, D, F and H were identical. Calibration bar illustrated in panel A.

REFERENCES

1. Albarwani S, Robertson BE, Nye PC, and Kozlowski RZ. Biophysical properties of Ca^{2+}- and Mg-ATP-activated K^+ channels in pulmonary arterial smooth muscle cells isolated from the rat. *Pflugers Arch* 428: 446-454, 1994.

2. Archer SL, Huang JM, Reeve HL, Hampl V, Tolarova S, Michelakis E, and Weir EK. Differential distribution of electrophysiologically distinct myocytes in conduit and resistance arteries determines their response to nitric oxide and hypoxia. *Circ Res* 78: 431-442, 1996.

3. Archer SL, Souil E, Dinh-Xuan AT, Schremmer B, Mercier JC, El Yaagoubi A, Nguyen-Huu L, Reeve HL, and Hampl V. Molecular identification of the role of voltage-gated K^+ channels, Kv1.5 and Kv2.1, in hypoxic pulmonary vasoconstriction and control of resting membrane potential in rat pulmonary artery myocytes. *J Clin Invest* 101: 2319-2330, 1998.

4. Ausubel FM, Brent R, Kingston RE, Moore DD, Seidman JG, Smith JA, and Struhl K. Preparation and analysis of RNA. Current Protocols in Molecular Biology - Volume 1. New York: Wiley. 1997, p. 4.2-4.3.

5. Ausubel FM, Brent R, Kingston RE, Moore DD, Seidman JG, Smith JA, and Struhl K. One-dimensional SDS gel electrophorsis of proteins. Current Protocols in Molecular Biology - Volume 2. New York: Wiley. 1999, p. 10.2A.1-10.2A.29.

6. Conforti L, Bodi I, Nisbet JW, and Millhorn DE. O_2-sensitive K^+ channels: role of the Kv1.2 -subunit in mediating the hypoxic response. *J Physiol (Lond)* 524 (Pt 3): 783-793, 2000.

7. Deal KK, Lovinger DM, and Tamkun MM. The brain Kv1.1 potassium channel: in vitro and in vivo studies on subunit assembly and posttranslational processing. *J Neurosci* 14: 1666-1676, 1994.

8. Garcia-Guzman M, Sala F, Criado M, and Sala S. A delayed rectifier potassium channel cloned from bovine adrenal medulla. Functional analysis after expression in Xenopus oocytes and in a neuroblastoma cell line. *FEBS Lett* 354: 173-176, 1994.

9. Grissmer S, Nguyen AN, Aiyar J, Hanson DC, Mather RJ, Gutman GA, Karmilowicz MJ, Auperin DD, and Chandy KG. Pharmacological characterization of five cloned voltage-gated K^+ channels, types Kv1.1, 1.2, 1.3, 1.5, and 3.1, stably expressed in mammalian cell lines. *Mol Pharmacol* 45: 1227-1234, 1994.

10. Gulbis JM, Mann S, and MacKinnon R. Structure of a voltage-dependent K^+ channel beta subunit. *Cell* 97: 943-952, 1999.

11. Hulme JT, Coppock EA, Felipe A, Martens JR, and Tamkun MM. Oxygen sensitivity of cloned voltage-gated K^+ channels expressed in the pulmonary vasculature. *Circ Res* 85: 489-497, 1999.

12. Kwak YG, Hu N, Wei J, George AL, Jr., Grobaski TD, Tamkun MM, and Murray KT. Protein kinase A phosphorylation alters Kvbeta1.3 subunit-mediated inactivation of the Kv1.5 potassium channel. *J Biol Chem* 274: 13928-13932, 1999.

13. Madden JA, Dawson CA, and Harder DR. Hypoxia-induced activation in small isolated pulmonary arteries from the cat. *J Appl Physiol* 59: 113-118, 1985.

14. Mays DJ, Foose JM, Philipson LH, and Tamkun MM. Localization of the Kv1.5 K+ channel protein in explanted cardiac tissue. *J Clin Invest* 96: 282-292, 1995.

15. Nakahira K, Shi G, Rhodes KJ, and Trimmer JS. Selective interaction of voltage-gated K^+ channel beta-subunits with alpha-subunits. *J Biol Chem* 271: 7084-7089, 1996.

16. Osipenko ON, Tate RJ, and Gurney AM. Potential role for kv3.1b channels as oxygen sensors [see comments]. *Circ Res* 86: 534-540, 2000.

17. Patel AJ, Lazdunski M, and Honore E. Kv2.1/Kv9.3, a novel ATP-dependent delayed-rectifier K^+ channel in oxygen-sensitive pulmonary artery myocytes. *EMBO J* 16: 6615-6625, 1997.

18. Perez-Garcia MT, Lopez-Lopez JR, and Gonzalez C. Kvbeta1.2 subunit coexpression in HEK293 cells confers O_2 sensitivity to Kv4.2 but not to Shaker channels. *J Gen Physiol* 113: 897-907, 1999.

19. Post JM, Gelband CH, and Hume JR. $[Ca^{2+}]_i$ inhibition of K+ channels in canine pulmonary artery. Novel mechanism for hypoxia-induced membrane depolarization. *Circ Res* 77: 131-139, 1995.

20. Post JM, Hume JR, Archer SL, and Weir EK. Direct role for potassium channel inhibition in hypoxic pulmonary vasoconstriction. *Am J Physiol* 262: C882-C890, 1992.

21. Sham JS, Crenshaw BR, Jr., Deng LH, Shimoda LA, and Sylvester JT. Effects of hypoxia in porcine pulmonary arterial myocytes: roles of K(V) channel and endothelin-1. *Am J Physiol Lung Cell Mol Physiol* 279: L262-L272, 2000.

22. Snyders DJ, Tamkun MM, and Bennett PB. A rapidly activating and slowly inactivating potassium channel cloned from human heart. Functional analysis after stable mammalian cell culture expression. *J Gen Physiol* 101: 513-543, 1993.

23. Tucker A, McMurtry IF, Reeves JT, Alexander AF, Will DH, and Grover RF. Lung vascular smooth muscle as a determinant of pulmonary hypertension at high altitude. *Am J Physiol* 228: 762-767, 1975.

24. Xu C, Lu Y, Tang G, and Wang R. Expression of voltage-dependent K^+ channel genes in mesenteric artery smooth muscle cells. *Am J Physiol* 277: G1055-G1063, 1999.

25. Yuan XJ, Goldman WF, Tod ML, Rubin LJ, and Blaustein MP. Hypoxia reduces potassium currents in cultured rat pulmonary but not mesenteric arterial myocytes. *Am J Physiol* 264: L116-L123, 1993.

26. Yuan XJ, Tod ML, Rubin LJ, and Blaustein MP. Contrasting effects of hypoxia on tension in rat pulmonary and mesenteric arteries. *Am J Physiol* 259: H281-H289, 1990.

27. Yuan XJ, Wang J, Juhaszova M, Golovina VA, and Rubin LJ. Molecular basis and function of voltage-gated K^+ channels in pulmonary arterial smooth muscle cells. *Am J Physiol* 274: L621-L635, 1998.

28. Zhu WH, Conforti L, Czyzyk-Krzeska MF, and Millhorn DE. Membrane depolarization in PC-12 cells during hypoxia is regulated by an O_2-sensitive K^+ current. *Am J Physiol* 271: C658-C665, 1996.

CHAPTER 5

LOCALIZATION OF Kv2.1 TO LIPID RAFTS IN THE PULMONARY ARTERY

INTRODUCTION

Several mechanisms have been addressed in the literature in an attempt to explain the inhibition of pulmonary arterial voltage-gated K^+ (Kv) channels by hypoxia; however, no clear consensus has been reached. Kv channels could be the O_2-sensors themselves through direct interaction of O_2 with the channel, or they may be an effector, responding through some indirect mechanism (28). The indirect hypothesis seems more likely, however, as Kv channel sensitivity to hypoxia is dependent on the system used for heterologous expression (7). Therefore, the localization of Kv channels with various signal transduction molecules should be considered in both heterologous and native systems as this localization may prove to be an important determinant of Kv channel inhibition by hypoxia.

Recent advances in the study of cell membrane structure have led to the idea that distinct lipid microdomains exist within the fluid bilayer of the plasma membrane (6,12,29). These dynamic structures, termed lipid rafts, are enriched in cholesterol and sphingolipids. These rafts, which are present in both excitable and non-excitable cells, localize a number of membrane proteins, including multiple signal transduction

molecules, while excluding others (6,12,29). The concentration of some proteins and separation of others, is the basic principle by which lipid microdomains are thought to exert their function (11,29).

Different types of lipid rafts are likely to exist based on ultrastructure data and the presence or absence of specific marker proteins (25,27). Caveolae represent one type of lipid raft that forms an invagination at the cell surface (1). Caveolae are associated with proteins referred to as caveolins, which serve as markers for caveolae in cell fractionation procedures (1,20). Caveolae have been implicated in a variety of cell functions including the localized generation of Ca^{2+} sparks in both cardiac and arterial smooth muscle cells (16).

A recurring theme in modern biology is that cellular structure is highly ordered, with signal transduction molecules being clustered into signaling centers near their substrates. An emerging body of evidence suggests that caveolae and caveolae-like domains form the basis of such signaling centers (1). Indeed, numerous signal transduction molecules have been localized to lipid rafts (1). Of particular note, is the localization of various tyrosine kinases to lipid rafts, in light of the fact that like hypoxia, tyrosine kinase inhibitors have been shown to markedly inhibit whole cell K^+ current with no other effects on channel kinetics (31). Therefore, the targeting of Kv channels, and their associated signaling molecules, to resistance pulmonary arterial smooth muscle cell (PASMC) lipid rafts, may represent a mechanism through which hypoxia inhibits Kv channel activity. While many proteins have been localized to lipid rafts, Kv channel raft association in the pulmonary artery has not been examined. As discussed in Chapters 3 and 4, Kv2.1 is an O_2-sensitive K^+ channel, present in both conduit and resistance

pulmonary arteries, which is easily detected via immunoblotting. Therefore, the main objective of this study was to test for raft association of the Kv2.1 channel in smooth muscle cells of the pulmonary arterial circulation. Specifically, as it has been shown that raft association is cell-type specific (21), we determined if Kv2.1 was targeted to lipid rafts in PASMCs of resistance vessels, where hypoxic pulmonary vasoconstriction is thought to occur, while excluded from lipid rafts in PASMCs of conduit vessels.

MATERIALS AND METHODS

Materials

Anti-human-Kv1.5-T antibody was produced and characterized in the Tamkun Laboratory. Anti-Kv2.1 polyclonal antibody was purchased from Upstate Biotechnology (Lake Placid, NY). Anti-caveolin polyclonal antibody, which recognizes caveolin isoforms 1, 2, and 3, was purchased from Transduction Laboratories (Lexington, KY). Anti-Kv4.2 polyclonal antibody was provided by Dr. Peter Backx.

Immunohistochemistry

Bovine conduit and resistance pulmonary artery sections were cut and processed as detailed in Chapter 4. Anti-human-Kv1.5-T and anti-caveolin were both utilized at a dilution of 1:500.

L-Cell Raft Isolation

Low-density, triton-insoluble raft fractions were isolated as previously described (18,26). Mouse L-cells stably expressing either rat Kv2.1 or rat Kv4.2 were cultured as described in Chapter 3. Cells from 10, 100-mm dishes (near confluent), were incubated

with 2 μmol/liter dexamthasone in the culture medium for 18 to 24 h in order to induce channel expression. Cells were rinsed with PBS, scraped off the dishes with a rubber policeman, and homogenized in 1 ml of 1% Triton X-100 in MES –buffered saline (25 mmol/liter MES, pH 6.5, 0.15 mol/liter NaCl) plus 1 mM pefablock protease inhibitor (Boehringer Mannheim) with a glass douncer. Sucrose was added to the homogenate to a final concentration of 40%. The detergent extract was placed at the bottom of a centrifuge tube and a 5-30% linear sucrose gradient was formed on top. The samples were centrifuged at 39,000 rpm for 18-20 h at 4 °C in a Beckman SW41 rotor. Following centrifugation, the samples were removed from the rotor, placed on ice and 20, 600 μl, gradient fractions were collected from the top. Approximately 150 μl from each fraction was boiled in 1XSDS sample buffer for 5 min and approximately 30 μl samples were separated by SDS-PAGE and analyzed by Western blot.

Rat and Bovine Brain Raft Isolation

For rat brain raft isolation, one brain (approximately 1 g) was homogenized with a glass douncer in 10 ml MES buffer containing 1% Triton X-100 and the following protease inhibitors: benzamidine 0.31 mg/ml, N-ethylmaleamide 0.62 mg/ml, bacitracin 1 mg/ml (Sigma), pepstatin 1 μg/ml, leupeptin 1 μg/ml and pefablock 0.07 μg/ml (Boehringer Mannheim). The homogenate was centrifuged at 3,000 rpm at 4 °C for 15 min (Beckman JA25.5) in order to sediment debris. Following centrifugation, the sample was processed as described above. For bovine brain raft isolation, approximately 1 g of bovine brain, dissected from the hippocampus region, was processed as described above.

Rat Lung Raft Isolation

For rat lung raft isolation, approximately 1 g of rat lung tissue was homogenized, as described above for rat and bovine brain raft isolation, with the following exceptions. Tissues were first minced with scissors, homogenized for 1 min with a polytron homogenizer (Tekmar), centrifuged at 3,000 rpm to sediment debris, filtered through 1 layer of gauze and homogenized further with a glass douncer. Due to concerns that our triton to tissue ratio was too high for some preparations, we processed some samples in 0.5% or 0.2% Triton X-100 (instead of 1%).

Bovine Pulmonary Artery Smooth Muscle Cell Raft Isolation

Conduit and resistance blood vessels from freshly slaughtered cattle were isolated, removed, and stripped of adventitial and endothelial layers as described in Chapter 4. Approximately 1 g of conduit or resistance pulmonary arterial tissue was then processed as described above in rat lung raft isolation.

Detergent-Free Raft Isolation

The detergent-free raft isolations were performed as previously described (32). This method uses a sonication step to disrupt the cellular membranes. Approximately, 1-2 g of tissue (which had been minced with scissors) was homogenized on ice in 10 ml 500 mM NaCarbonate (pH 11.0) with 2 μg/ml pepstatin and 2 μg/ml leupeptin with 3 X 10 sec pulses with a polytron homogenizer followed by 18 strokes in a loose fitting douncer and an additional 3 X 10 sec pulses with the polytron homogenizer. The homogenate was sonicated with 3 X 20 sec bursts and centrifuged at 3,000 rpm at 4 °C for 15 min (Beckman JA25.5) to sediment debris. Following centrifugation, the

supernatant was processed further with 18 strokes in a loose fitting douncer and then adjusted to 45% sucrose with a MES –buffer solution containing 25 mmol/liter MES, pH 6.5, 0.15 mol/liter NaCl and 90% sucrose. The 45% sucrose solution was placed at the bottom of a centrifuge tube and a 5-35% discontinuous sucrose gradient, in a buffer containing sodium carbonate, pH 11.0, was used to fractionate the sample. The samples were centrifuged at 39,000 rpm for 18-20 h at 4 °C in a Beckman SW41 rotor. Samples were removed from the rotor and processed as described above.

Western Blot Analysis

Samples were separated by SDS-PAGE and transferred to nitrocellulose as described in Chapter 4. Anti-Kv2.1 (1:500), anti-Kv4.2 (1:200) or anti-caveolin (1:1000) were diluted in S1A with 5% nonfat milk and immunoblots were processed as detailed in Chapter 4.

RESULTS

Kv1.5 and Caveolin Expression in Bovine PASMCs

Anti-human Kv1.5-T and anti-caveolin antibodies give a similar staining pattern in bovine PASMCs (Figure 5.1). This figure shows high magnification images of caveolin (A-D) and Kv1.5 (E-H) expression in the smooth muscle layer of bovine conduit and resistance pulmonary arteries. Both antibodies gave a similar punctate staining pattern that was mainly confined to the cell surface. As mentioned in Chapter 4, no experiments comparing the localization of Kv2.1 with that of caveolin in the pulmonary artery were performed as no Kv2.1 antibody was available that immunstained pulmonary arterial tissue. However, the similar staining pattern of Kv1.5 and caveolin led us to

consider the possibility of Kv channel targeting to lipid raft domains within the pulmonary artery.

Localization of Kv2.1, but not Kv4.2, to Lipid Rafts in Transfected L-Cells

Before looking at raft association in the pulmonary artery, raft association of Kv2.1 and Kv4.2 was first examined in transfected cells. Low-density, Triton X-100-insoluble complexes were isolated from mouse L-cells stably expressing Kv2.1 or Kv4.2. Western blot analysis of Kv2.1 expression of sucrose gradient fractions revealed that the majority of Kv2.1 floats in a low-density, triton-insoluble fraction together with caveolin, a raft marker protein (Figure 5.2). In contrast to Kv2.1, Kv4.2 did not float in the low-density fractions and was found strictly in the non-raft fractions at the bottom of the gradient (Figure 5.2), thus suggesting that Kv2.1 raft association was not an artifact of the cell system and experimental conditions. Furthermore, endogenous Na^+/K^+ ATPase, actin and tubulin were also found at the bottom of the gradient (18). Additionally, we confirmed the results of Kv2.1 and caveolin localization to lipid rafts in transfected L-cells using a detergent-free method of raft isolation to show that raft targeting was not artificially induced by the detergent (Figure 5.3). Once again these results illustrate that Kv2.1 and caveolin are found almost exclusively in the raft fractions.

Localization of Kv2.1 to Lipid Rafts in Rat Lung

In order to determine if Kv2.1 targets to a lipid raft in the pulmonary vasculature, Kv2.1 raft association was examined in rat lung. Western blot analysis of Kv2.1 sucrose gradient fractions of 1% Triton X-100-solubilized extracts from rat lung lysates demonstrated that Kv2.1 was at the bottom of the gradient (Figure 5.4). This result was

inconsistent with the Kv2.1 raft association observed in mouse L-cells (Figure 5.2) and HEK293 cells (data not shown). Concerned that the solubilization of Kv2.1 in the rat lung preparation was caused by too much detergent, Kv2.1 raft association was also examined from 0.5% Triton X-100-solubilized extracts. Western blot analysis of Kv2.1 sucrose gradient fractions of 0.5% Triton X-100-solubilized extracts from rat lung lysates revealed that nearly all of the Kv2.1 was found in low-density lipid raft fractions, suggesting that Kv2.1 targets to a lipid raft in the rat lung (Figure 5.4).

Determination of Kv2.1 Localization to Lipid Rafts in Bovine Conduit and Resistance PASMCs

Because there are multiple cell types in whole lung tissue, it could not be ascertained if the "floating" Kv2.1 came from PASMCs or some other cell type. Therefore, a large-scale model was used in order to examine Kv2.1 raft localization in smooth muscle cells from conduit and resistance pulmonary arteries. Western blot analysis of Kv2.1 sucrose gradient fractions of 1%, or 0.5%, Triton X-100-solubilized extracts from bovine conduit PASMCs lysates detected Kv2.1 at the bottom of the gradient (Figure 5.5). Analysis of the same blots for caveolin revealed that while some caveolin was associated with the floating lipid raft fractions, caveolin was also found at the bottom of the gradient in the non-raft fractions.

Results from Kv2.1 raft association experiments in bovine resistance PASMCs were similar to that in bovine conduit PASMCs. Western blot analysis of Kv2.1 sucrose gradient fractions of 1%, or 0.2%, Triton X-100-solubilized extracts from bovine resistance PASMCs lysates demonstrated that Kv2.1 was at the bottom of the gradient (Figure 5.6). Also similar to the results from bovine conduit PASMCs, caveolin was

found in both the floating and non-floating fractions. The fact that caveolin was spread throughout the gradient in the bovine preparations, when it was confined to the floating fractions in the other preparations (L-cell, HEK 293 cell, and rat lung), suggested that there was too much detergent for the amount and type of tissue we were using. Alternatively, the lipid of bovine rafts could be more sensitive to triton solubilization than the rodent and human rafts. Therefore, we were unable at this point to make any conclusions regarding the localization of Kv2.1 to lipid rafts in the pulmonary artery.

Localization of Kv2.1 to Lipid Rafts in Rat and Bovine Brain

The results for Kv2.1 raft association in bovine conduit and resistance PASMCs were different from that in rat lung or mouse L-cells. Therefore, Kv2.1 raft association was compared between rat and bovine brain in order to reduce the variability. Western blot analysis of Kv2.1 gradient fractions of 1% Triton X-100-solubilized rat brain extracts demonstrated that almost all of the Kv2.1 protein was found in the low-density lipid fractions (Figure 5.7). In contrast, Western blot analysis of Kv2.1 sucrose gradient fractions of 1%, or even 0.5%, Triton X-100-solubilized extracts from bovine brain demonstrated that, while some of the Kv2.1 protein was found in the floating lipid raft fractions, the majority of the protein was at the bottom of the gradient (Figure 5.8). Furthermore, caveolin, which is expressed in small quantities in the bovine brain (but was not detectable in rat brain), was found in both the raft and non-raft fractions. This suggested that different species may have different lipid compositions (and thus different detergent solubilities) or, perhaps, because whole rat brain was used while only a portion of the bovine brain (equal in weight to the rat brain, but not necessarily equal in lipid

amount or composition) was used, these difference may simply reflect a different detergent to lipid ratio in the two different preparations.

Localization of Kv2.1 to Lipid Rafts in Bovine Conduit and Resistance PASMCs Using a Detergent-Free Method of Raft Extraction

Concerned that the rafts were being solubilzed in the Triton X-100 raft extraction experiments from bovine PASMCs, a detergent-free method of raft extraction (32) was utilized. Western blot analysis of Kv2.1 gradient fractions of sodium carbonate solubilized extracts from both conduit and resistance PASMC lysates revealed that Kv2.1 was found exclusively in the floating light membrane fractions, along with the majority of the caveolin protein (Figure 5.9). These data indicate that Kv2.1 is localized to lipid rafts in both conduit and resistance PASMCs.

DISCUSSION

High magnification images of Kv1.5 and caveolin expressed in bovine PASMCs revealed a similar staining pattern (Figure 5.1). This staining pattern was punctate in nature and confined mainly to the cell surface. This result led us to hypothesize that certain pulmonary arterial Kv channels are not uniformly expressed on the cell surface of PASMCs and led us to the idea that this targeting to lipid rafts could be a mechanism for Kv channel O_2-sensing in resistance PASMCs. For instance, current from Kv channels targeted to caveolae could be mediated by caveolar neck closure. This mechanism could potentially allow for the rapid regulation of surface channel number without having to rely on the usual mechanisms of membrane protein insertion or internalization. Alternatively, since many ion channels are regulated directly by protein kinases (14,15)

and G-proteins (9,13), simply targeting Kv channels to regions enriched in signaling molecules could serve to regulate Kv channel function. Indeed, it was recently reported that L-type Ca^{2+} channels are targeted to lipid rafts, along with various Ca^{2+} handling proteins, in canine airway smooth muscle (8).

Before examining Kv2.1 localization to lipid rafts in the pulmonary artery, raft association of Kv2.1 was first examined in a heterologous expression system. The results from this study indicated that Kv2.1, but not Kv4.2 is localized to lipid rafts in transfected L-cells (Figure 5.2). These experiments were repeated in HEK293 cells and similar results were obtained. Caveolin, a marker for raft association was found in similar raft fractions as Kv2.1; however, additional experiments revealed that Kv2.1 was localized to a non-caveolar raft (18).

Targeting of Kv2.1 to lipid rafts was also examined in rat lung. When using a 1% Triton X-100-solubilization protocol, Kv2.1 was found at the bottom of the gradient, suggesting that Kv2.1 channel protein was solubilized and therefore not in a lipid raft (Figure 5.4). This result was inconsistent with the Kv2.1 raft association found in mouse L-cells, HEK293 cells and rat brain, suggesting that Kv2.1 raft association is tissue specific, or, there was simply too much detergent in the rat lung preparation. Previous studies suggest that detergent may partially solubilize rafts and that this effect may be more pronounced with excess detergent (4). Additionally, the detergent:protein ratio has been shown to affect recovery of raft localized proteins (23). Therefore, as it is likely that the different result obtained in rat lung was due to excess detergent, the experiment was repeating using 0.5%, instead of 1%, Triton X-100. In this case, Kv2.1 was found primarily in the low-density lipid raft fractions (Figure 5.4), suggesting that Kv2.1 is in a

lipid raft in rat lung. Kv2.1 is expressed in both conduit and resistance pulmonary arterial smooth muscle cells (Figure 4.8). Additionally, Kv2.1 has been reported in airway smooth muscle cells (3). Therefore, it could not be determined if the Kv2.1 protein associated with the light membrane fractions was due to pulmonary arterial Kv2.1, pulmonary airway Kv2.1, or both. However, since the majority of Kv2.1 was found in the raft fractions, it is likely that both pulmonary arterial and airway Kv2.1 proteins are associated with lipid rafts.

Ultimately the purpose of this study was to determine if Kv2.1 was localized to lipid rafts in PASMCs and, if so, to determine whether this association was different between conduit and resistance PASMCs. A bovine model was utilized for these experiments in order to obtain enough tissue for the resistance vessel raft association experiments. When raft association of Kv2.1 in bovine conduit PASMC tissue was examined using a Triton X-100 solubilization buffer containing either 1% or 0.5% triton, Kv2.1 was found at the bottom of the gradient (Figure 5.5). Analysis of these samples for caveolin revealed that although some of the protein was associated with the floating lipid raft fractions, a large portion of the protein was found at the bottom of the gradient in the non-raft fractions. This is in contrast to the caveolin results in rat lung in which caveolin was only detected in the raft fractions (Compare Figure 5.5 with Figure 5.4). Kv2.1 raft association was also examined in resistance PASMCs and again, both Kv2.1 and caveolin were found at the bottom of the gradient in the non-raft fractions. This result was puzzling as caveolin, a marker protein for caveolae, is found almost exclusively in the floating raft fractions (32). Therefore, Kv2.1 raft association was compared between rat and bovine brain in an attempt to determine if the differences

between rat lung and bovine conduit and resistance PASMCs were attributed to a species difference, a tissue difference, or simply a matter of the detergent:protein ratio. When bovine brain samples were analyzed for Kv2.1 raft association using 1% or 0.5% Triton X-100, the majority of the Kv2.1 protein was found at the bottom of the gradient (Figure 5.7). Caveolin, which is expressed in small quantities in brain (5,10) was detected in the light membrane fractions only after extended film exposures. This result suggested that bovine Kv2.1-containing rafts do exist; however, because both Kv2.1 and caveolin were at least partially solubilized in the bovine brain preparations, it is likely that the rafts themselves were partially solubilized by too much detergent.

Pharmacological disruption of lipid rafts with demecolcine, a microtubule disrupter, revealed that Kv2.1 is not localized to the same type of lipid raft as caveolin (18). Furthermore, Kv2.1 raft populations are more sensitive to detergent extraction than caveolin raft populations (19). Recently, several investigators have used detergent-free methods of raft isolation to look at raft association of various proteins (30,32). Detergent-free methods, which use sonication to disrupt the cell membranes in place of detergent, have allowed for the identification of certain proteins, more sensitive to detergent extraction, that had been previously undetected in raft fractions using the Triton X-100 extraction method (30). As it was difficult to find a detergent concentration that wouldn't solubilize the more detergent-resistance caveolin protein in our bovine preparations, a detergent-free method of raft extraction was utilized in order to determine if the more detergent-sensitive Kv2.1 protein was localized to a lipid raft in bovine PASMCs. Under detergent-free conditions, the majority of Kv2.1 was found to be raft associated in both conduit and resistance PASMCs (Figure 5.9). Although this result was

not obtained using both a detergent-free and a detergent-based method of raft extraction, it is likely that Kv2.1 is raft associated in the pulmonary artery *in vivo*. As mentioned previously, detergent-free methods have been used in order to detect raft-association that had previously gone undetected using a detergent-based protocol (30,32). Furthermore, in the bovine preparations, even the more detergent-resistant protein, caveolin, was partially solubilized. While it is likely that there is some species variation in the amount and type of lipid in a given raft population, it is also likely that the discrepancies lie with a variable detergent:protein ratio between preparations.

Although Kv2.1 localization to lipid rafts in the pulmonary artery does not by itself explain the differential responses of conduit and resistance pulmonary arteries to hypoxia reported by several investigators (2,17,24), it does not exclude the possibility that the targeting of Kv channels to lipid rafts is important for pulmonary arterial O_2-sensing. For instance, channel localization to lipid rafts in the pulmonary artery has the potential of clustering various signaling molecules and their substrates, thereby maximizing signal transduction and minimizing cross-talk. Indeed, numerous signaling proteins have already been localized to lipid rafts (1). Although Kv2.1 is not differentially targeted to a lipid raft between conduit and resistance vessels, it is possible that other O_2-sensitive channels, such as Kv3.1b (22), are differentially targeted. Or, perhaps, an important O_2-sensing protein, or β subunit, that interacts with the channel, is localized to lipid rafts in resistance, but not in conduit PASMCs, thereby accounting for the differential hypoxic effects.

In summary, these data indicate that Kv2.1 targets to lipid rafts in both conduit and resistance PASMCs. Although it is not likely that Kv2.1 raft association alone

accounts for the differential responses of conduit and resistance pulmonary arteries to hypoxia, the targeting of Kv channels to these important signaling centers is likely to be a key component of PASMC O_2-sensing. Future work is needed to examine the composition of raft proteins in the pulmonary artery. Additionally, other O_2-sensitive Kv channels should be examined for differential raft association between conduit and resistance pulmonary arteries.

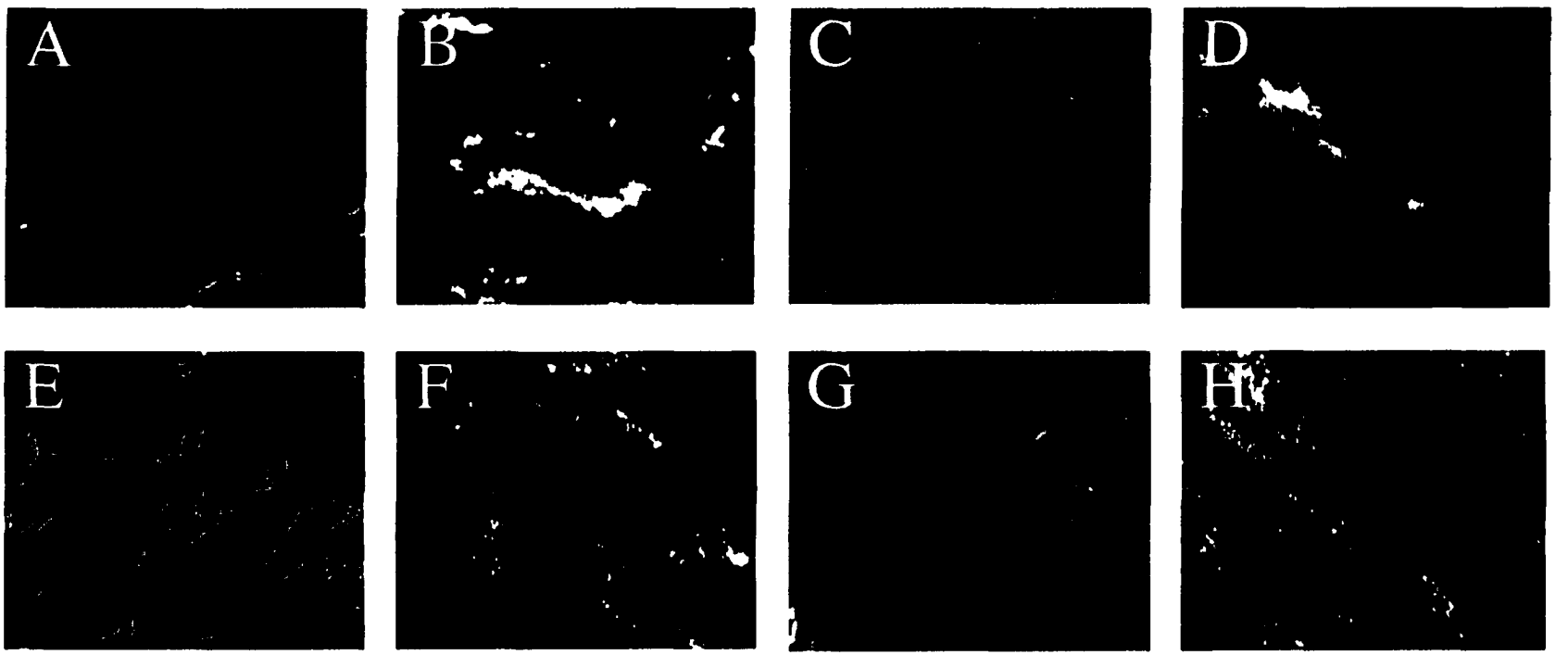

Figure 5.1. Immunolocalization of caveolin and Kv1.5 to bovine conduit and resistance pulmonary arteries. Panels A-D show high magnification DIC images and caveolin (Cy3) immunostaining of bovine conduit (A &B) and resistance (C & D) pulmonary arteries. Panels E-H show high magnification DIC images and Kv1.5 (Cy3) immunostaining of bovine conduit (E & F) and resistance (G & H) pulmonary arteries. Calibration bar illustrated in panel A.

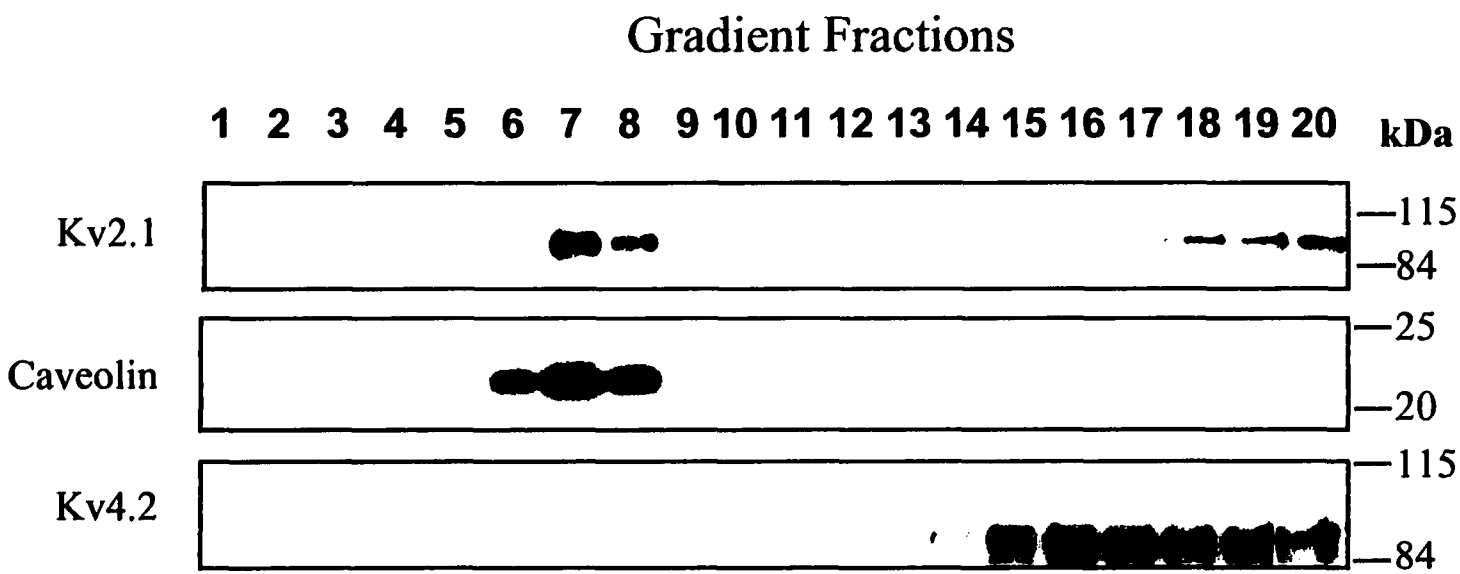

Figure 5.2. Sucrose density gradient centrifugation of 1% Triton X-100-solubilized extracts from mouse L-cells stably expressing Kv2.1 or Kv4.2. Kv2.1 immunoblot was stripped and reprobed for caveolin as shown.

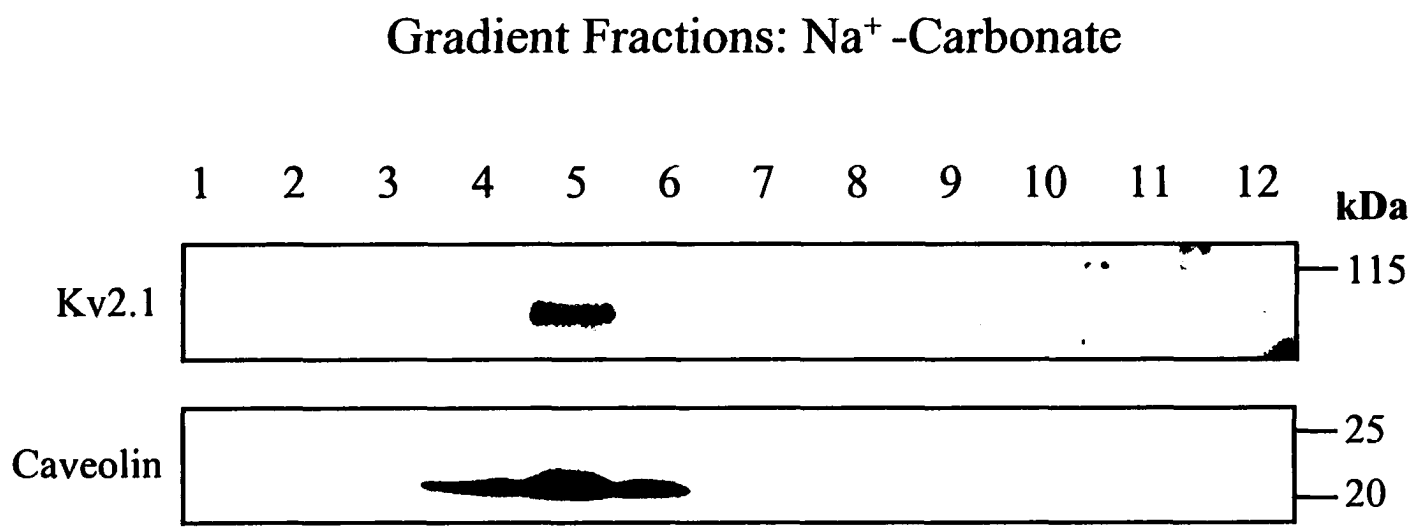

Figure 5.3. Sucrose density gradient centrifugation of detergent-free solubilized extracts from mouse L-cells stably expressing Kv2.1 analyzed for Kv2.1 and caveolin immunoreactivity.

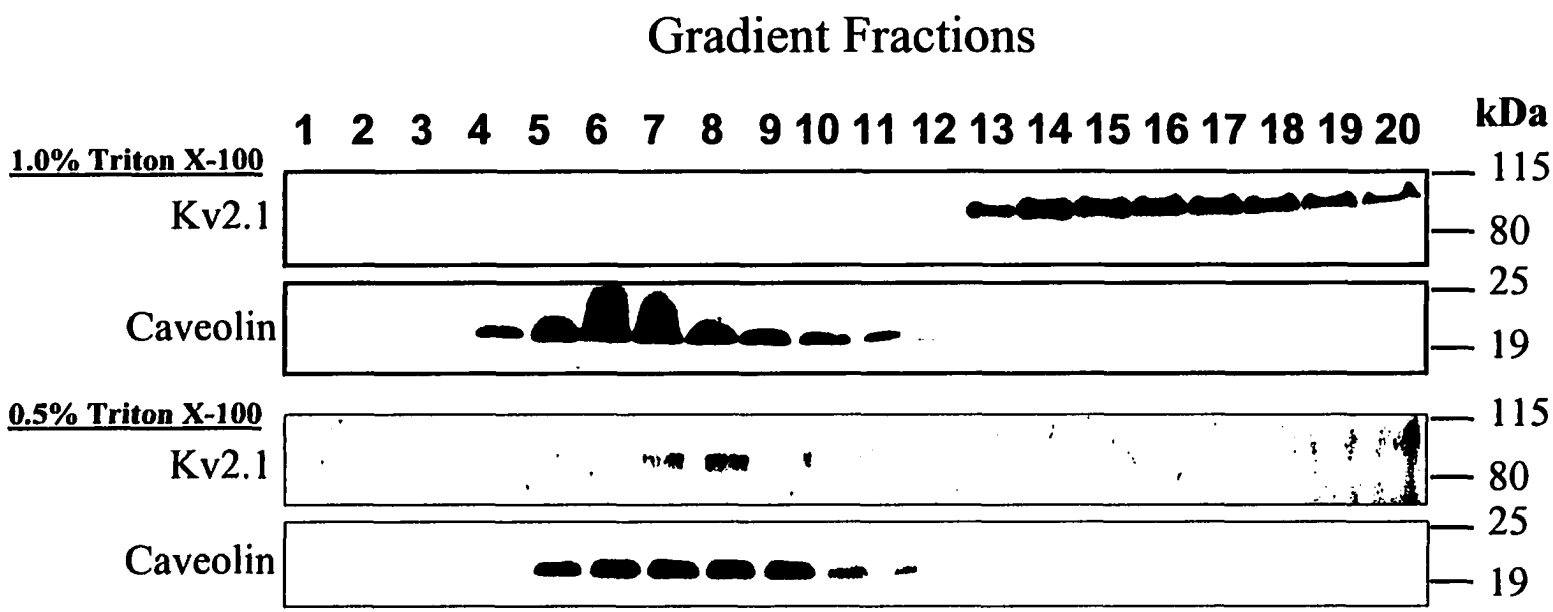

Figure 5.4. Sucrose density gradient centrifugation of 1% & 0.5% Triton X-100-solubilized extracts from rat lung lysates analyzed for Kv2.1 and caveolin immunoreactivity.

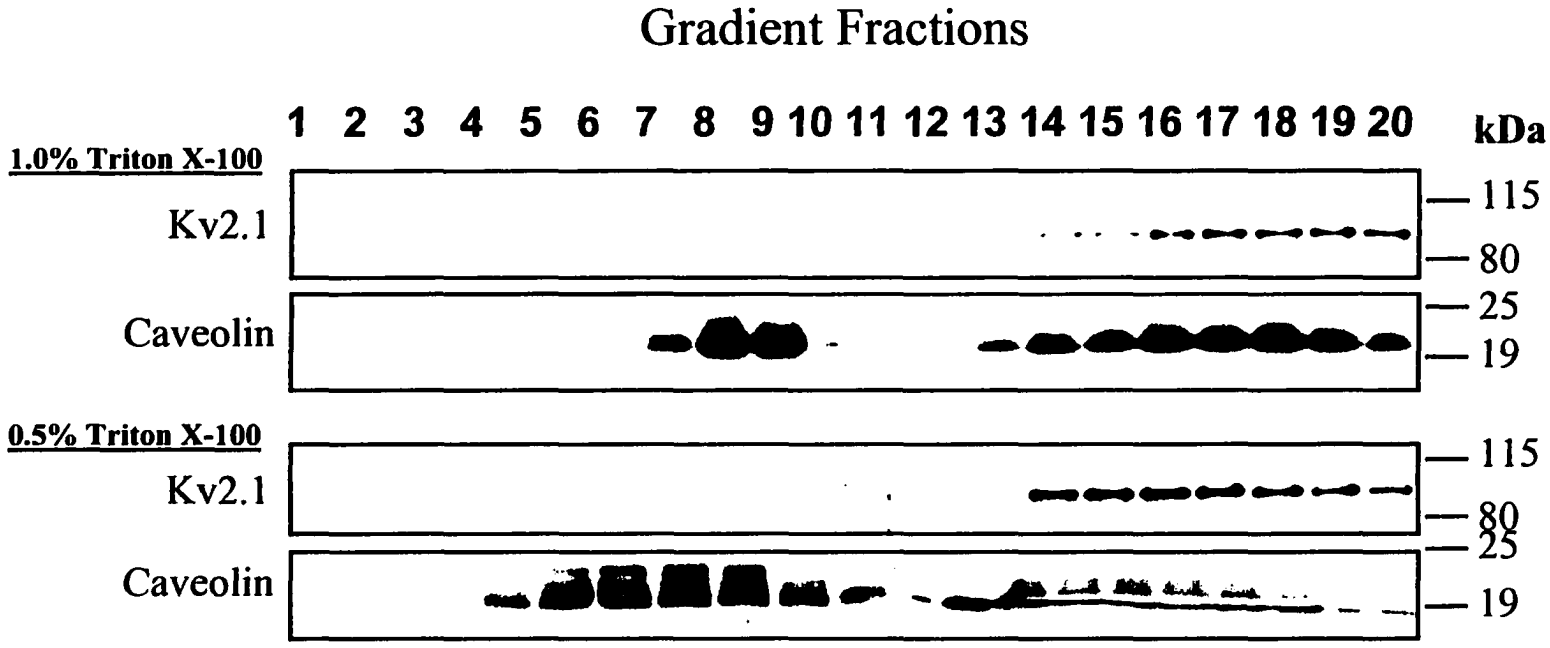

Figure 5.5. Sucrose density gradient centrifugation of 1% & 0.5% Triton X-100-solubilized extracts from bovine conduit pulmonary artery smooth muscle cell lysates analyzed for Kv2.1 and caveolin immunoreactivity.

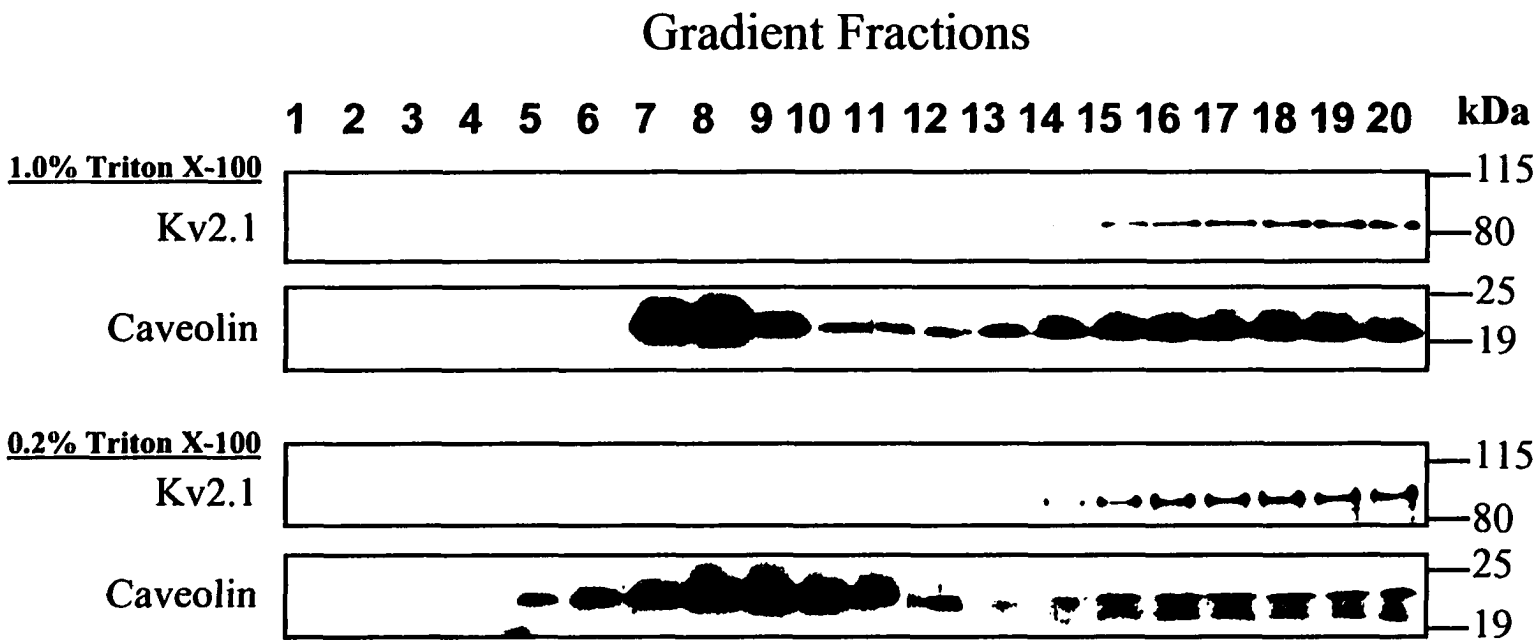

Figure 5.6. Sucrose density gradient centrifugation of 1% & 0.2% Triton X-100-solubilized extracts from bovine resistance pulmonary artery smooth muscle cell lysates analyzed for Kv2.1 and caveolin immunoreactivity.

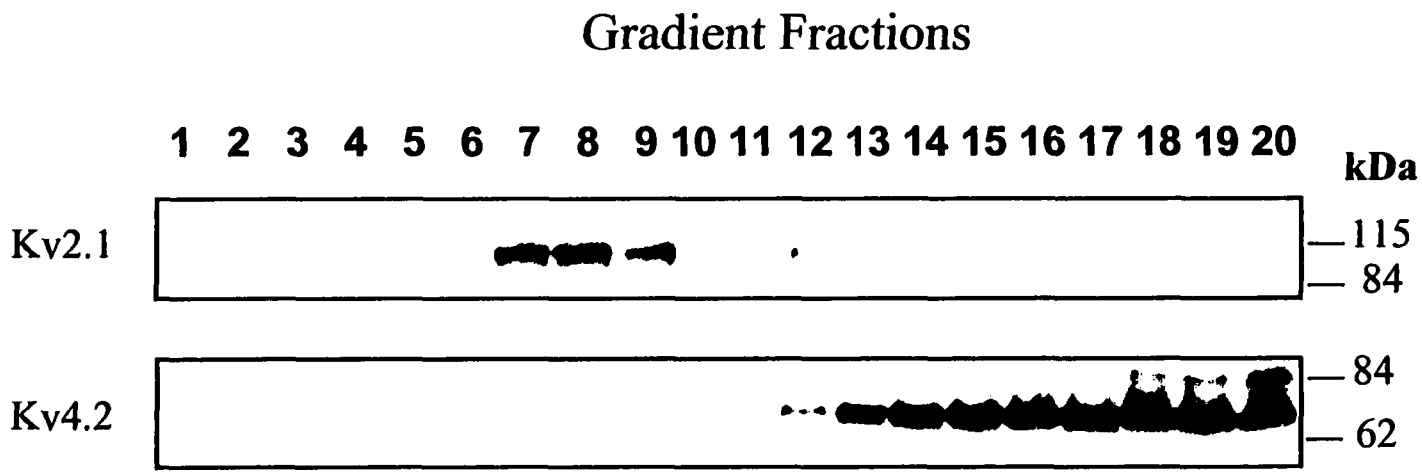

Figure 5.7. Sucrose density gradient centrifugation of 1% Triton X-100-solubilized extracts from rat brain lysates analyzed for Kv2.1 and Kv4.2 immunoreactivity.

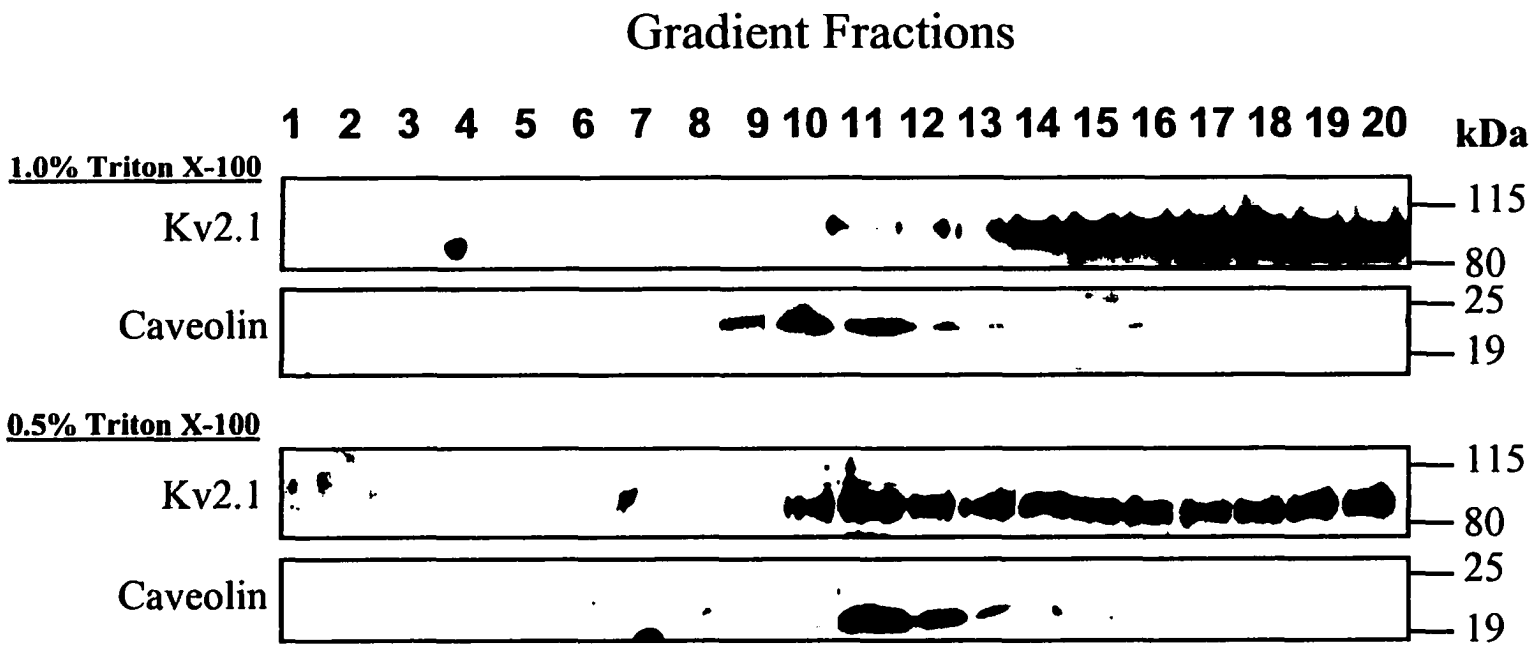

Figure 5.8. Sucrose density gradient centrifugation of 1% & 0.5% Triton X-100-solubilized extracts from bovine brain lysates analyzed for Kv2.1 and caveolin immunoreactivity.

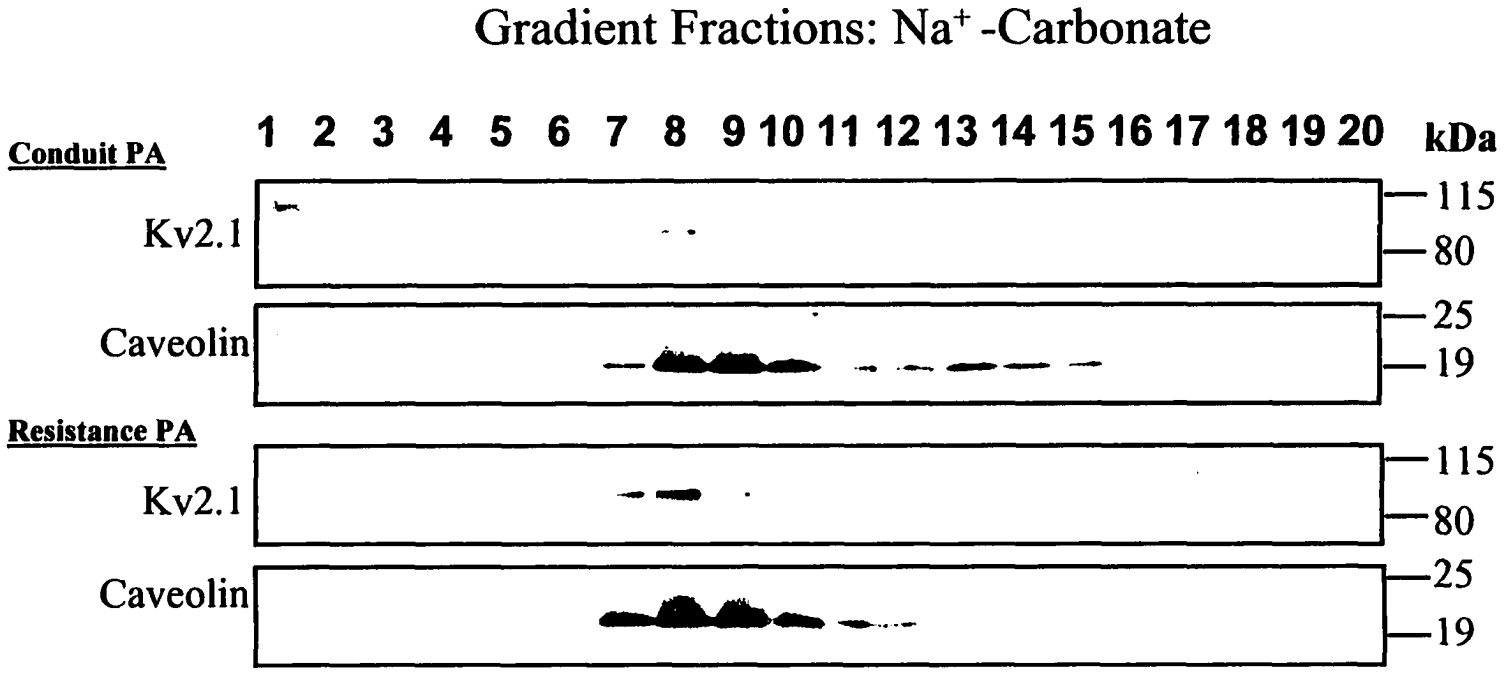

Figure 5.9. Sucrose density gradient centrifugation of detergent-free solubilized extracts from bovine conduit and resistance pulmonary artery smooth muscle cell lysates analyzed for Kv2.1 and caveolin immunoreactivity.

REFERENCES

1. Anderson RG. The caveolae membrane system. *Annu Rev Biochem* 67: 199-225, 1998.

2. Archer SL, Huang JM, Reeve HL, Hampl V, Tolarova S, Michelakis E, and Weir EK. Differential distribution of electrophysiologically distinct myocytes in conduit and resistance arteries determines their response to nitric oxide and hypoxia. *Circ Res* 78: 431-442, 1996.

3. Archer SL, Souil E, Dinh-Xuan AT, Schremmer B, Mercier JC, El Yaagoubi A, Nguyen-Huu L, Reeve HL, and Hampl V. Molecular identification of the role of voltage-gated K^+ channels, Kv1.5 and Kv2.1, in hypoxic pulmonary vasoconstriction and control of resting membrane potential in rat pulmonary artery myocytes. *J Clin Invest* 101: 2319-2330, 1998.

4. Arni S, Keilbaugh SA, Ostermeyer AG, and Brown DA. Association of GAP-43 with detergent-resistant membranes requires two palmitoylated cysteine residues. *J Biol Chem* 273: 28478-28485, 1998.

5. Bickel PE, Scherer PE, Schnitzer JE, Oh P, Lisanti MP, and Lodish HF. Flotillin and epidermal surface antigen define a new family of caveolae- associated integral membrane proteins. *J Biol Chem* 272: 13793-13802, 1997.

6. Brown DA and London E. Functions of lipid rafts in biological membranes. *Annu Rev Cell Dev Biol* 14: 111-136, 1998.

7. Coppock EA, Martens JR, and Tamkun MM. Molecular mechanisms of hypoxia-induced pulmonary vasoconstriction: Role of voltage-gated K^+ channels. *Am J Physiol.* In Press 2001.

8. Darby PJ, Kwan CY, and Daniel EE. Caveolae from canine airway smooth muscle contain the necessary components for a role in Ca^{2+} handling. *Am J Physiol* 279: L1226-L1235, 2000.

9. Duprat F, Lesage F, Guillemare E, Fink M, Hugnot JP, Bigay J, Lazdunski M, Romey G, and Barhanin J. Heterologous multimeric assembly is essential for K^+ channel activity of neuronal and cardiac G-protein-activated inward rectifiers. *Biochem Biophys Res Commun* 212: 657-663, 1995.

10. Galbiati F, Volonte D, Goltz JS, Steele Z, Sen J, Jurcsak J, Stein D, Stevens L, and Lisanti MP. Identification, sequence and developmental expression of invertebrate flotillins from Drosophila melanogaster. *Gene* 210: 229-237, 1998.

11. Harder T and Simons K. Caveolae, DIGs, and the dynamics of sphingolipid-cholesterol microdomains. *Curr Opin Cell Biol* 9: 534-542, 1997.

12. Jacobson K and Dietrich C. Looking at lipid rafts? *Trends Cell Biol* 9: 87-91, 1999.

13. Krapivinsky G, Gordon EA, Wickman K, Velimirovic B, Krapivinsky L, and Clapham DE. The G-protein-gated atrial K^+ channel IKACh is a heteromultimer of two inwardly rectifying K^+-channel proteins. *Nature* 374: 135-141, 1995.

14. Kwak YG, Hu N, Wei J, George AL, Jr., Grobaski TD, Tamkun MM, and Murray KT. Protein kinase A phosphorylation alters Kvbeta1.3 subunit-mediated inactivation of the Kv1.5 potassium channel. *J Biol Chem* 274: 13928-13932, 1999.

15. Kwak YG, Navarro-Polanco RA, Grobaski T, Gallagher DJ, and Tamkun MM. Phosphorylation is required for alteration of kv1.5 K^+ channel function by the Kvbeta1.3 subunit. *J Biol Chem* 274: 25355-25361, 1999.

16. Lohn M, Furstenau M, Sagach V, Elger M, Schulze W, Luft FC, Haller H, and Gollasch M. Ignition of calcium sparks in arterial and cardiac muscle through caveolae. *Circ Res* 87: 1034-1039, 2000.

17. Madden JA, Dawson CA, and Harder DR. Hypoxia-induced activation in small isolated pulmonary arteries from the cat. *J Appl Physiol* 59: 113-118, 1985.

18. Martens JR, Navarro-Polanco R, Coppock EA, Nishiyama A, Parshley L, Grobaski TD, and Tamkun MM. Differential targeting of Shaker-like potassium channels to lipid rafts. *J Biol Chem* 275: 7443-7446, 2000.

19. Martens JR, Sakamoto N, Sullivan SA, Grobaski TD, and Tamkun MM. Isoform-specific localization of voltage-gated K^+ channels to distinct lipid raft populations: targeting of Kv1.5 to caveolae. J Biol Chem. In Press 2001.

20. Okamoto T, Schlegel A, Scherer PE, and Lisanti MP. Caveolins, a family of scaffolding proteins for organizing "preassembled signaling complexes" at the plasma membrane. *J Biol Chem* 273: 5419-5422, 1998.

21. Oliferenko S, Paiha K, Harder T, Gerke V, Schwarzler C, Schwarz H, Beug H, Gunthert U, and Huber LA. Analysis of CD44-containing lipid rafts: Recruitment of annexin II and stabilization by the actin cytoskeleton. *J Cell Biol* 146: 843-854, 1999.

22. Osipenko ON, Tate RJ, and Gurney AM. Potential role for Kv3.1b channels as oxygen sensors. *Circ Res* 86: 534-540, 2000.

23. Ostermeyer AG, Beckrich BT, Ivarson KA, Grove KE, and Brown DA. Glycosphingolipids are not essential for formation of detergent- resistant membrane rafts in melanoma cells. methyl-beta-cyclodextrin does not affect cell surface transport of a GPI-anchored protein. *J Biol Chem* 274: 34459-34466, 1999.

24. Post JM, Gelband CH, and Hume JR. $[Ca^{2+}]_i$ inhibition of K^+ channels in canine pulmonary artery. Novel mechanism for hypoxia-induced membrane depolarization. *Circ Res* 77: 131-139, 1995.

25. Roper K, Corbeil D, and Huttner WB. Retention of prominin in microvilli reveals distinct cholesterol-based lipid micro-domains in the apical plasma membrane. *Nat Cell Biol* 2: 582-592, 2000.

26. Sargiacomo M, Sudol M, Tang Z, and Lisanti MP. Signal transducing molecules and glycosyl-phosphatidylinositol-linked proteins form a caveolin-rich insoluble complex in MDCK cells. *J Cell Biol* 122: 789-807, 1993.

27. Schnitzer JE, McIntosh DP, Dvorak AM, Liu J, and Oh P. Separation of caveolae from associated microdomains of GPI-anchored proteins. *Science* 269: 1435-1439, 1995.

28. Semenza GL. Perspectives on oxygen sensing. *Cell* 98: 281-284, 1999.

29. Simons K and Ikonen E. Functional rafts in cell membranes. *Nature* 387: 569-572, 1997.

30. Smart EJ, Ying YS, Mineo C, and Anderson RG. A detergent-free method for purifying caveolae membrane from tissue culture cells. *Proc Natl Acad Sci U S A* 92: 10104-10108, 1995.

31. Sobko A, Peretz A, and Attali B. Constitutive activation of delayed-rectifier potassium channels by a src family tyrosine kinase in Schwann cells. *EMBO J* 17: 4723-4734, 1998.

32. Song KS, Li S, Okamoto T, Quilliam LA, Sargiacomo M, and Lisanti MP. Co-purification and direct interaction of Ras with caveolin, an integral membrane protein of caveolae microdomains. Detergent-free purification of caveolae microdomains. *J Biol Chem* 271: 9690-9697, 1996.

CHAPTER 6

SUMMARY AND FUTURE DIRECTIONS

The hypoxia-induced membrane depolarization and subsequent constriction of small resistance pulmonary arteries is thought to occur via inhibition of vascular smooth muscle cell voltage-gated K^+ (Kv) channels that are open at the resting membrane potential. As inhibition of these channels has been implicated as an important step in hypoxic pulmonary vasoconstriction (HPV), a better understanding of the molecular nature of the Kv channels, and the potential mechanisms, involved in this response should aid the development of more specifically targeted pharmacological agents for the alleviation of excessive HPV and its subsequent pathological consequences. In the present study, the O_2-sensitivity of cloned Kv channels, expressed in a heterologous expression system, and the expression of Kv channel α and β subunits in the pulmonary artery, were examined in order to identify, from a molecular perspective, which Kv channels are likely to contribute to the native pulmonary arterial smooth muscle cell (PASMC) O_2-sensitive K^+ current. Additionally, Kv channel localization to lipid rafts in the pulmonary artery was also examined as it may represent a novel mechanism of Kv channel inhibition by hypoxia. Results from our study include the following general findings: 1) Kv channel subunit composition dramatically affects O_2 sensitivity, 2) Kv channel subunit expression changes along the pulmonary arterial tree, and 3) Kv channels

are localized to lipid raft microdomains in PASMCs. Major findings and future directions are summarized below.

Kv channel subunit composition dramatically affects O_2-sensitivity. Homomeric Kv1.2 and Kv2.1 channels are O_2-sensitive, but only at non-physiological membrane potentials, while homomeric Kv1.5 channels are not O_2-sensitive at any membrane potential. In contrast, heteromeric Kv1.2/Kv1.5 and Kv2.1/Kv9.3 channels are O_2-sensitive in the voltage range of the PASMC resting membrane potential, making these heteromeric channels good candidates for the native PASMC O_2-sensitive K^+ current. Therefore, any attempt to describe the molecular nature of the PASMC O_2-sensitive K^+ current must take into consideration the possibility of heteromeric channel formation. Future work in this area should include detection of these heteromeric channels in vivo. Additionally, chimeras between O_2-sensitive subunits (such as Kv1.2) and O_2-insensitive subunits (Kv1.5) should be made in order to determine what regions of the channel are important for O_2 sensing.

Kv channel subunit expression changes along the pulmonary arterial tree. Specifically, expression of Kv3.1b and Kv9.3 α subunits, and members of the Kvβ1 subfamily, is increased in the resistance pulmonary arteries where HPV is thought to occur. Comparisons of these molecular data, and that of previous studies of native current in PASMCs, allow us to make tentative hypotheses about the involvement of Kv3.1b and Kv9.3 α subunits, and Kvβ1 subunits, in the physiological response of resistance PASMCs to hypoxia. Future work should include studies in which the O_2-sensitivity of Kv3.1b is examined as well as possible heteromeric assembly of Kv3.1b with other α subunits and β subunits. These studies would help to determine whether or

not it is likely that Kv3.1b associates with other subunits in vivo, and, if so, if these heteromeric channels are O_2-sensitive at physiologically important membrane potentials. Additional studies examining the role of the Kv β subunit on the hypoxic-inhibition of Kv channel current should also be examined. This work should include studies in which the β subunit NADPH binding site is mutated in order to determine if this site is responsible for the β subunit-induced O_2-sensitivity of certain Kv α subunits.

The O_2-sensitive Kv2.1 channel is localized to lipid raft microdomains in the pulmonary artery. As these lipid microdomains have been shown to be involved in a variety of cell functions, any attempt to examine the molecular mechanism of Kv channel inhibition by hypoxia should keep these important signaling centers in mind. Future work should examine raft targeting of other O_2-sensitive channels, such as Kv3.1b, as well as the effect of Kv β subunits on raft targeting. Additionally, the O_2-sensitivity of a Kv channel that mistargets out of a raft should be examined.